

Maximum mass of relativistic self-gravitating Bose-Einstein condensates with repulsive or attractive $|\varphi|^4$ self-interaction

Pierre-Henri Chavanis

Laboratoire de Physique Théorique, Université de Toulouse, CNRS, UPS, Toulouse, France

 (Received 23 November 2022; accepted 28 March 2023; published 4 May 2023)

We derive an approximate analytical expression of the maximum mass of relativistic self-gravitating Bose-Einstein condensates with repulsive or attractive $|\varphi|^4$ self-interaction. This expression interpolates between the general relativistic maximum mass of noninteracting bosons stars, the general relativistic maximum mass of bosons stars with a repulsive self-interaction in the Thomas-Fermi limit, and the Newtonian maximum mass of dilute axion stars with an attractive self-interaction [P. H. Chavanis, *Phys. Rev. D* **84**, 043531 (2011)]. We obtain the general structure of our formula from simple considerations and determine the numerical coefficients in order to recover the exact asymptotic expressions of the maximum mass in particular limits. As a result, our formula should provide a relevant approximation of the maximum mass of relativistic boson stars for any value (positive and negative) of the self-interaction parameter. We discuss the evolution of the system above the maximum mass and consider application of our results to dark matter halos and inflaton clusters. We also make a short review of boson stars and Bose-Einstein condensate dark matter halos and point out analogies with models of extended elementary particles.

DOI: [10.1103/PhysRevD.107.103503](https://doi.org/10.1103/PhysRevD.107.103503)

I. INTRODUCTION

The concept of boson stars was introduced by Kaup [1] and Ruffini and Bonazzola [2] (see also Refs. [3–5]) in the 1960s in a rather academic manner without explicit connection to any astrophysical object. They were just hypothetical stars governed by the laws of general relativity and quantum mechanics. In a sense, boson stars are the descendants of the so-called “geons” of Wheeler [6], except that they are built from scalar particles of spin 0 instead of electromagnetic field, i.e., spin-1 bosons.¹ Kaup [1] and Ruffini and Bonazzola [2] considered the $T = 0$ limit in which bosons form Bose-Einstein condensates (BECs). In that case, all the

¹The geon, which is a gravitational electromagnetic entity, was originally introduced by Wheeler [6] as a localized nonsingular solution of the Einstein-Maxwell equations. A geon consists of a spherical shell of electromagnetic radiation held together by its own gravitational attraction. It realizes to some extent the proposal of Einstein [7] and Einstein and Rosen [8]: “Is an atomistic theory of matter and electricity conceivable which, while excluding singularities in the field, makes use of no other fields than those of the gravitational field and those of the electromagnetic field in the sense of Maxwell?” and some of the goals of the unitary field theory [9–15]. These objects, however, were found to be unstable [6,16] leading to the belief that gravitational collapse is inevitable. In the following years, transferring the ideas of Mach and Einstein to the microcosmos, many researchers tried to find a model that describes an elementary particle in terms of a semiclassical field coupled to the Einstein equations. These extended particles resemble geons [6] or wormholes [17–19]. Kaup [1] presented the notion of a Klein-Gordon geon that was later called a boson star.

bosons are in the same quantum state described by a unique complex wave function $\varphi(x^\mu)$ satisfying the Klein-Gordon-Einstein (KGE) equations.² This semiclassical equation is valid in the Hartree-Fock approximation for the second quantized two-body problem [2]. Boson stars can be regarded as macroscopic quantum states that are only prevented from collapsing gravitationally by the Heisenberg uncertainty principle. No Schwarzschild-type event horizon occurs in these objects since their density profile extends to infinity. Kaup [1] and Ruffini and Bonazzola [2] showed that equilibrium states can exist only below a maximum mass $M_{\max}^{\text{GR}} = 0.633M_P^2/m$ set by general relativity, where $M_P = (\hbar c/G)^{1/2}$ is the Planck mass. Above this maximum mass, the star is expected to collapse and form a black hole (or evaporate). Their results were rederived and confirmed in Refs. [21–27]. The maximum mass of boson stars is the counterpart of the maximum mass of fermion stars, such as white dwarf stars and neutron stars. The maximum mass of white dwarf stars $M_{\max}^{\text{WD}} = 3.10 M_P^3/(\mu H)^2$, where H is the proton mass and μ is the molecular weight, was found by Chandrasekhar [28] and the maximum mass of neutron stars $M_{\max}^{\text{NS}} = 0.384 M_P^3/m^2$, where m is the neutron mass, was found by Oppenheimer and Volkoff [29].

Boson stars can be viewed as complex scalar fields (SFs) or anisotropic fluids [1,2], while fermion stars are isotropic

²See Ref. [20] for a short account of the early history of wave mechanics (Schrödinger, Klein-Gordon, Dirac, and Gross-Pitaevskii equations) and an exhaustive list of references.

fluids [30]. Despite this distinguished feature, there exist remarkable similarities between boson stars and fermion stars. The mass-central density relation $M(\rho_0)$ and the radius-central density relation $R(\rho_0)$ of boson stars exhibit damped oscillations [1,2,23,26,31–38] and the mass-radius relation $M(R)$ has a snail-like (spiral) structure [23,35,38]. The series of equilibria becomes unstable after the first mass peak and a new mode of stability is lost at each subsequent turning point of mass like in the case of neutron stars [30]. These stability results can be established from the study of the pulsation equation [32–34,39,40]³ or from the energy principle [26] stating that a stable equilibrium state is a minimum of mass energy Mc^2 at fixed particle number N (the charge or the number of bosons minus antibosons is conserved for a complex SF). The variational principle for the first variations $\delta M - \alpha \delta N = 0$ implies that $M(\rho_0)$ and $N(\rho_0)$ are extremal at the same points, precisely where a mode of pulsation vanishes [26,27]. The mass-particle number relation $M(N)$ is plotted in Refs. [26,27,36–38]. The $M(N)$ curve presents cusps at the critical points where $M(\rho_0)$ and $N(\rho_0)$ are extremal. It forms a zigzag course of smaller and smaller extension associated with the spiral nature of the mass-radius relation. Kusmartsev *et al.* [36–38] used the $M(N)$ curve interpreted as a bifurcation diagram to investigate the dynamical stability of boson stars by invoking Arnold’s classification of singularities in catastrophe theory [42,43] and the Whitney theorem [44], which were previously applied in Ref. [45] to nongravitational solitons. If the mass becomes larger after a cusp, a new mode of instability appears. Inversely, if the mass becomes smaller after a cusp, a mode of instability disappears.⁴ Seidel and Suen [35],

³The pulsation equation for boson stars was derived by Gleiser [32] and Jetzer [33] who generalized the approach developed by Chandrasekhar [41] for an isotropic fluid in general relativity. Since the SF is complex, they obtained a system of two coupled eigenvalue equations. Using the method of test functions, they could only prove that equilibrium states with a central density much larger than the critical density (corresponding to the maximum mass) are unstable. They first suggested that the instability point may not coincide with the maximum mass because of anisotropic effects. But soon after, Gleiser [39], Gleiser and Watkins [34], and Jetzer [40], following the work of Lee and Pang [27], showed that the instability actually occurs at the maximum mass and that a new mode becomes unstable at each successive critical point. This is due to the fact that the functions $M(\rho_0)$ and $N(\rho_0)$ are extremal at the same points (see below), implying that the pulsation vanishes at these points [27].

⁴One can also deduce the stability of boson stars from the Poincaré theorem [46,47] (see, e.g., Appendix C of [48] for a brief exposition of this theorem). This approach was previously applied to the series of equilibria of isothermal self-gravitating systems that present features similar to those of fermion and boson stars (damped oscillations, spirals, zigzags, cusps, etc.) [48,49]. Using the Poincaré turning point argument, the stability of boson stars can be directly inferred from Fig. 8 of [26], returning the results of [36–38]. One can also use the Poincaré turning point argument to determine the stability of fermion stars (white dwarfs and neutron stars) [50], returning the results of [30] based on the Wheeler $M(R)$ theorem.

Kusmartsev *et al.* [36–38], and Guzmán [51,52] showed that a stable boson star that is slightly perturbed will oscillate with a fundamental frequency, emit SF radiation, and settle down into a new equilibrium configuration with less mass, while an unstable boson star will, in general, collapse to a black hole or migrate to the stable branch. They also mentioned that the binding energy $E_b = (M - Nm)c^2$ can become positive, signaling the existence of configurations with excess energy. Such configurations are always unstable against a collective transformation in which they are dispersed into free particles at infinity [1,31]. These results are remarkably similar to those obtained for neutron stars [30]. However, there also exist crucial differences between boson and fermion stars. In particular, boson stars are stabilized by the Heisenberg uncertainty principle, while fermion stars are stabilized by the Pauli exclusion principle. This difference is reflected in the scaling with m of the maximum mass of stable configurations. The maximum mass of boson stars scales as $M_{\max}^{\text{GR}} \sim M_P^2/m$ [1,2], instead of $M_{\max}^{\text{GR}} \sim M_P^3/m^2$ [28,29] for fermion stars. As a result, for the same particle mass m , the maximum mass of boson stars is smaller than the mass of fermion stars by a factor $m/M_P \ll 1$. For example, for $m \sim 1 \text{ GeV}/c^2$ (of the order of the neutron mass) for which $m/M_P \sim 10^{-19}$, the maximum mass of boson stars is $M \sim 10^{-19}M_\odot$, while the maximum mass of neutron stars is on the order of the solar mass. This leads to the concept of miniboson stars [23,24,27] or minisoliton stars [25–27] with small mass, small radius, and extremely high densities. This property may facilitate the formation of small black holes made of cold invisible axions (bosonic black holes [22] or axion black holes [24]) in the axion dominated universe. The maximum mass of boson stars becomes on the order of the solar mass if the mass of the bosons is very small, typically $m \sim 10^{-10} \text{ eV}/c^2$.

Friedberg *et al.* [26] (see also [5,53–55]) computed the radial solutions of the static KGE equations with nodes, which correspond to excited states. They found that the critical mass grows approximately linearly with the number of nodes (see also [31]). Jetzer [40] showed that the excited Bose star configurations are stable for central densities up to the critical density.⁵ As a result, as noted by Lee [25,56], by increasing the node number n there exists an equilibrium state for any value of the mass (at least classically). Since a boson star is a stationary solution of the Klein-Gordon (KG) equation in its own gravitational field, a boson star is also called a “gravitational atom” [57]. The energy levels of these gravitational atoms present an interesting fine structure for high values of the principal quantum number. This fine splitting of the

⁵Lee and Pang [27] previously argued that excited modes are always unstable, but their claim is incorrect because they did not require the particle number to be constant in their stability analysis.

energy levels may indicate a rich particlelike structure of the quantized geons [53]. In the last stages of boson star formation, one expects that a highly excited configuration first forms with several nodes and that it eventually decays into the ground state (with no node) by a combined emission of scalar radiation and gravitational radiation. This mechanism has been analyzed by Ferrell and Gleiser [57] in a Newtonian approximation.

Colpi *et al.* [58] considered the case of bosons stars with a repulsive $\frac{\lambda}{4\hbar c}|\varphi|^4$ ($\lambda > 0$) self-interaction and found that the resulting configurations differ markedly from the noninteracting case.⁶ In the Thomas-Fermi (TF) limit, the maximum mass set by general relativity is $M_{\max}^{\text{GR}} = 0.0612\sqrt{\lambda}M_p^3/m^2$.⁷ For $\lambda \sim 1$ it exhibits the same scaling as the maximum mass of fermion stars (Chandrasekhar's mass). This leads to much bigger structures than in the noninteracting case, making them much more astrophysically interesting. They are called “massive boson stars.” In a sense, the repulsive self-interaction for bosons plays a role similar to the quantum pressure arising from the Pauli exclusion principle for fermions. Like for fermion stars and noninteracting

boson stars, the $M(\rho_0)$, $R(\rho_0)$, and $N(\rho_0)$ curves exhibit damped oscillations [32,33,36–38,58,79,82–86], the $M(R)$ curve has a snail-like (spiral) structure [38,86], and the $M(N)$ curve displays cusps and forms a zigzag course of smaller and smaller extension [36–38,84]. A detailed discussion of the analogy between boson stars and neutron stars is given in Ref. [38]. Colpi *et al.* [58] (see also [81]) showed that, in the TF limit, a boson star with a repulsive quartic self-interaction is equivalent to an isotropic barotropic fluid with a well-defined equation of state $P(\epsilon)$.⁸ This equation of state reduces to that of an $n = 1$ polytrope at low densities (nonrelativistic limit) and to the linear law $P \sim \epsilon/3$ similar to the equation of state of radiation at high densities (ultrarelativistic limit). This strengthens the analogy between boson stars and neutron stars that display the same asymptotics at high densities. In these objects, the speed of sound is always less than the speed of light. However, ultrarelativistic configurations are dynamically unstable according to the Poincaré criterion because they are located after the first turning point of mass [86]. Cold mixed boson-fermion stars have been studied by Henriques *et al.* [88–90] and Jetzer [91].

Jetzer and Scialom [92,93] showed that the static solutions of the KGE equation for a real SF have a naked singularity at the origin and that they are always dynamically unstable. This result is in agreement with the cosmic censorship conjecture, which excludes spacetimes with naked singularities [94]. In particular, general relativistic real massless SFs are unstable.⁹ This conclusion is in agreement with the result of Christodoulou [105,106] (see also [107,108]) who showed that all time-dependent spherically symmetric solutions of the KGE equations with $m = \lambda = 0$ must either disperse to infinity or form a black hole. Real SFs (like axions) do not admit regular static solutions to the KGE equations because there is no conserved Noether current leading to particle number (or charge) conservation.¹⁰ It is possible to construct regular solutions that are periodic in time when $M < M_{\max}^{\text{GR}} = 0.606 M_p^2/m$ [111,112]. However,

⁶The first investigations of the KGE equations with a self-interaction potential were carried out by Mielke and Scherzer [53] (see also [54,55,59–61]). They used a $-|\varphi|^4 + |\varphi|^6$ potential obtained from a nonlinear Heisenberg-Pauli-Weyl [62–64] spinor equation in a curved spacetime produced by the energy-momentum tensor of the spinor fields via the Einstein equations. This work was done in the context of particle physics (independent from the context of boson stars) in order to describe classically extended particles consisting of confined quarks. In that case, the Einstein-type field equations account for strong interactions on a curved spacetime of hadronic dimensions characterized by a modified Planck length of strong gravity [65–74]. Algebraic complications resulting from the spinor structure were avoided by considering SFs coupled to gravity. In order to maintain a similar dynamics, a scalar self-interaction $V(\varphi)$ was formally obtained by “squaring” the fundamental nonlinear spinor equation. This provides a model for a unitary field theory of extended particles resembling the geons of Wheeler, which are held together by self-generated gravitational forces and are composed of localized fundamental classical fields described by the Einstein-Maxwell equations. The coupling of gravity to neutrino fields had been previously considered by Brill and Wheeler [75]. Their work provided the appropriate groundwork for an extension to nonlinear “spinor geons” satisfying the Dirac-Einstein equations considered in [53]. On the other hand, Lee and co-workers [25,76,77] investigated a Higgs-type potential [78] with symmetry breaking of the degenerate vacuum form. They called the solutions of their KGE equations “nontopological soliton stars” and found that the maximum mass of these scalar [76] or fermion [77] soliton stars has units of M_p^3/m^3 , which is huge—on the order of the mass of the Universe $\sim 10^{20}M_\odot$ —in comparison with a boson or a neutron star (for the case of comparable boson and fermion masses $m \sim 1 \text{ GeV}/c^2$). Nishimura and Yamaguchi [79] constructed a neutron star using an equation of state of an isotropic fluid built from Higgs bosons. Their work showed that the limit for such boson stars can possibly exceed the limiting mass of $3.2M_\odot$ for neutron stars [80].

⁷Tkachev [81] independently considered the case of bosons stars with a repulsive $|\varphi|^4$ self-interaction and obtained the scaling of the maximum mass $M_{\max}^{\text{GR}} \sim \sqrt{\lambda}M_p^3/m^2$ from qualitative arguments.

⁸See Ref. [87] and Appendix B for a detailed derivation of this equation of state. The hydrodynamic description of boson stars with a repulsive self-interaction in the TF limit has been studied in detail by Chavanis and Harko [86] in the framework of the Oppenheimer-Volkoff equations.

⁹Real massless SFs coupled to Einstein gravity were first considered by Bergmann and Leipnik [95] and Yilmaz [96] (see also [97]). They are known to admit exact static solutions which were discovered by Buchdahl [98] for a special case. In the framework of the Jordan-Brans-Dicke-Thiry theory, these solutions already appeared in Ref. [99] and correspond to those found by Majumdar [100] for the Einstein-Maxwell system. Later, the solutions discovered by Buchdahl [98] were rederived by Wyman [101] (see also [102,103]) and generalized to spacetimes of arbitrary dimensions by Xanthopoulos and Zannias [104].

¹⁰Note that particle number conservation is approximately restored in the nonrelativistic limit so that Newtonian boson stars made of a real SF, like dilute axion stars, become stable in that limit [109,110].

on a long timescale (which can nevertheless exceed the age of the Universe), these “oscillatons” are unstable and disperse to infinity or form a black hole.

Nontopological solitons [12–14,54,55,60,61,113–137] may be regarded as the nongravitational precursors of boson stars.¹¹ For a specific Higgs-type self-interaction potential $V(\varphi)$, they are localized solutions of a nonlinear KG equation in flat spacetime. These solitons were meant to represent elementary particles extending in space (i.e., particles with a structure), pursuing the initial goal of Einstein and Rosen [7–9], Menius and Rosen [10], Finkelstein *et al.* [11,12,15], Dirac [150–153], and de Broglie [154]. In flat spacetime, according to Derrick’s theorem [118], no stable time-independent solution of finite energy exists for a nonlinearly coupled real SF in dimension larger than 1. Nontopological solitons may, however, have a very long lifetime if their rate of dissolution is small [119]. Objects similar to nontopological solitons are called Q balls [155], fermion Q balls [156–159], neutrino balls [160], and quark nuggets [161] in the case of spinors. Q balls [155] are stabilized by their conserved charge Q . Bound further by their self-gravity, Q stars [156–159] may model neutron stars with a mass larger than $\sim 3M_{\odot}$. Other SFs arise from axion [162–166], inflaton or dilaton fields [167] with their corresponding compact objects axion stars [81,163,168] and dilaton stars [167]. The dilaton field arises in the process of a Kaluza-Klein–type dimensional reduction of supergravity or superstring models. These real SFs couple to gravity similarly to the Brans-Dicke field of scalar-tensor theories. The dilaton stars [167] are stable because of a conserved dilaton current and charge in such models. In an extended model [169] with Higgs field and dilaton coupling, there occur, however, unstable branches with diverging mass for high central values of the Higgs field. Nonsingular, time-dependent, spherically symmetric solutions of nonlinear SF theories were constructed in [170–173] and called pulsions [170,171] or oscillons [172,173]. They characterize 3D nongravitational self-interacting real SFs described by the KG equation. Although unstable, they are extremely long-lived. Spherically symmetric solutions (including excited states) of the KG equations for a real or complex SF in a prescribed Schwarzschild, de Sitter, or Friedmann-Lemaître-Robertson-Walker metric were constructed in Refs. [54,61,72,174–177] in the context of black holes, particle physics, and cosmology. More recently, Rosen [178,179] revived his old idea of an elementary particle built out of SFs within the framework of the KG or Proca equations coupled to the Einstein equations.¹² He developed a model of particles (interpreted as gravitational solitons) closely related to the model of boson stars, being apparently unaware of the vast literature on this subject.¹³ In a sense, Wheeler’s geon concept has

¹¹The KG equation with an attractive $|\varphi|^4$ self-interaction was introduced by Finkelstein *et al.* [12] and by Rosen and Rosenstock [13,14] (see Schiff [138,139] and Malenka [140] for the case of a repulsive φ^4 self-interaction in the context of nonlinear meson theory for heavy nuclei; see also Goldstone [141], Higgs [78], and Nielsen and Olesen [142] for a Mexican hat potential with $m^2 < 0$ and $\lambda > 0$). The sine-Gordon equation was introduced by Petiau [114], Skyrme [115,116], and Enz [117] in the context of particle physics (see also the analogy with Bloch walls in magnetic crystals [143] and the motion of a slide dislocation in a crystalline structure [144–147]). The name “sine-Gordon equation” first appeared in Ref. [127] and was coined by Kruskal (it is more precise than the name “nonlinear KG equation” [126]). The concept and the name “soliton” were introduced by Zabusky and Kruskal [148] in the context of the Korteweg–de Vries (KdV) equation [149]. The analogy between the sine-Gordon equation and the KdV equation was first pointed out by Rubinstein [127].

¹²See also the concept of Proca stars introduced in [180,181].

¹³It is fascinating to realize that the KG equation coupled to the Maxwell and Einstein equations have been introduced independently by different communities to describe either boson stars in astrophysics (with the usual gravitational constant G) or elementary particles (with a modified gravitational constant G_f). This was foreseen by Einstein [7] in 1919: “There are reasons for thinking that the elementary formations which go to make up the atom are held together by gravitational forces.” Models of extended elementary particles have been constructed from the Maxwell equations with Poincaré stress [153,182–186], nonlinear Maxwell equations [187–190], Maxwell-Einstein equations [6,7,191], KG-Maxwell equations [9–11], (multifield) self-interacting KG equations [12–14,54,55,60,61,113–137], (massless) self-interacting Dirac equations [12,15,59,113,128,192–202], Dirac-Maxwell equations [203–207], KG-Maxwell-Einstein equations [3,208–210], (multifield) self-interacting KG-Maxwell equations [209,211–213], self-interacting Dirac-Maxwell equations [214–216], self-interacting Dirac-KG equations [131,217], self-interacting Dirac-KG-Maxwell equations [218], self-interacting KG-Einstein equations [53,219–221], KG-Einstein equations [72,178], Einstein-Maxwell equations for a charged fluid with a vacuum equation of state $P = -\epsilon$ [222–226], Yang-Mills-Einstein equations [227,228], Proca equations [179], Weyl equations [229], Dirac-Einstein equations [230], Dirac-Maxwell-Einstein equations [231,232], self-interacting (Higgs) KG-Maxwell-Einstein equations [233], and gravitational Dirac-Maxwell [234] equations. In Maxwell’s theory of electromagnetism, charged particles appear as singularities in the field. The field equations break down at singular points, and so separate equations of motion have to be prescribed for the particles. Einstein and Infeld [235] emphasized that a proper field theory knows only fields and not particles and that particles should only emerge from the fields themselves. They write: “Could we not reject the concept of matter and build a pure field physics? We could regard matter as the region in space where the field is extremely strong.” In the unitary field theories listed above, particles appear not as singularities but as small volumes in which the energy and the charge of the field are concentrated. These unitary field models are necessarily nonlinear in order to avoid singularities. All the properties of the particles, such as their equation of motion, follow from the field equations. Other authors [65–72,191,236–240] developed analogies between elementary particles and Schwarzschild [241,242], Kerr-Newmann [243–245], and Reissner-Nordström [246,247] black holes. Carneiro [248] writes: “The strong gravity approach [71–74] tries to derive the hadron properties from a scaling down of gravitational theory, treating particles as black-hole-type solutions. It is based on the scale invariance of general relativity. With this philosophy, we can think the Universe as a self-similar structure, with the same physical laws appearing at different scales.” Kodama [220,221] found a stable static, singularity-free, finite energy solution of the KGE equations with a φ^4 potential that extends the usual 1D kink solution [132,133]. The spacetime geometry implied resembles that of the Einstein-Rosen bridge [8] of the Schwarzschild geometry, i.e., two asymptotically flat spaces connected by a bridge (a “black soliton” or a kind of wormhole in the sense of Wheeler [6,17–19]).

anticipated the nonintegrable soliton solutions of classical nonlinear field theory. We refer to specific reviews on solitons in particle physics [249–251], soliton stars [252], and boson stars [253–261] for more information on the subject.

Boson stars associated with a complex SF can be formed from a dissipationless relaxation process called “gravitational cooling” [262]. This process has a counterpart in stellar dynamics. Collisionless stellar systems are known to experience a process of violent relaxation [263] during which they form a centrally dense core by sending some stars at large distances in an extended halo. Similarly, a bosonic cloud will settle to a unique boson star by ejecting part of the scalar matter.¹⁴ Since there is no viscous term in the KG equation, the radiation of the SF is the only mechanism. The emission of gravitational waves also occurs in the absence of spherical symmetry. Boson star solutions in their ground state or in excited configurations have been used in the context of dark matter (DM) to fit the observed rotation curves of dwarf and spiral galaxies (see the introduction of Ref. [265] for a short review of early works on this topic). Indeed, if bosons are ultralight, with a mass $m \sim 10^{-22}$ eV/ c^2 , they can form compact objects of Galactic size (see [266,267] and references therein).¹⁵ Therefore, ultralight axions (ULAs) have been invoked in models of DM halos. In the context of DM, Newtonian gravity is usually a good approximation, so we can use the Schrödinger-Poisson or Gross-Pitaevskii-Poisson (GPP) equations instead of the KGE equations. A Newtonian boson star is a stationary solution of these equations. However, models of DM halos based on a pure boson star solution (soliton) are usually not successful, especially in the case of large DM halos. Indeed, the mechanism of gravitational cooling [262] typically leads to a “core-halo” structure with a quantum core (soliton) in its ground state surrounded by an extended halo resulting from the quantum interferences of the excited states. This core-halo structure has been evidenced in numerical simulations of the Schrödinger-Poisson equations [268–276] and can be heuristically explained by an adaptation of Lynden-Bell’s statistical theory of violent relaxation [263,277] as discussed in Ref. [264]. The quantum core may solve the core-cusp problem [278] of the cold dark matter model and the halo, which is similar to an isothermal or a Navarro-Frenk-White profile, accounts for the flat rotation curves of the galaxies. This type of core-halo configuration leads to more realistic models of DM halos than a pure BEC solution and has been the subject of intensive research over the last few years (see, e.g., an exhaustive list of references in [267] and in the recent reviews [279–286]).

¹⁴See [264] for a description of the analogy between gravitational cooling and violent relaxation.

¹⁵More massive bosons with a mass $10^{-22} \leq m \leq 10^{-3}$ eV/ c^2 can also form compact objects of Galactic size provided that they are self-interacting with a dimensionless self-interacting constant in the range $0 \leq \lambda \leq 10^{-15}$ [267].

In the nonrelativistic limit, the KGE equations reduce to the Schrödinger-Poisson equations in the noninteracting limit or to the GPP equations when the bosons interact through a $|\varphi|^4$ potential.¹⁶ Using the Madelung [289] transformation, one can introduce a hydrodynamic representation of these equations in the form of compressible Euler equations with an additional quantum potential. The complete mass-radius relation of nonrelativistic self-gravitating BECs with repulsive or attractive self-interactions was obtained in [265,290], either exactly by solving the GPP equations numerically, or analytically (approximately) by using variational methods based on the minimization of energy at fixed mass and employing a Gaussian ansatz for the wave function. For noninteracting bosons, one obtains the mass-radius relation $M = 9.95\hbar^2/(Gm^2R_{99})$ [290,291], showing that the radius of the star decreases as its mass increases [similar to the mass-radius relation $M = 1.49 \times 10^{-3} \hbar^6/[G^3m^3(\mu H)^5R^3]$ of nonrelativistic white dwarf stars [292]]. For a repulsive self-interaction, the mass-radius relation is modified at high masses. In the TF regime, corresponding to $M \rightarrow +\infty$, the star is equivalent to a polytrope of index $n = 1$, and the radius of the BEC tends to a minimum value $R_{\text{TF}} = \pi(a_s\hbar^2/Gm^3)^{1/2}$ [81,265,293–297] independent of its mass. These latter results were extended in the general relativistic regime by Chavanis and Harko [86] using a hydrodynamic approach (see also [298] for a complementary discussion). This leads to the concept of general relativistic BEC stars with a maximum mass $M_{\text{max}}^{\text{GR}} = 0.307 \hbar c^2 \sqrt{a_s}/(Gm)^{3/2}$ [86] equivalent to the one found in Ref. [58]. Chavanis and Harko [86] suggested that, because of their superfluid core, neutron stars could be considered as BEC stars. Indeed, neutrons could form Cooper pairs and behave as bosons of mass $2m_n$ (where m_n is the neutron mass). Since the maximum mass of BEC stars depends on the self-interaction parameter, it can be larger than the Oppenheimer-Volkoff limit $M_{\text{OV}} = 0.376(\hbar c/G)^{3/2}/m_n^2 = 0.7M_{\odot}$ obtained when the neutron star is modeled as an ideal Fermi gas. This could explain certain observations of neutron stars with a mass $\sim 2M_{\odot}$ [299], which cannot be explained with the Oppenheimer-Volkoff model.

On the other hand, bosons can have an attractive $\frac{\lambda}{4\hbar c}|\varphi|^4$ ($\lambda < 0$) self-interaction. This is the case, in particular, for quantum chromodynamics (QCD) axions with a mass $m \sim 10^{-4}$ eV/ c^2 and a negative scattering length $a_s \sim -5.8 \times 10^{-53}$ m (corresponding to a self-interaction constant $\lambda \sim -7.39 \times 10^{-49}$ and a decay constant $f = 5.82 \times 10^{10}$ GeV). Axions are hypothetical pseudo-Nambu-Goldstone bosons

¹⁶The nonrelativistic limit of the KGE equations is discussed in [20,287,288] for a complex SF and in [109,110] for a real SF. In the case of a complex SF, the potential that appears in the GP equation is the same as the potential that appears in the KG equation. In the case of a real SF, they are usually different (see Appendices B and C for a detailed discussion).

of the Peccei-Quinn [300] phase transition associated with a $U(1)$ symmetry that solves the strong charge parity (CP) problem of QCD. They are described by a real SF φ with a cosine self-interaction potential. Axions are possible DM candidates [301]. Their role in cosmology has been first investigated in Refs. [302–305]. The cosmological evolution of axions was considered by Hogan and Rees [162] and Kolb and Tkachev [163–166]. In the early Universe, self-gravity between axions can be neglected so they are governed by the (relativistic) sine-Gordon equation in an expanding background. Because of the attractive self-interaction, axions can form miniclusters of mass $M_{\text{axiton}} \sim 10^{-12} M_{\odot}$ and size $R_{\text{axiton}} \sim 10^9$ m called axion miniclusters [162] or “axitons” [164]. Tkachev [81,168] took self-gravity into account and considered the possibility to form axion stars by Jeans instability.¹⁷ He assumed a repulsive $\frac{\lambda}{4\hbar c} |\varphi|^4$ ($\lambda > 0$) self-interaction between axions and found a maximum mass $M_{\text{max}}^{\text{GR}} \sim \sqrt{\lambda} M_p^3 / m^2$ (see footnote 7). However, when the self-interaction is attractive ($\lambda < 0$), the equilibrium state of axion stars results from the balance between the gravitational attraction, the attractive self-interaction, and the repulsive quantum potential. There is an equilibrium state only below a maximum mass $M_{\text{max}}^{\text{NR}} = 1.012\hbar / \sqrt{Gm|a_s|}$ or $M_{\text{max}}^{\text{NR}} = 5.073M_p / \sqrt{|\lambda|}$, which was first identified by Chavanis [265,281,290]. This is the maximum mass of dilute axion stars [306]. Note that this maximum mass is a purely nonrelativistic (NR) result, contrary to the maximum mass of boson and fermion stars discussed above, which is due to general relativity (GR). For dilute QCD axion stars, one finds $M_{\text{max}}^{\text{NR}} = 6.46 \times 10^{-14} M_{\odot}$ and a corresponding radius $R_{99}^* = 227$ km, which are on the order of the mass and size of asteroids (by comparison, the Kaup mass is $M_{\text{max}}^{\text{GR}} = 8.46 \times 10^{-7} M_{\odot}$ and the Kaup radius is $R_*^{\text{GR}} = 1.19 \times 10^{-2}$ m). This leads to the notion of “axteroids.” For ULAs, we can have a much larger maximum mass, on the order of Galactic masses. Its precise value depends, however, on the values of m and a_s , which are not well known. Taking $m = 2.92 \times 10^{-22}$ eV/ c^2 and $a_s = -3.18 \times 10^{-68}$ fm (corresponding to $\lambda = -1.18 \times 10^{-96}$ and $f = 1.34 \times 10^{17}$ GeV) predicted in [267], we get $M_{\text{max}}^{\text{NR}} = 5.10 \times 10^{10} M_{\odot}$ and $R_{99}^* = 1.09$ pc (by comparison, the Kaup mass is $M_{\text{max}}^{\text{GR}} = 2.90 \times 10^{11} M_{\odot}$ and the Kaup radius is $R_*^{\text{GR}} = 0.132$ pc). For $M < M_{\text{max}}^{\text{NR}}$, the mass-radius relation displays two branches of solutions [265,290]. There are two possible equilibrium states for the same mass. The equilibrium states with $R > R_*$ are stable (energy minima) and the equilibrium states with $R < R_*$ are unstable (energy maxima). The stability of axion stars can be determined by applying the Poincaré turning point argument [265,290]. The stable solutions

¹⁷He introduced the names “gravitationally bound axion condensates” [81] and “axionic Bose stars” [168], becoming later “axion stars.”

define the branch of dilute axion stars and the mass $M_{\text{max}}^{\text{NR}}$ represents their maximum mass (the unstable solutions correspond to nongravitational BECs) [265,290]. For $M > M_{\text{max}}^{\text{NR}}$, there is no equilibrium state and the axion star collapses [307]. This leads to (i) a bosenova with the emission of relativistic axions if we take special relativity into account [308], (ii) a black hole if the conditions where general relativity prevails are fulfilled [309,310], or (iii) the formation of a dense axion star [311] if we take into account higher order terms in the expansion of the self-interaction potential like, e.g., a repulsive $|\varphi|^6$ self-interaction [109,312] that can stabilize the star against gravitational collapse.¹⁸ The axion star can also fragment into several stable pieces (axion “drops”) of mass $M' < M_{\text{max}}$ [318,319], thereby preventing its complete collapse. We refer to [260,316] and to the Introduction of [110] for recent reviews on axion stars and for an exhaustive list of references.

These results have been applied to DM halos made of ULAs. Bose-Einstein condensate dark matter (BECDM) halos, also called fuzzy dark matter (FDM) halos or scalar field DM halos, typically have a core-halo structure made of a quantum core (soliton) in its ground state surrounded by an approximately isothermal envelope (atmosphere) arising from the quantum interferences of excited states [264,272,320,321]. This core-halo structure results from a process of gravitational cooling [262] and violent relaxation [263,277]. The results given in Refs. [265,290] describe the ground state of a self-gravitating BEC so they apply either to the “minimum halo” of mass $(M_h)_{\text{min}} \sim 10^8 M_{\odot}$, which is a completely condensed object without envelope (atmosphere), or to the quantum core M_c of large DM halos of mass $M_h \geq (M_h)_{\text{min}}$. A general expression of the core mass-halo mass relation $M_c(M_h)$ for BECDM halos with an arbitrary self-interaction has been obtained in [267,321–324] from thermodynamical considerations (see also [269,271,273,325,326] for other justifications). The mass M_c of the quantum core increases with the halo mass M_h . For noninteracting bosons and for bosons with a repulsive self-interaction, it can be shown that the core mass

¹⁸Visinelli *et al.* [313] and Eby *et al.* [314] argue that relativistic effects are crucial on the branch of dense axion stars while self-gravity is negligible. As a result, dense axion stars correspond to “pseudobreathers,” “oscillons,” or “axitons,” which are described by the sine-Gordon equation (they can be viewed as the 3D version of usual 1D “breathers” [315]). For a real SF, these objects are known to be unstable due to a particle number changing process, such as the $3 \rightarrow 1$ process, and to decay via emission of relativistic axions. Visinelli *et al.* [313] and Eby *et al.* [314] argue that the decay timescale is much shorter than any cosmological timescale so that dense axion stars are not physically relevant. This conclusion is, however, contested by Braaten and Zhang [316] who argue that dense axion stars can be long-lived. Note that dense axion stars described by a complex SF (axion boson stars [317]) would be stable in the relativistic regime because of charge conservation.

TABLE I. Maximum mass M_{\max} of different types of fermion and boson stars. It is interesting to note that all the scalings M_p , M_p^2/m , M_p^3/m^2 , and M_p^4/m^3 are represented. We have also indicated the minimum radius R_* and the maximum compactness $C_{\max} = GM_{\max}/R_*c^2$ of the star. The compactness of a Schwarzschild black hole is $C_S = 1/2$. The Buchdahl inequality for a barotropic relativistic star imposes $C \leq 4/9 = 0.444$. The ratio between the star radius R and the Schwarzschild radius $R_S = 2GM/c^2$ is $R/R_S = Rc^2/(2GM) = 1/(2C)$. It is restricted by the Buchdahl inequality $R \geq (9/8)R_S$ so that a barotropic relativistic star cannot be a black hole.

	M_{\max}	R_*	C_{\max}	R_*/R_S
White dwarfs [28]	$3.10 M_p^3/(\mu H)^2$	0	∞	0
Neutron stars [29]	$0.384 M_p^3/m^2$	$3.35(\hbar^3/Gm^4c)^{1/2}$	0.114	4.37
Miniboson (minisoliton) stars [1,2]	$0.633 M_p^2/m$	$6.03 \hbar/mc$	0.105	4.76
Massive boson stars [58,86]	$0.0612\sqrt{\lambda}M_p^3/m^2$	$0.383\sqrt{\lambda}(\hbar^3/Gm^4c)^{1/2}$	0.160	3.13
Soliton star [25,56,76,77]	M_p^4/m^3			
Oscillatons (real SF) [111,112]	$0.606 M_p^2/m$			
Dilute axion stars [265,290]	$5.07 M_p/\sqrt{ \lambda }$	$1.10\sqrt{ \lambda }(\hbar^3/Gm^4c)^{1/2}$	$4.61 (m/M_p)^2/ \lambda $	

M_c is always much smaller than the maximum mass M_{\max}^{GR} set by general relativity, so the quantum core cannot collapse toward a supermassive black hole (SMBH) [267,323,324]. For bosons with an attractive self-interaction, the core mass M_c could reach the maximum mass M_{\max}^{NR} of Ref. [265] in sufficiently large DM halos and collapse [267,323,324]. The outcome of the collapse in that case would be a dense axion “star” (soliton),¹⁹ a black hole, a bosenova, or axion drops [109,307–314,316,318,319]. The conditions for this collapse require, however, stronger self-interactions ($f < 10^{15}$ GeV) than those ($10^{16} \leq f \leq 10^{18}$ GeV) commonly allowed by particle physics and cosmology (see [267,306] for more details). Furthermore, since $f \ll M_p$ the collapse leads to a dense axion star or to a bosenova, not to a SMBH. These results can also find applications in the context of inflaton clusters and inflaton stars that could form in the very early Universe [327–330]. There is a complete analogy between inflaton clusters and BECDM halos, so that most of the results obtained for BECDM halos (core-halo solution, core mass-radius relation, core mass-halo mass relation, etc.) can be exported to the context of inflaton clusters. In particular, if the SF has an attractive self-interaction, inflaton stars can be stable only below the maximum mass M_{\max}^{NR} of Ref. [265]. Padilla *et al.* [331] argued that, above that critical mass, the inflaton star collapses and forms a black hole. That could be a new mechanism to form primordial black holes (PBHs) during the phase of reheating following inflation. However, according to the results of Refs. [109,308,311], it is also possible that the collapse of inflaton stars leads to a bosenova or a dense inflaton star rather than a black hole. Primordial black holes of mass ~ 1 g can form only in sufficiently massive inflaton clusters of mass $M_h \sim 10^{14}$ g and they rapidly evaporate on a timescale 10^{-30} s. We suggest that bosenova and dense inflaton stars may occur in less massive inflaton

clusters if the bosons have a sufficiently attractive self-interaction. In addition to the quantum core of DM halos [267,322–324] and inflaton clusters [331], other applications of the maximum mass of self-gravitating BECs with an attractive self-interaction (like dilute axion stars) [265,290] have been discussed in Refs. [332–339].

In this paper, we provide a simple approximate analytical expression of the maximum mass of relativistic self-gravitating BECs with an arbitrary $|\varphi|^4$ self-interaction. This expression interpolates between the general relativistic maximum mass of noninteracting bosons stars, the general relativistic maximum mass of bosons stars with a repulsive self-interaction in the TF limit, and the nonrelativistic maximum mass of dilute axion stars with an attractive self-interaction. It therefore connects the different expressions obtained in the literature reviewed above (see Table I for a summary). We obtain the general structure of our formula from simple considerations and determine the numerical coefficients in order to recover the exact asymptotic expressions of the maximum mass in particular limits. We also show that the predictions from the Gaussian ansatz are in good agreement with the exact values. As a result, our formula should provide a relevant approximation of the maximum mass of relativistic boson stars for any value (positive or negative) of the self-interaction parameter.

The paper is organized as follows. In Sec. II, we recall the basic equations describing nonrelativistic self-gravitating BECs. In Sec. III, we discuss the exact mass-radius relation of nonrelativistic self-gravitating BECs obtained by solving the GPP equations numerically. In Sec. IV, we show that we can obtain an analytical approximation of the mass-radius relation from an f ansatz. We determine the coefficients of this relation so as to recover the exact results in particular limits. In Sec. V, we recall the expression of the exact maximum mass of general relativistic BECs obtained by solving the KGE equations numerically. In Secs. VI and VII, we obtain an analytical approximation of the maximum mass

¹⁹By an abuse of language, we will sometimes use the term axion star to designate the quantum core of axionic DM halos.

of self-gravitating BECs as a function of the scattering length a_s of the bosons for a repulsive or an attractive self-interaction. We determine the coefficients of this relation so as to recover the exact results in the noninteracting limit ($a_s = 0$), in the TF limit (for $a_s > 0$), and in the non-relativistic limit (for $a_s < 0$). In Sec. VIII, we summarize the main results of our study. In Sec. IX, we reexpress our results in terms of the dimensionless self-interaction constant λ or in terms of the axion decay constant f , and we discuss whether the collapse of the BEC star above the maximum mass leads to a black hole or a bosonova. In Sec. X, we apply our results to DM halos and inflaton clusters and discuss whether the solitonic core of these systems can become unstable in realistic situations. We conclude in Sec. XI. The Appendices provide complements to our main results. In particular, we develop interesting analogies between self-gravitating BECs and models of extended elementary particles.

II. NONRELATIVISTIC SELF-GRAVITATING BECs

In this section, we recall basic results applying to nonrelativistic self-gravitating BECs at $T = 0$ described by the GPP equations (see Refs. [265,290,320] for more details).

A. Gross-Pitaevskii-Poisson equations

We assume that DM is made of bosons (like the axion) in the form of BECs at $T = 0$. We use a nonrelativistic approach based on Newtonian gravity. The evolution of the wave function $\psi(\mathbf{r}, t)$ of a self-gravitating BEC is governed by the GPP equations

$$i\hbar \frac{\partial \psi}{\partial t} = -\frac{\hbar^2}{2m} \Delta \psi + \frac{4\pi a_s \hbar^2}{m^2} |\psi|^2 \psi + m\Phi \psi, \quad (1)$$

$$\Delta \Phi = 4\pi G |\psi|^2, \quad (2)$$

where $\Phi(\mathbf{r}, t)$ is the gravitational potential and m is the mass of the bosons.²⁰ The mass density of the BEC is $\rho(\mathbf{r}, t) = |\psi|^2$. The first term in Eq. (1) is the kinetic term, which accounts for the Heisenberg uncertainty principle. The second term takes into account the self-interaction of the bosons via a $|\psi|^4$ potential [see Eq. (B55)],

$$V(|\psi|^2) = \frac{2\pi a_s \hbar^2}{m^3} |\psi|^4, \quad (3)$$

where a_s is the scattering length of the bosons. The interaction between the bosons is repulsive when $a_s > 0$ and attractive when $a_s < 0$. The third term accounts for the self-gravity of the BEC.

²⁰The derivation of the GPP equations (1) and (2) from the KGE equations is discussed in Appendices B and C and references therein.

The GPP equations conserve the mass

$$M = \int |\psi|^2 d\mathbf{r} \quad (4)$$

and the energy

$$E_{\text{tot}} = \frac{\hbar^2}{2m^2} \int |\nabla \psi|^2 d\mathbf{r} + \frac{2\pi a_s \hbar^2}{m^3} \int |\psi|^4 d\mathbf{r} + \frac{1}{2} \int |\psi|^2 \Phi d\mathbf{r}, \quad (5)$$

which is the sum of the kinetic energy Θ , the internal energy $U = \int V(|\psi|^2) d\mathbf{r}$, and the gravitational energy W (i.e., $E_{\text{tot}} = \Theta + U + W$).

B. Madelung transformation

Writing the wave function as

$$\psi(\mathbf{r}, t) = \sqrt{\rho(\mathbf{r}, t)} e^{iS(\mathbf{r}, t)/\hbar}, \quad (6)$$

where $\rho(\mathbf{r}, t)$ is the mass density and $S(\mathbf{r}, t)$ is the action, and making the Madelung [289] transformation

$$\rho(\mathbf{r}, t) = |\psi|^2 \quad \text{and} \quad \mathbf{u} = \frac{\nabla S}{m}, \quad (7)$$

where $\mathbf{u}(\mathbf{r}, t)$ is the velocity field, the GPP equations (1) and (2) can be written under the form of hydrodynamic equations

$$\frac{\partial \rho}{\partial t} + \nabla \cdot (\rho \mathbf{u}) = 0, \quad (8)$$

$$\frac{\partial S}{\partial t} + \frac{(\nabla S)^2}{2m} + Q + \frac{4\pi a_s \hbar^2}{m^2} \rho + m\Phi = 0, \quad (9)$$

$$\frac{\partial \mathbf{u}}{\partial t} + (\mathbf{u} \cdot \nabla) \mathbf{u} = -\frac{1}{m} \nabla Q - \frac{1}{\rho} \nabla P - \nabla \Phi, \quad (10)$$

$$\Delta \Phi = 4\pi G \rho, \quad (11)$$

where

$$Q = -\frac{\hbar^2}{2m} \frac{\Delta \sqrt{\rho}}{\sqrt{\rho}} = -\frac{\hbar^2}{4m} \left[\frac{\Delta \rho}{\rho} - \frac{1}{2} \frac{(\nabla \rho)^2}{\rho^2} \right] \quad (12)$$

is the quantum potential taking into account the Heisenberg uncertainty principle,

$$h(\rho) = V'(\rho) = \frac{4\pi a_s \hbar^2}{m^3} \rho \quad (13)$$

is the enthalpy, and

$$P = \rho V'(\rho) - V(\rho) = \rho^2 \left[\frac{V(\rho)}{\rho} \right]' = \frac{2\pi a_s \hbar^2}{m^3} \rho^2 \quad (14)$$

is the pressure arising from the self-interaction of the bosons $V(\rho) = 2\pi a_s \hbar^2 \rho^2 / m^3$ (see Appendix B). This quadratic equation of state is a particular polytropic equation of state $P = K\rho^\gamma$ of index $\gamma = 2$ and polytropic constant $K = 2\pi a_s \hbar^2 / m^3$. The hydrodynamic equations (8)–(11) are called the quantum Euler-Poisson equations. Equation (8) is the continuity equation, Eq. (9) is the quantum Hamilton-Jacobi (or Bernoulli) equation, Eq. (10) is the quantum Euler equation, and Eq. (11) is the Poisson equation. In the TF limit where the quantum potential Q can be neglected (formally $\hbar = 0$),²¹ they become equivalent to the classical Euler-Poisson equations for a barotropic gas [340].

The quantum Euler equations conserve the mass

$$M = \int \rho d\mathbf{r} \quad (15)$$

and the energy

$$E_{\text{tot}} = \Theta_c + \Theta_Q + U + W, \quad (16)$$

which is the sum of the classical kinetic energy

$$\Theta_c = \int \rho \frac{\mathbf{u}^2}{2} d\mathbf{r}, \quad (17)$$

the quantum kinetic energy

$$\Theta_Q = \frac{\hbar^2}{8m^2} \int \frac{(\nabla\rho)^2}{\rho} d\mathbf{r} = \frac{1}{m} \int \rho Q d\mathbf{r}, \quad (18)$$

the internal energy

$$U = \int V(\rho) d\mathbf{r} = \int \rho \int^\rho \frac{P(\rho')}{\rho'^2} d\rho' d\mathbf{r} = \int \frac{2\pi a_s \hbar^2}{m^3} \rho^2 d\mathbf{r}, \quad (19)$$

and the gravitational energy

$$W = \frac{1}{2} \int \rho \Phi d\mathbf{r}. \quad (20)$$

At equilibrium, the classical (macroscopic) kinetic energy vanishes and we get

$$E_{\text{tot}} = \Theta_Q + U + W. \quad (21)$$

²¹We note that \hbar appears in the quantum potential Q and in the self-interaction constant $g = 4\pi a_s \hbar^2 / m^3$. The TF limit (corresponding to $\hbar \rightarrow 0$ with fixed $4\pi a_s \hbar^2 / m^3$) amounts to neglecting Q but not g .

C. Equilibrium states

A stationary solution of GPP equations is of the form

$$\psi(\mathbf{r}, t) = \phi(\mathbf{r}) e^{-iEt/\hbar}, \quad (22)$$

where $\phi(\mathbf{r}) = \sqrt{\rho(\mathbf{r})}$ and E are real. Substituting Eq. (22) into Eqs. (1) and (2), we obtain the eigenvalue problem

$$-\frac{\hbar^2}{2m} \Delta\phi + \frac{4\pi a_s \hbar^2}{m^2} \phi^3 + m\Phi\phi = E\phi, \quad (23)$$

$$\Delta\phi = 4\pi G\phi^2, \quad (24)$$

determining the eigenfunctions $\phi_n(\mathbf{r})$ and the eigenvalues E_n . For the fundamental mode (the one with the lowest energy) the wave function $\phi(r)$ is spherically symmetric and has no node so that the density profile decreases monotonically with the radial distance. Dividing Eq. (23) by ϕ and using $\rho = \phi^2$, we obtain the identity

$$Q + \frac{4\pi a_s \hbar^2}{m^2} \rho + m\Phi = E, \quad (25)$$

which can also be obtained from the quantum Hamilton-Jacobi (or Bernoulli) equation (9) by setting $S = -Et$.

Equivalent results can be obtained from the hydrodynamic equations (8)–(11). Indeed, the condition of quantum hydrostatic equilibrium, corresponding to a steady state of the quantum Euler equation (10), reads

$$\frac{\rho}{m} \nabla Q + \nabla P + \rho \nabla \Phi = \mathbf{0}. \quad (26)$$

Dividing Eq. (26) by ρ and integrating the resulting expression with the help of Eq. (14), we recover Eq. (25), where E appears as a constant of integration. On the other hand, combining Eq. (26) with the Poisson equation (11), we obtain the fundamental differential equation of quantum hydrostatic equilibrium

$$\frac{\hbar^2}{2m^2} \Delta \left(\frac{\Delta\sqrt{\rho}}{\sqrt{\rho}} \right) - \frac{4\pi a_s \hbar^2}{m^3} \Delta\rho = 4\pi G\rho. \quad (27)$$

This equation describes the balance between the quantum potential taking into account the Heisenberg uncertainty principle, the pressure due to the self-interaction of the bosons, and the self-gravity.

These results can also be obtained from an energy principle. Indeed, one can show (see Appendix B of [267]) that (i) an equilibrium state of the GPP equations is an extremum of energy E_{tot} at fixed mass M and that (ii) an equilibrium state is stable if, and only if, it is a minimum of

energy at fixed mass. We are led, therefore, to considering the minimization problem

$$\min\{E_{\text{tot}} \mid M \text{ fixed}\}. \quad (28)$$

Writing the variational problem for the first variations (extremization problem) as

$$\delta E_{\text{tot}} - \frac{\mu}{m} \delta M = 0, \quad (29)$$

where μ (global chemical potential) is a Lagrange multiplier taking into account the mass constraint, we obtain $\mathbf{u} = \mathbf{0}$ and

$$Q + \frac{4\pi a_s \hbar^2}{m^2} \rho + m\Phi = \mu. \quad (30)$$

This relation is equivalent to Eq. (25) provided that we make the identification $E = \mu$. Therefore, the eigenenergy E coincides with the global chemical potential μ . Equation (30) is also equivalent to the condition of quantum hydrostatic equilibrium (26). Therefore, an extremum of energy at fixed mass is an equilibrium state of the GPP equations. Furthermore, among all possible equilibria, only minima of energy at fixed mass are dynamically stable with respect to the GPP equations (maxima or saddle points are linearly unstable). The stability of an equilibrium state can be established by studying the sign of the second variations of energy or by solving an equation of pulsations. These methods are equivalent and lead to a complicated eigenvalue problem (see Appendix B of [267]). The stability of an equilibrium state can also be directly established, without having to solve an eigenvalue problem, by plotting the series of equilibria and using the Poincaré [46,47] turning point criterion applied to the curve $\mu(M)$, the Wheeler [30] theorem applied to the curve $M(R)$, or the Whitney theorem [44] applied to the curve $E_{\text{tot}}(M)$ (see Refs. [109,265,290] for a specific application of these methods to the case of axion stars).

III. EXACT MASS-RADIUS RELATION OF NONRELATIVISTIC SELF-GRAVITATING BECs

The fundamental equation (27) of quantum hydrostatic equilibrium for a self-gravitating BEC has been solved numerically (exactly) in our previous paper [290] for an arbitrary $|\psi|^4$ self-interaction (repulsive or attractive). The nodeless solution describes a compact gravitational quantum object (soliton/BEC) in its ground state. From this solution, we have determined the exact mass-radius relation of nonrelativistic BEC stars (see Figs. 1 and 2 below). Here, we recall some exact results obtained in particular limits that will be useful in the following.

A. Noninteracting bosons

For noninteracting bosons ($a_s = 0$), the equation of quantum hydrostatic equilibrium (27) reduces to

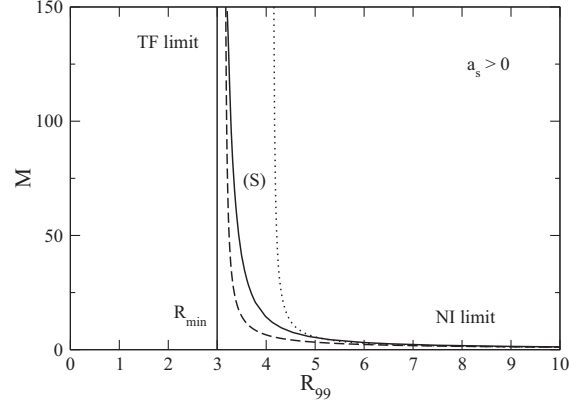


FIG. 1. Mass-radius relation of self-gravitating BECs with $a_s > 0$ [full line, exact result [290]; dotted line, Gaussian ansatz [265]; dashed line, fit from Eq. (53) with $a = 9.946$ and $b = \pi$]. The mass is normalized by $M_a = \hbar/\sqrt{Gma_s}$ and the radius by $R_a = (a_s \hbar^2/Gm^3)^{1/2}$.

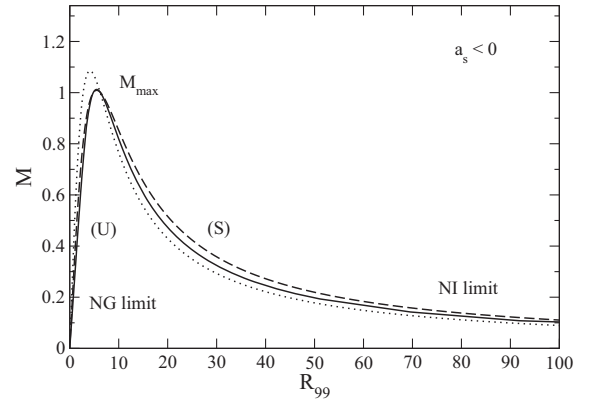


FIG. 2. Mass-radius relation of self-gravitating BECs with $a_s < 0$ [full line, exact result [290]; dotted line, Gaussian ansatz [265]; dashed line, fit from Eq. (53) with $a = 11.1$ and $b = 5.5$]. The mass is normalized by $M_a = \hbar/\sqrt{Gm|a_s|}$ and the radius by $R_a = (|a_s| \hbar^2/Gm^3)^{1/2}$.

$$\frac{\hbar^2}{2m^2} \Delta \left(\frac{\Delta \sqrt{\rho}}{\sqrt{\rho}} \right) = 4\pi G\rho. \quad (31)$$

It can be solved numerically to obtain the density profile. The mass-radius relation is given by [290,291]

$$M = 9.95 \frac{\hbar^2}{Gm^2 R_{99}}, \quad (32)$$

where R_{99} represents the radius containing 99% of the mass (the density profile extends to infinity, so it has not a compact support). The mass decreases as the radius increases. The equilibrium states are all stable.

Remark.—The scaling of the mass-radius relation (32) can be understood by writing that the radius R of the BEC is on the order of the de Broglie wavelength of the bosons

$\lambda_{\text{dB}} = \hbar/(mv)$ constructed with the virial velocity $v \sim (GM/R)^{1/2}$.

B. Bosons with a repulsive self-interaction

For bosons with a repulsive self-interaction ($a_s > 0$), the exact mass-radius relation is represented in Fig. 1. The mass decreases as the radius increases. In the TF limit $M \gg M_a = \hbar/\sqrt{Gma_s}$, where the quantum potential can be neglected, the system is equivalent to a polytrope of index $\gamma = 2$. The equation of quantum hydrostatic equilibrium (27) reduces to

$$\Delta\rho + \frac{Gm^3}{a_s\hbar^2}\rho = 0. \quad (33)$$

This equation is equivalent to the Lane-Emden equation of index $n = 1$ [292]. It can be solved analytically leading to a density profile of the form²²

$$\rho(r) = \frac{\rho_0 R_{\text{TF}}}{\pi r} \sin\left(\frac{\pi r}{R_{\text{TF}}}\right). \quad (34)$$

In the TF limit, the equilibrium states have a unique radius given by [81,265,293–297]

$$R_{\text{TF}} = \pi \left(\frac{a_s \hbar^2}{Gm^3} \right)^{1/2}, \quad (35)$$

which is independent of their mass M . This is the minimum radius of self-gravitating BECs with a repulsive self-interaction. In the noninteracting (NI) limit $M \ll M_a = \hbar/\sqrt{Gma_s}$ and $R \gg R_{\text{TF}}$, we recover Eq. (32).

Remark.—Let us recall some basic results valid in the TF limit [265] that we shall need later. The central density of the self-gravitating BEC is determined by its mass according to

$$\rho_0 = \frac{\pi M}{4R_{\text{TF}}^3}. \quad (36)$$

Its total energy is

$$E_{\text{tot}} = -\frac{GM^2}{2R_{\text{TF}}}. \quad (37)$$

When slightly displaced from its equilibrium configuration, the BEC oscillates with a pulsation that is on the order of the inverse dynamical time (see [265] for more precise results)

$$t_D \sim \frac{1}{\sqrt{G\rho_0}} \sim \left(\frac{R_{\text{TF}}^3}{GM} \right)^{1/2}. \quad (38)$$

²²This analytical solution was first given by Ritter [341] in the context of self-gravitating polytropic spheres. It was previously used by Laplace [342] to model the Earth's interior (see footnote 10 in [267]).

C. Bosons with an attractive self-interaction

For bosons with an attractive self-interaction ($a_s < 0$), the exact mass-radius relation is represented in Fig. 2. The mass increases as the radius increases, reaches a maximum value [265,290]

$$M_{\text{max}}^{\text{NR}} = 1.012 \frac{\hbar}{\sqrt{Gm|a_s|}} \quad (39)$$

at

$$R_{99}^* = 5.5 \left(\frac{|a_s| \hbar^2}{Gm^3} \right)^{1/2}, \quad (40)$$

and decreases. $M_{\text{max}}^{\text{NR}}$ is the maximum mass of dilute axion stars [306]. There is no equilibrium state with $M > M_{\text{max}}^{\text{NR}}$. In that case, the BEC is expected to collapse [307]. The outcome of the collapse (dense axion star, black hole, bosonova, axion drops, etc.) is discussed in [109,307–313,318,319]. For $M < M_{\text{max}}$, there are two possible equilibrium states with the same mass. The equilibrium states with $R > R_{99}^*$ are stable and the equilibrium states with $R < R_{99}^*$ are unstable. This can be shown by using the Poincaré criterion, the Wheeler theorem, the Whitney theorem, or by investigating the sign of the squared pulsation [109,265,290]. We note that the maximum mass is connected to the minimum stable radius by

$$M_{\text{max}}^{\text{NR}} = 5.57 \frac{\hbar^2}{Gm^2 R_{99}^*}, \quad (41)$$

which presents the same scaling as Eq. (32).

In the nongravitational (NG) limit $M \ll M_{\text{max}}^{\text{NR}}$ and $R \ll R_{99}^*$, the equation of quantum hydrostatic equilibrium (27) reduces to

$$-\frac{\hbar^2}{2m} \frac{\Delta\sqrt{\rho}}{\sqrt{\rho}} + \frac{4\pi a_s \hbar^2}{m^2} \rho = E. \quad (42)$$

This equation is equivalent to the ordinary (nongravitational) GP equation with an attractive self-interaction. It can be solved numerically to obtain the density profile. The mass-radius relation is given by (see, e.g., [290])

$$M = 0.275 \frac{m R_{99}}{|a_s|}. \quad (43)$$

These equilibrium states are unstable. In the NI limit $M \ll M_{\text{max}}^{\text{NR}}$ and $R \gg R_{99}^*$, we recover Eq. (32). These equilibrium states are stable.

IV. APPROXIMATE MASS-RADIUS RELATION OF NONRELATIVISTIC SELF-GRAVITATING BECs FROM THE f ANSATZ

In Ref. [265], using a Gaussian ansatz for the wave function, we have obtained an approximate analytical expression of the mass-radius relation of self-gravitating BECs. In Ref. [267], we have shown that the form of this relation is independent of the precise shape of the wave function. The shape of the wave function just determines the coefficients entering in this relation. We have then proposed to determine these coefficients by matching the asymptotic expressions of the analytical (approximate) mass-radius relation with the asymptotic expressions of the exact (numerical) mass-radius relation obtained in [290]. We briefly recall this procedure below.

A. f ansatz

Stable BEC stars (axion stars or the quantum core of BECDM halos) correspond to minima of energy E_{tot} at fixed mass M . We can obtain an approximate analytical form of the mass-radius relation by making an ansatz for the wave function.²³ To be as general as possible, we consider an ansatz of the form (that we call f ansatz)

$$\rho(\mathbf{r}, t) = \frac{M}{R(t)^3} f\left[\frac{\mathbf{r}}{R(t)}\right], \quad (44)$$

where $f(\mathbf{x})$ is an arbitrary (physical) function. We impose $\int f(\mathbf{x}) d\mathbf{x} = 1$ to satisfy the normalization condition (or the conservation of mass). On the other hand, the gravitational potential can be determined from the Poisson equation (11). Using Eq. (44), we obtain

$$\Phi(\mathbf{r}, t) = \frac{GM}{R(t)} g\left[\frac{\mathbf{r}}{R(t)}\right], \quad (45)$$

where $g(\mathbf{x})$ is the solution of

$$\Delta g = 4\pi f(\mathbf{x}). \quad (46)$$

We can now use the ansatz (44)–(46) to determine the different functionals that appear in the energy from Eq. (16). We find

$$\Theta_Q = \sigma \frac{\hbar^2 M}{m^2 R^2} \quad \text{with} \quad \sigma = \frac{1}{8} \int \frac{(\nabla f)^2}{f} d\mathbf{x}, \quad (47)$$

$$U = \zeta \frac{2\pi a_s \hbar^2 M^2}{m^3 R^3} \quad \text{with} \quad \zeta = \int f^2(\mathbf{x}) d\mathbf{x}, \quad (48)$$

$$W = -\nu \frac{GM^2}{R} \quad \text{with} \quad \nu = -\frac{1}{2} \int f(\mathbf{x}) g(\mathbf{x}) d\mathbf{x}. \quad (49)$$

²³Here, we restrict ourselves to the equilibrium state, so we just need to make an ansatz for the density profile. See Sec. 8 of [320] for a more general study.

If we use a Gaussian ansatz $f(\mathbf{x}) = \frac{1}{\pi^{3/2}} e^{-x^2}$, the values of the coefficients are $\sigma_G = 3/4$, $\zeta_G = 1/(2\pi)^{3/2}$, and $\nu_G = 1/\sqrt{2\pi}$ [265].

With the ansatz from Eq. (44), the total energy can be written as

$$E_{\text{tot}}(R) = \sigma \frac{\hbar^2 M}{m^2 R^2} - \nu \frac{GM^2}{R} + \zeta \frac{2\pi a_s \hbar^2 M^2}{m^3 R^3}. \quad (50)$$

At equilibrium, the condition $E'_{\text{min}}(R) = 0$ (extremum of energy) gives the mass-radius relation²⁴

$$-2\sigma \frac{\hbar^2 M}{m^2 R^3} + \nu \frac{GM^2}{R^2} - 6\pi\zeta \frac{a_s \hbar^2 M^2}{m^3 R^4} = 0 \quad (51)$$

or, equivalently,

$$M = \frac{\frac{2\sigma}{\nu} \frac{\hbar^2}{Gm^2 R}}{1 - \frac{6\pi\zeta}{\nu} \frac{a_s \hbar^2}{Gm^3 R^2}}. \quad (52)$$

The BEC is stable provided that $E''_{\text{tot}}(R) > 0$, which corresponds to the requirement that the equilibrium state is a minimum of energy or, equivalently, that the squared pulsation is positive [265].

We see that the form of the analytical mass-radius relation is independent of the ansatz. Indeed, it is always given by

$$M = \frac{a \frac{\hbar^2}{Gm^2 R}}{1 - b^2 \frac{a_s \hbar^2}{Gm^3 R^2}}, \quad (53)$$

where only the values of the coefficients a and b depend on the ansatz. Following Ref. [267], we shall determine the coefficients a and b so as to recover the exact mass-radius relation in some particular limits. We finally note that the mass-radius relation can be written under the normalized form

$$\frac{M}{M_s} = \frac{\frac{R_s}{R}}{1 \mp \left(\frac{R_s}{R}\right)^2}, \quad (54)$$

with $R_s = b(|a_s| \hbar^2 / Gm^3)^{1/2}$ and $M_s = (a/b) \hbar / \sqrt{Gm|a_s|}$ (the upper sign corresponds to a repulsive self-interaction and the lower sign to an attractive self-interaction).

Remark.—With the Gaussian ansatz, we get $a_G^* = 2\sigma_G / \nu_G = 3.76$ and $b_G^* = (6\pi\zeta_G / \nu_G)^{1/2} = 1.73$. However, below, we shall identify the radius R with R_{99} , not with the radius R of the f ansatz defined in Eq. (44). Since $R_{99} = 2.38167R$ with the Gaussian ansatz [265], we obtain $a_G = 2.38167a_G^* = 8.96$ and $b_G = 2.38167b_G^* = 4.12$ to

²⁴As shown in [265,307,320], the mass-radius relation can also be obtained from the equilibrium virial theorem or from the Lagrangian formalism.

be compared with the more exact values of a and b found below [see Eqs. (57) and (60)].

B. Noninteracting bosons

For noninteracting bosons ($a_s = 0$), the mass-radius relation from Eq. (53) reduces to

$$M = a \frac{\hbar^2}{Gm^2 R}. \quad (55)$$

If we identify R with the radius R_{99} containing 99% of the mass and compare Eq. (55) with the exact mass-radius relation of noninteracting self-gravitating BECs from Eq. (32), we get $a = 9.946$.

Remark.—The density profile of a noninteracting self-gravitating BEC (soliton) is often fitted by the empirical profile introduced by Schive *et al.* [268,269]. In Ref. [321], we have shown that a Gaussian profile [265], which is simpler, also fits the soliton quite well up to the halo radius (see Fig. 2 of [321]). A Gaussian profile with the mass-radius relation from Eq. (53) may also provide a convenient approximation of the density profile of self-gravitating BECs with repulsive or attractive self-interaction.

C. Repulsive self-interaction

For bosons with a repulsive self-interaction ($a_s > 0$), in the TF limit ($\hbar \rightarrow 0$ with fixed $g = 4\pi a_s \hbar^2 / m^3$), the mass-radius relation from Eq. (53) reduces to

$$R = b \left(\frac{a_s \hbar^2}{Gm^3} \right)^{1/2}. \quad (56)$$

If we identify R with the radius at which the density vanishes and compare Eq. (56) with the exact radius of self-gravitating BECs in the TF limit from Eq. (35), we get $b = \pi$. On the other hand, in the noninteracting limit, we recover the result from Eq. (55) leading to $a = 9.946$. We shall adopt these values of a and b in the repulsive case (see Fig. 1 for a comparison with the exact result). Therefore, we take

$$a = 9.946, \quad b = \pi \quad (\text{repulsive}). \quad (57)$$

D. Attractive self-interaction

For bosons with an attractive self-interaction ($a_s < 0$), the mass-radius relation from Eq. (53) displays a maximum mass

$$M_{\max} = \frac{a}{2b} \frac{\hbar}{\sqrt{Gm|a_s|}} \quad \text{at } R_* = b \left(\frac{|a_s| \hbar^2}{Gm^3} \right)^{1/2}. \quad (58)$$

They are connected by

$$M_{\max} = \frac{a}{2} \frac{\hbar^2}{Gm^2 R_*}. \quad (59)$$

If we identify R_* with the radius $(R_*)_{99}$ containing 99% of the mass and compare Eq. (58) with the exact values of the maximum mass and of the corresponding radius from Eqs. (39) and (40), we get $b = 5.5$ and $a/2b = 1.012$, leading to $a = 11.1$. We shall adopt these values in the attractive case (see Fig. 2 for a comparison with the exact result). Therefore, we take

$$a = 11.1, \quad b = 5.5 \quad (\text{attractive}). \quad (60)$$

We note that the value $a = 11.1$ obtained from the maximum mass is relatively close to the value $a = 9.946$ obtained in the noninteracting limit (see Sec. IV B). In the nongravitational limit, the mass-radius relation from Eq. (53) reduces to

$$M = \frac{a}{b^2} \frac{mR}{|a_s|}. \quad (61)$$

The value $a/b^2 = 0.367$ obtained from the maximum mass is relatively close to the exact value 0.275 from Eq. (43). This is a consistency check.

V. EXACT MAXIMUM MASS OF BOSON STARS DUE TO GENERAL RELATIVITY

In this section, we recall the expression of the maximum mass of general relativistic BECs (boson stars) at $T = 0$ described by the KGE equations. Above that maximum mass, the system collapses toward a black hole.

A. Noninteracting bosons

The maximum mass and the minimum radius of a noninteracting boson star set by general relativity are [1,2]

$$M_{\max}^{\text{GR}} = 0.633 \frac{\hbar c}{Gm}, \quad R_*^{\text{GR}} = 6.03 \frac{\hbar}{mc}. \quad (62)$$

They satisfy the relation

$$R_*^{\text{GR}} = 9.53 \frac{GM_{\max}}{c^2}. \quad (63)$$

The compactness at the maximum mass is $\mathcal{C} \equiv GM_{\max} / R_*^{\text{GR}} c^2 = 0.105$.²⁵ These scalings can be obtained as

²⁵We have adopted the value of the radius $R_*^{\text{GR}} = 6.03 \hbar / mc$ given by Seidel and Suen [35]. This is the radius containing 95% of the mass. The radius containing 99% of the mass is larger, implying a smaller compactness. For example, Choi *et al.* [343] consider the radius containing 99% of the mass and find a maximum compactness $\mathcal{C} \simeq 0.08$ (see also [344]). This yields $R_*^{\text{GR}} = 7.91 \hbar / mc$.

explained in Appendix B.2 of [265] (see also Secs. VI and VII). The Kaup radius is on the order of the Compton wavelength of the boson.

B. Repulsive self-interaction in the TF limit

The maximum mass and the minimum radius of a boson star with a repulsive $|\varphi|^4$ self-interaction in the TF limit set by general relativity are [58,86]

$$M_{\max}^{\text{GR}} = 0.307 \frac{\hbar c^2 \sqrt{a_s}}{(Gm)^{3/2}}, \quad R_* = 1.92 \left(\frac{a_s \hbar^2}{Gm^3} \right)^{1/2}. \quad (64)$$

They satisfy the relation

$$R_*^{\text{GR}} = 6.25 \frac{GM_{\max}}{c^2}. \quad (65)$$

The compactness at the maximum mass is $\mathcal{C} \equiv GM_{\max}/R_*^{\text{GR}} c^2 = 0.16$ [86]. These scalings can be obtained as explained in Appendix B 3 of [265] (see also Sec. VI). The critical radius R_* is of the same order as the minimum radius R_{TF} of a nonrelativistic self-interacting BEC in the TF approximation (see Sec. III B).

Remark.—In the TF limit, a self-interacting complex SF is equivalent to a fluid with a barotropic equation of state $P(\epsilon)$ determined by the potential $V(|\varphi|^2)$ (see Appendix B). In the case of a repulsive $|\varphi|^4$ self-interaction [see Eq. (B76)], the equation of state is given by Eq. (B83). The mass-radius relation of the boson star, and its maximum mass (64), may therefore be obtained by solving the Oppenheimer-Volkoff equation of hydrostatic equilibrium, as done in Ref. [86], instead of solving the KGE equations, as done in Ref. [58].

VI. RELATIVISTIC CORRECTIONS AS WE APPROACH THE SCHWARZSCHILD RADIUS

A relativistic star becomes dynamically unstable when its radius approaches the Schwarzschild radius $R_S = 2GM/c^2$ [41]. The condition $R \sim R_S$ combined with the nonrelativistic mass-radius relation of the star determines the order of magnitude of its maximum mass M_{\max}^{GR} due to general relativity (see Appendix B of [265]). Let us apply this argument to BEC stars (see Figs. 3 and 4 for an illustration).

Substituting $R = kGM/c^2$ with $k \sim 1$ into Eq. (53), we obtain after simplification

$$M_{\max} = \left(\frac{a}{k} \right)^{1/2} \frac{\hbar c}{Gm} \sqrt{1 + \frac{b^2 a_s c^2}{ak Gm}}. \quad (66)$$

This equation is of the form

$$M_{\max} = A \frac{\hbar c}{Gm} \sqrt{1 + B \frac{a_s c^2}{Gm}}, \quad (67)$$

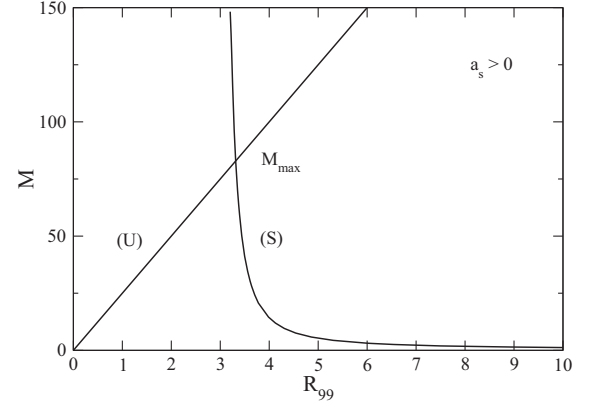


FIG. 3. Graphical construction determining the maximum mass of self-gravitating BECs with $a_s > 0$ due to general relativity. We use the normalization of Fig. 1. The maximum mass M_{\max} is qualitatively obtained by taking the intersection between the mass-radius relation $M(R)$ of Newtonian BECs and the Schwarzschild line $R = kGM/c^2$ (in scaled variables its slope is $kGm/|a_s|c^2$).

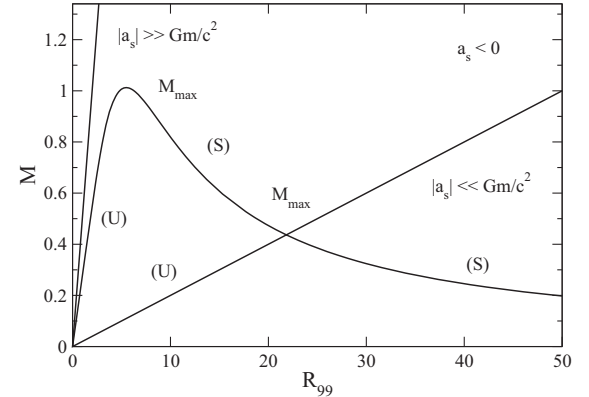


FIG. 4. Same as Fig. 3 for $a_s < 0$. An intersection exists only when $|a_s|c^2/Gm$ is sufficiently small (see the main text for details). When $|a_s|c^2/Gm$ is large, the maximum mass is given by the nonrelativistic limit (39) or by relativistic corrections in the quantum potential (see Sec. VII).

with $A = (a/k)^{1/2}$ and $B = b^2/ak$. The radius corresponding to the maximum mass is

$$R_* = \frac{kGM_{\max}}{c^2}. \quad (68)$$

Substituting Eqs. (66) and (67) into Eq. (68), we get

$$R_* = \sqrt{ka} \frac{\hbar}{mc} \sqrt{1 + \frac{b^2 a_s c^2}{ak Gm}} \quad (69)$$

and

$$R_* = kA \frac{\hbar}{mc} \sqrt{1 + B \frac{a_s c^2}{Gm}}. \quad (70)$$

If we define the compactness of the relativistic star at the maximum mass by

$$\mathcal{C} = \frac{GM_{\max}}{R_* c^2}, \quad (71)$$

we obtain

$$\mathcal{C} = \frac{1}{k}. \quad (72)$$

By construction, our approximations assume that the compactness is independent of the value of a_s . Of course, this is not rigorously true. However, this is a reasonable approximation, as we can see by considering the exact values of the compactness of boson stars in two extreme limits (see Sec. V), namely, the noninteracting limit ($\mathcal{C} = 0.105$) and the TF limit ($\mathcal{C} = 0.16$).

We shall now determine the values of A and B in Eq. (67) in order to match the exact results from Secs. VA and VB.

A. Noninteracting limit

In the noninteracting limit ($a_s = 0$), Eqs. (66)–(70) reduce to

$$M_{\max} = \left(\frac{a}{k}\right)^{1/2} \frac{\hbar c}{Gm} = A \frac{\hbar c}{Gm} \quad (73)$$

and

$$R_* = \sqrt{ka} \frac{\hbar}{mc} = kA \frac{\hbar}{mc}. \quad (74)$$

This returns the maximum mass (62) of miniboson stars [1]. Comparing Eqs. (73) and (74) with Eqs. (62) and (63), we get $A = 0.633$ and $k = 1/\mathcal{C} = 9.53$.

Remark.—With these values of A and k we obtain $a = kA^2 = 3.82$ instead of the value $a = 9.946$ (or $a_G = 8.96$) computed in Sec. IV.

B. TF limit

For boson stars with a repulsive self-interaction in the TF limit ($\hbar \rightarrow 0$ with fixed $g = 4\pi a_s \hbar^2/m^3$), Eqs. (66)–(70) reduce to

$$M_{\max} = \frac{b}{k} \left(\frac{a_s \hbar^2 c^4}{G^3 m^3}\right)^{1/2} = A\sqrt{B} \left(\frac{a_s \hbar^2 c^4}{G^3 m^3}\right)^{1/2} \quad (75)$$

and

$$R_* = b \left(\frac{a_s \hbar^2}{Gm^3}\right)^{1/2} = kA\sqrt{B} \left(\frac{a_s \hbar^2}{Gm^3}\right)^{1/2}. \quad (76)$$

This returns the maximum mass (64) of massive boson stars [58,86]. Note that R_* is independent of k . Comparing Eqs. (75) and (76) with Eqs. (64) and (65), we get $A\sqrt{B} = 0.307$ and $k = 1/\mathcal{C} = 6.25$. Taking $A = 0.633$ from Sec. VI A, we get $B = 0.235$.

Remark.—With these values of A and k we obtain $a = kA^2 = 2.50$ and $b = kA\sqrt{B} = 1.92$ instead of the values $a = 9.946$ and $b = \pi$ (or $a_G = 8.96$ and $b_G = 4.12$) computed in Sec. IV.

C. Interpolation formulas

Using the previous results, we can obtain simple interpolation formulas for the maximum mass and minimum radius of boson stars. We shall take

$$A = 0.633, \quad B = 0.235, \quad k = 6.25. \quad (77)$$

In this manner, the asymptotic expressions of the maximum mass are exact. The value of the radius is also exact in the TF limit. By contrast, the value of the radius is not exact (but approximately correct) for noninteracting bosons because of the slow change of compactness with the self-interaction, which is not taken into account in our approach. We propose therefore the interpolation formulas

$$M_{\max} = 0.633 \frac{\hbar c}{Gm} \sqrt{1 + 0.235 \frac{a_s c^2}{Gm}}, \quad (78)$$

$$R_* = 3.96 \frac{\hbar}{mc} \sqrt{1 + 0.235 \frac{a_s c^2}{Gm}}. \quad (79)$$

We note that these expressions are defined only for $a_s > -4.25Gm/c^2$ (see Fig. 4). This suggests that the present treatment is only reliable for positive values of the scattering length. This is because the maximum mass of boson stars with an attractive self-interaction ($a_s < 0$) is essentially a nonrelativistic result [265]. Therefore, relativistic corrections in the maximum mass do not come from the fact that the radius of the star approaches the Schwarzschild radius, but rather from relativistic corrections arising in the quantum potential as discussed in Sec. VII below.

For $a_s \rightarrow 0$, Eqs. (78) and (79) reduce to

$$M_{\max} \simeq 0.633 \frac{\hbar c}{Gm} \left(1 + 0.118 \frac{a_s c^2}{Gm}\right), \quad (80)$$

$$R_* \simeq 3.96 \frac{\hbar}{mc} \left(1 + 0.118 \frac{a_s c^2}{Gm}\right). \quad (81)$$

D. Improved interpolation formulas

We can improve the preceding interpolation formulas by allowing the parameter B to be different in the expressions (67) and (70) determining the maximum mass and the corresponding radius. We write

$$M_{\max} = A \frac{\hbar c}{Gm} \sqrt{1 + B \frac{a_s c^2}{Gm}}, \quad (82)$$

$$R_* = A' \frac{\hbar}{mc} \sqrt{1 + B' \frac{a_s c^2}{Gm}}, \quad (83)$$

and we determine the constants A , B , A' , and B' so as to reproduce the exact asymptotic behaviors from Eqs. (62) and (64). In this manner, we obtain

$$A = 0.633, \quad B = 0.235, \quad A' = 6.03, \quad B' = 0.101, \quad (84)$$

leading to

$$M_{\max} = 0.633 \frac{\hbar c}{Gm} \sqrt{1 + 0.235 \frac{a_s c^2}{Gm}}, \quad (85)$$

$$R_* = 6.03 \frac{\hbar}{mc} \sqrt{1 + 0.101 \frac{a_s c^2}{Gm}}. \quad (86)$$

This gives a maximum compactness

$$\mathcal{C} = 0.105 \frac{\sqrt{1 + 0.235 \frac{a_s c^2}{Gm}}}{\sqrt{1 + 0.101 \frac{a_s c^2}{Gm}}}, \quad (87)$$

depending on a_s , and going from $\mathcal{C} = 0.105$ in the noninteracting limit $a_s = 0$ to $\mathcal{C} = 0.160$ in the TF limit $a_s \rightarrow +\infty$.

VII. RELATIVISTIC CORRECTIONS IN THE QUANTUM POTENTIAL

A. Relativistic Hamiltonian

In the weak gravity limit, the relativistic Hamiltonian is given by $H = \int_0^{+\infty} T_0^0 4\pi r^2 dr$, where the time-time component T_0^0 of the energy-momentum tensor is given by Eq. (B53). If we introduce the pseudo-wave-function $\psi(\mathbf{r}, t) = e^{-iEt/\hbar} \phi(\mathbf{r})$, where E includes relativistic corrections, one can show [343,345] that the Hamiltonian decomposes into $H = Mc^2 + H_{\text{NR}} + H_{\text{R}}$, where the first term is the rest-mass energy (with $M = Nm$), the second term is the nonrelativistic Hamiltonian, and the third term is the relativistic correction to the kinetic energy (or quantum potential). From Eq. (B53), we see that the kinetic energy is equal to

$$H_{\text{kin}} = \frac{\hbar^2}{2m^2} \int \left(1 + \frac{2\Phi}{c^2}\right) |\nabla\psi|^2 d\mathbf{r}. \quad (88)$$

Consequently, the relativistic correction to the kinetic energy is

$$H_{\text{R}} = \frac{\hbar^2}{m^2 c^2} \int \Phi |\nabla\psi|^2 d\mathbf{r}. \quad (89)$$

Using the hydrodynamic representation of the SF (see Sec. II B) and ignoring the rest-mass term, which is just a constant, the total energy taking into account relativistic corrections in the quantum potential is $E_{\text{tot}} = E_{\text{NR}} + E_{\text{R}}$, where E_{NR} is given by Eq. (16) and

$$E_{\text{R}} = \frac{\hbar^2}{m^2 c^2} \int (\nabla\sqrt{\rho})^2 \Phi d\mathbf{r}. \quad (90)$$

Using the f ansatz of Sec. IV, we obtain

$$E_{\text{R}} = \frac{\hbar^2 GM^2}{m^2 c^2 R^3} \int (\nabla\sqrt{f})^2 g d\mathbf{x}. \quad (91)$$

Since the value of the integral is negative, we can write

$$E_{\text{R}} = -\chi \frac{\hbar^2 GM^2}{m^2 c^2 R^3} \text{ with } \chi = - \int (\nabla\sqrt{f})^2 g d\mathbf{x} > 0. \quad (92)$$

If we use a Gaussian ansatz, we get $\chi_G \simeq 0.997$ (see Appendix A).

Combining Eqs. (50) and (92), we find that the total energy is

$$E_{\text{tot}}(R) = \sigma \frac{\hbar^2 M}{m^2 R^2} - \nu \frac{GM^2}{R} + \zeta \frac{2\pi a_s \hbar^2 M^2}{m^3 R^3} - \chi \frac{\hbar^2 GM^2}{m^2 c^2 R^3}. \quad (93)$$

Remarkably, the scaling of the relativistic correction E_{R} is the same as the scaling of the internal energy U arising from the self-interaction of the bosons (for a $|\varphi|^4$ self-interaction). As a result, the total energy of a relativistic BEC star can be rewritten as

$$E_{\text{tot}}(R) = \sigma \frac{\hbar^2 M}{m^2 R^2} - \nu \frac{GM^2}{R} + \zeta \frac{2\pi a_s \hbar^2 M^2}{m^3 R^3} \left(1 - \kappa \frac{Gm}{a_s c^2}\right) \quad (94)$$

with

$$\kappa = \frac{\chi}{2\pi\zeta}. \quad (95)$$

If we use a Gaussian ansatz, we get $\kappa_G = 2.50$. We see that the results of the nonrelativistic study [265] remain valid provided that we make the substitution

$$a_s \rightarrow a_s \left(1 - \kappa \frac{Gm}{a_s c^2}\right) \equiv a_s^*. \quad (96)$$

In particular, according to Eqs. (53) and (96), the mass-radius relation of relativistic BEC stars is

$$M = \frac{a \frac{\hbar^2}{Gm^2 R}}{1 - b^2 \frac{a_s \hbar^2}{Gm^2 R^2} \left(1 - \kappa \frac{Gm}{a_s c^2}\right)}. \quad (97)$$

Since we have used scaled variables, Figs. 1 and 2 remain the same. We just have to replace a_s by a_s^* in the normalization. There is a critical scattering length

$$(a_s)_c = \kappa \frac{Gm}{c^2} = \kappa \frac{r_S}{2}, \quad (98)$$

where $r_S = 2Gm/c^2$ is the Schwarzschild (gravitational) radius of the bosons [346]. When $a_s = (a_s)_c$, the effective scattering length vanishes ($a_s^* = 0$). When $a_s \geq (a_s)_c$ (i.e., $a_s^* \geq 0$), the mass-radius relation is monotonic like in Fig. 1. When $a_s < (a_s)_c$ (i.e., $a_s^* < 0$), it displays a maximum mass like in Fig. 2. Therefore, when relativistic corrections are taken into account in the quantum potential, we find the existence of a maximum mass not only when $a_s < 0$ but also when $0 \leq a_s < \kappa Gm/c^2$. Using Eqs. (58) and (96), the maximum mass and the corresponding radius are given by

$$M_{\max} = \frac{a}{2b} \frac{\hbar}{\sqrt{Gm|a_s - \kappa \frac{Gm}{c^2}|}}, \quad (99)$$

$$R_* = b \left(\frac{|a_s - \kappa \frac{Gm}{c^2}| \hbar^2}{Gm^3} \right)^{1/2}. \quad (100)$$

They can be written as

$$M_{\max} = C \frac{\hbar}{\sqrt{Gm|a_s - \kappa \frac{Gm}{c^2}|}}, \quad (101)$$

$$R_* = D \left(\frac{|a_s - \kappa \frac{Gm}{c^2}| \hbar^2}{Gm^3} \right)^{1/2}, \quad (102)$$

with $C = a/2b$ and $D = b$.

Remark.—Using the values $a = 11.1$ and $b = 5.5$ of Eq. (60) we obtain $C = 1.012$ and $D = 5.5$. Using the values $a_G = 8.96$ and $b_G = 4.12$ of the Gaussian ansatz, we find that $C = 1.09$ and $D = 4.12$.

B. Noninteracting limit

In the noninteracting limit ($a_s = 0$), Eqs. (99)–(102) reduce to

$$M_{\max} = \frac{a}{2b\sqrt{\kappa}} \frac{\hbar c}{Gm} = \frac{C}{\sqrt{\kappa}} \frac{\hbar c}{Gm}, \quad (103)$$

$$R_* = b\sqrt{\kappa} \frac{\hbar}{mc} = D\sqrt{\kappa} \frac{\hbar}{mc}, \quad (104)$$

$$R_* = \frac{2b^2\kappa GM_{\max}}{a c^2} = \frac{D\kappa GM_{\max}}{C c^2}. \quad (105)$$

This returns the maximum mass (62) of miniboson stars [1]. The compactness at the maximum mass is $C = a/(2b^2\kappa) = C/(D\kappa)$. Comparing Eqs. (103)–(105) with Eqs. (62) and (63), we get $C/\sqrt{\kappa} = 0.633$ and $D\sqrt{\kappa} = 6.03$.

Remark.—Using the values $a_G = 8.96$, $b_G = 4.12$, and $\kappa_G = 2.50$ of the Gaussian ansatz, we find that $M_{\max} = 0.688 \hbar c/Gm$, $R_* = 6.51 \hbar/mc$, and $C = 0.106$ in good agreement with the exact values $M_{\max} = 0.633 \hbar c/Gm$, $R_* = 6.03 \hbar/mc$, and $C = 0.105$ [1]. This is remarkable because these predictions are obtained without numerical calculation. In particular, the compactness is predicted almost exactly. We also find that the relativistic mass-radius relation is given by [see Eq. (97) with $a_s = 0$]

$$M = \frac{a \frac{\hbar^2}{Gm^2 R}}{1 + b^2 \kappa \frac{\hbar^2}{m^2 c^2 R^2}}. \quad (106)$$

Its graphical representation can be deduced from Fig. 2 by taking $M_a = \hbar c/(\sqrt{\kappa} Gm)$ and $R_a = \sqrt{\kappa} \hbar/mc$ (corresponding to $a_s \rightarrow a_s^* = -\kappa Gm/c^2$).

C. Attractive self-interaction

For bosons with an attractive self-interaction ($a_s < 0$), the expression (101) of the maximum mass is defined for all a_s . When $a_s \rightarrow -\infty$, we obtain

$$M_{\max} = \frac{a}{2b} \frac{\hbar}{\sqrt{Gm|a_s|}} = C \frac{\hbar}{\sqrt{Gm|a_s|}}, \quad (107)$$

$$R_* = b \left(\frac{|a_s| \hbar^2}{Gm^3} \right)^{1/2} = D \left(\frac{|a_s| \hbar^2}{Gm^3} \right)^{1/2}. \quad (108)$$

This returns the maximum mass (39) of nonrelativistic dilute axion stars [265]. Comparing Eqs. (107) and (108) with Eqs. (39) and (40) we get $C = 1.012$ and $D = 5.5$. Combined with the results of Sec. VII B, we see that we cannot satisfy all the constraints (we have four equations for three unknowns). The idea is to privilege exact asymptotic results for the maximum mass with respect to the radius. Therefore, we will take $C = 1.012$ and $C/\sqrt{\kappa} = 0.633$. This gives $\kappa = 2.56$ in good agreement with the value $\kappa_G = 2.50$ obtained from the Gaussian ansatz. Then, from the results of Sec. VII B, we get $D = 6.03/\sqrt{\kappa} = 3.77$ and from the results of this section $D = 5.5$. The disagreement between these two values is not too strong. In the following, we shall adopt $D = 5.5$.

Remark.—Using the values $a_G = 8.96$ and $b_G = 4.12$ of the Gaussian ansatz, we get $M_{\max} = 1.09 \hbar/\sqrt{Gm|a_s|}$, $R_* = 4.12 \sqrt{|a_s| \hbar^2/Gm^3}$, and $C = 0.264 Gm/|a_s| c^2$ in good agreement with the exact values

$M_{\max} = 1.012 \hbar / \sqrt{Gm|a_s|}$, $R_* = 5.5 \sqrt{|a_s| \hbar^2 / Gm^3}$, and $C = 0.184 Gm / |a_s| c^2$ [265]. This is remarkable because these predictions are obtained without numerical calculation. In particular, the maximum mass is predicted almost exactly.

D. Repulsive self-interaction

For bosons with a repulsive self-interaction ($a_s > 0$), the expression (101) of the maximum mass is defined only for $a_s < \kappa Gm / c^2$. In particular, it does not return the maximum mass of massive boson stars [58,86] from Eq. (64) in the TF limit (i.e., when $a_s \rightarrow +\infty$). Indeed, the maximum mass from Eq. (101) diverges when $a_s \rightarrow \kappa Gm / c^2$ and the mass-radius relation from Eq. (97) does not display a maximum mass when $a_s > \kappa Gm / c^2$. This means that relativistic corrections of strong gravity as we approach the Schwarzschild radius, besides the relativistic correction E_R of weak gravity in the quantum potential, are important in that case as discussed in Sec. VI.

E. Interpolation formulas

Using the previous results, we can obtain simple interpolation formulas for the maximum mass and minimum radius of boson stars. We shall take

$$C = 1.012, \quad D = 5.5, \quad \kappa = 2.56. \quad (109)$$

In this manner, the asymptotic expressions of the maximum mass for $a_s = 0$ and $a_s \rightarrow -\infty$ are exact. The asymptotic expression of the corresponding radius is also exact for $a_s \rightarrow -\infty$, while it is only approximate for $a_s = 0$. We propose, therefore, the interpolation formulas

$$M_{\max} = 1.012 \frac{\hbar}{\sqrt{Gm|a_s - 2.56 \frac{Gm}{c^2}|}}, \quad (110)$$

$$R_* = 5.5 \left(\frac{|a_s - 2.56 \frac{Gm}{c^2}| \hbar^2}{Gm^3} \right)^{1/2}. \quad (111)$$

We note that these expressions are defined only for $a_s < 2.56 Gm / c^2$.²⁶ This suggests that the present treatment is only reliable for negative values of the scattering length. This is because the maximum mass of boson stars with a repulsive self-interaction ($a_s \geq 0$) is a general relativistic result that is essentially due to the fact that the radius of the system approaches the Schwarzschild radius as shown in

²⁶The bound $a_s < 2.56 Gm / c^2$ obtained when we consider relativistic corrections to the quantum potential is “antisymmetric” with respect to the bound $a_s > -4.25 Gm / c^2$ found in Sec. VI when we consider the criterion based on the Schwarzschild radius. This shows that the two approaches are complementary to each other.

Sec. VI. It is not directly due to relativistic corrections in the quantum potential.

For $a_s \rightarrow 0$, Eqs. (110) and (111) reduce to

$$M_{\max} \simeq 0.633 \frac{\hbar c}{Gm} \left(1 + 0.195 \frac{a_s c^2}{Gm} \right), \quad (112)$$

$$R_* \simeq 8.8 \frac{\hbar}{mc} \left(1 - 0.195 \frac{a_s c^2}{Gm} \right). \quad (113)$$

Comparing Eqs. (112) and (113) with Eqs. (80) and (81), we see that the expressions coincide approximately for the maximum mass, while they strongly differ for the radius because the values of the radius at $a_s = 0$ and the signs in front of the correction $a_s c^2 / Gm$ are not the same. This is why we have privileged the behavior of R_* at $a_s \rightarrow \pm\infty$ rather than at $a_s = 0$.

Remark.—Using the values $a_G = 8.96$, $b_G = 4.12$, and $\kappa_G = 2.50$ of the Gaussian ansatz to evaluate the coefficients in Eqs. (99) and (100), we get

$$M_{\max} = 1.09 \frac{\hbar}{\sqrt{Gm|a_s - 2.50 \frac{Gm}{c^2}|}}, \quad (114)$$

$$R_* = 4.12 \left(\frac{|a_s - 2.50 \frac{Gm}{c^2}| \hbar^2}{Gm^3} \right)^{1/2}. \quad (115)$$

We stress that these results are obtained from the Gaussian ansatz without numerical calculation. They are in good agreement with the interpolation formulas (110) and (111), which rely on the exact asymptotic expressions of the maximum mass and minimum radius obtained numerically.

F. Improved interpolation formulas

We can improve the preceding interpolation formulas by allowing the parameter κ to be different in the expressions (101) and (102) determining the maximum mass and the corresponding radius. We write

$$M_{\max} = C \frac{\hbar}{\sqrt{Gm|a_s - \kappa \frac{Gm}{c^2}|}}, \quad (116)$$

$$R_* = D \left(\frac{|a_s - \kappa' \frac{Gm}{c^2}| \hbar^2}{Gm^3} \right)^{1/2}, \quad (117)$$

and we determine the constants C , D , κ , and κ' so as to reproduce the exact asymptotic behaviors from Eqs. (39), (40), and (62). In this manner, we obtain

$$C = 1.012, \quad D = 5.5, \quad \kappa = 2.56, \quad \kappa' = 1.20, \quad (118)$$

leading to

$$M_{\max} = 1.012 \frac{\hbar}{\sqrt{Gm|a_s - 2.56 \frac{Gm}{c^2}|}}, \quad (119)$$

$$R_* = 5.5 \left(\frac{|a_s - 1.20 \frac{Gm}{c^2}| \hbar^2}{Gm^3} \right)^{1/2}. \quad (120)$$

This gives a maximum compactness

$$C = \frac{0.184 \frac{Gm}{c^2}}{\sqrt{\left(a_s - 2.56 \frac{Gm}{c^2}\right) \left(a_s - 1.20 \frac{Gm}{c^2}\right)}}, \quad (121)$$

depending on a_s , and going from $C = 0.105$ in the noninteracting limit $a_s = 0$ to $C \sim 0.184 Gm/|a_s|c^2$ in the nonrelativistic limit $a_s \rightarrow -\infty$.

VIII. SUMMARY OF THE MAIN RESULTS

In this section, we summarize the results obtained previously for boson stars with repulsive or attractive self-interaction. The maximum mass, minimum radius, and maximum compactness are plotted as a function of the scattering length in Figs. 5–7.

For boson stars with a repulsive self-interaction ($a_s \geq 0$), we have obtained the following formulas [see Eqs. (85) and (86)]:

$$M_{\max} = 0.633 \frac{\hbar c}{Gm} \sqrt{1 + 0.235 \frac{a_s c^2}{Gm}}, \quad (122)$$

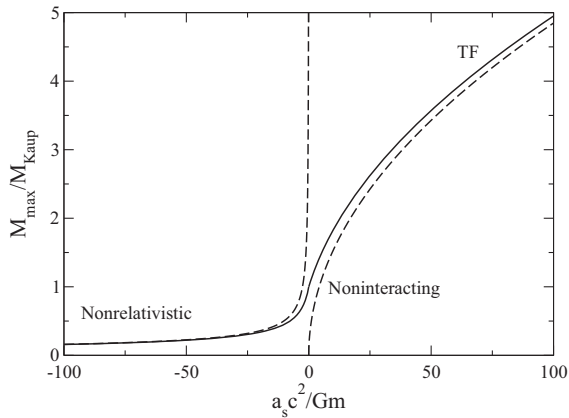


FIG. 5. Maximum mass M_{\max} of boson stars normalized by the Kaup mass M_{Kaup} corresponding to noninteracting bosons ($a_s = 0$) [1,2] as a function of the scattering length a_s of the bosons normalized by their semi-Schwarzschild radius Gm/c^2 . The dashed lines correspond to the TF limit ($a_s \rightarrow +\infty$) [58,86] and to the nonrelativistic limit ($a_s \rightarrow -\infty$) [265].

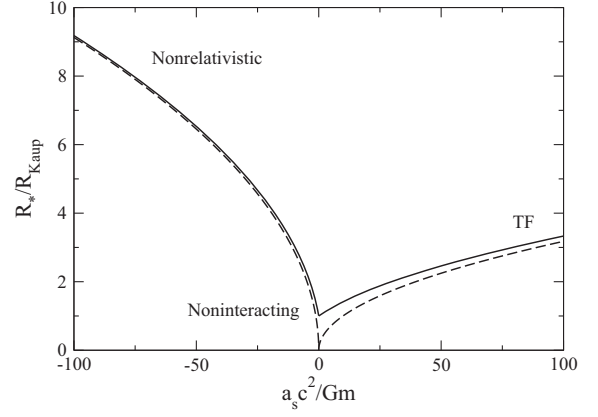


FIG. 6. Minimum radius R_* of boson stars normalized by the Kaup radius R_{Kaup} as a function of the scattering length a_s of the bosons normalized by their semi-Schwarzschild radius Gm/c^2 .

$$R_* = 6.03 \frac{\hbar}{mc} \sqrt{1 + 0.101 \frac{a_s c^2}{Gm}}, \quad (123)$$

or, equivalently,

$$M_{\max} = 0.307 \frac{\hbar c^2 \sqrt{a_s}}{(Gm)^{3/2}} \sqrt{1 + 4.25 \frac{Gm}{a_s c^2}}, \quad (124)$$

$$R_* = 1.92 \left(\frac{a_s \hbar^2}{Gm^3} \right)^{1/2} \sqrt{1 + 9.90 \frac{Gm}{a_s c^2}}. \quad (125)$$

These expressions interpolate between the maximum mass and minimum radius [see Eq. (62)] of noninteracting

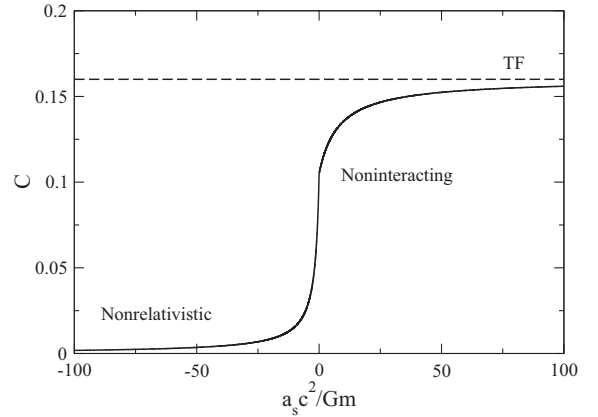


FIG. 7. Maximum compactness $C = GM_{\max}/R_*c^2$ of boson stars as a function of the scattering length a_s of the bosons normalized by their semi-Schwarzschild radius Gm/c^2 . The noninteracting limit ($a_s = 0$) corresponds to miniboson stars ($C = 0.105$) [1,2], the TF limit ($a_s \rightarrow +\infty$) corresponds to massive boson stars ($C = 0.16$) [58,86], and the nonrelativistic limit ($a_s \rightarrow -\infty$) corresponds to dilute axion stars ($C \rightarrow 0$) [265,290,306].

bosons stars [1,2] and the maximum mass and minimum radius [see Eq. (64)] of bosons stars with a strong repulsive self-interaction (TF limit) [58,86]. The maximum mass is due to general relativity in the strong gravity regime. We expect these approximate results to be more accurate for $a_s \gg r_S = Gm/c^2$ than for $a_s \ll r_S$. We see that a repulsive self-interaction increases the maximum mass and the minimum radius of noninteracting boson stars. Therefore, a repulsive self-interaction delays the collapse. Equations (124) and (125) also give the quantum corrections to the TF approximation used to obtain Eq. (64) [58,86]. We see that quantum corrections increase the maximum mass and minimum radius with respect to the TF approximation. The maximum compactness $\mathcal{C} = GM_{\max}/R_*c^2$ can be obtained as a function of the scattering length a_s from Eqs. (122)–(125) [see Eq. (87)]. It goes from $\mathcal{C} = 0.105$ in the noninteracting case ($a_s = 0$) to $\mathcal{C} = 0.16$ in the TF limit ($a_s \rightarrow +\infty$).

For boson stars with an attractive self-interaction ($a_s \leq 0$), like axions, we have obtained the following formulas [see Eqs. (119) and (120)]:

$$M_{\max} = 0.633 \frac{\hbar c}{Gm} \frac{1}{\sqrt{1 + 0.391 \frac{|a_s|c^2}{Gm}}}, \quad (126)$$

$$R_* = 6.03 \frac{\hbar}{mc} \sqrt{1 + 0.833 \frac{|a_s|c^2}{Gm}}, \quad (127)$$

or, equivalently,

$$M_{\max} = 1.012 \frac{\hbar}{\sqrt{Gm|a_s|}} \frac{1}{\sqrt{1 + 2.56 \frac{Gm}{|a_s|c^2}}}, \quad (128)$$

$$R_* = 5.5 \left(\frac{|a_s|\hbar^2}{Gm^3} \right)^{1/2} \sqrt{1 + 1.20 \frac{Gm}{|a_s|c^2}}. \quad (129)$$

These expressions interpolate between the general relativistic maximum mass and minimum radius [see Eq. (62)] of noninteracting bosons stars [1,2] and the nonrelativistic maximum mass and minimum radius [see Eqs. (39) and (40)] of boson stars with an attractive self-interaction [265]. The maximum mass is due to general relativity in the strong gravity regime when $|a_s| \ll r_S$ and to the attractive self-interaction + general relativity in the weak gravity regime when $|a_s| \gg r_S$. We expect these approximate results to be more accurate for $|a_s| \gg r_S = Gm/c^2$ than for $|a_s| \ll r_S$. We see that an attractive self-interaction decreases the maximum mass and increases the minimum radius of noninteracting boson stars. Therefore, an attractive self-interaction favors the collapse. Equations (128) and (129) also give the relativistic corrections to the nonrelativistic results from Eqs. (39) and (40) [265,290].

We see that relativistic corrections reduce the maximum mass and increase the minimum radius with respect to the nonrelativistic approximation. The maximum compactness $\mathcal{C} = GM_{\max}/R_*c^2$ can be obtained as a function of the scattering length a_s from Eqs. (126)–(129) [see Eq. (121)]. It goes from $\mathcal{C} = 0.105$ in the noninteracting case ($a_s = 0$) to $\mathcal{C} = 0$ in the nonrelativistic limit ($a_s \rightarrow -\infty$).

IX. BLACK HOLE OR BOSENOVA?

In the previous sections, we have expressed the maximum mass of boson stars in terms of the scattering length a_s of the bosons. In the present section, we reformulate these results in terms of the dimensionless self-interaction constant λ or in terms of the axion decay constant f (see Appendices B and C). Then, we discuss whether the collapse of the boson star above the maximum mass leads to a black hole or a bosenova. We introduce relevant transition scales separating these two regimes.

A. Maximum mass

The dimensionless self-interaction constant and the axion decay constant (when $a_s < 0$) are defined by²⁷

$$\frac{\lambda}{8\pi} = \frac{a_s mc}{\hbar}, \quad (130)$$

$$f = \left(\frac{\hbar c^3 m}{32\pi |a_s|} \right)^{1/2} = \frac{mc^2}{2\sqrt{|\lambda|}}. \quad (131)$$

In the noninteracting limit, the maximum mass of boson stars due to general relativity [see Eq. (62)] can be written as

$$M_{\max, \text{NI}}^{\text{GR}} = 0.633 \frac{M_P^2}{m}. \quad (132)$$

For $m \sim 1 \text{ GeV}/c^2$ (nucleon mass), we get $M_{\max, \text{NI}}^{\text{GR}} \sim 8.46 \times 10^{-20} M_\odot$ (miniboson star). The maximum mass becomes comparable to the solar mass $M_{\max, \text{NI}}^{\text{GR}} \sim M_\odot$ for $m \sim 10^{-10} \text{ eV}/c^2$.

On the other hand, for boson stars with a repulsive self-interaction, the maximum mass due to general relativity can be written, in the TF approximation, as [see Eq. (64)]

$$M_{\max, \text{TF}}^{\text{GR}} = 0.0612 \sqrt{\lambda} \frac{M_P^3}{m^2}. \quad (133)$$

²⁷Depending on whether we consider a real or a complex SF, there may be a multiplicative factor 2/3 in the expression of λ [see Eq. (C15)]. We adopt here the definitions from Eqs. (130) and (131) in order to be consistent with our previous papers.

Following Colpi *et al.* [58], we introduce the rescaled dimensionless self-interaction constant

$$\Lambda = \frac{\lambda}{4\pi} \frac{M_P^2}{m^2} \quad (134)$$

in terms of which

$$M_{\max, \text{TF}}^{\text{GR}} = 0.217\sqrt{\Lambda} \frac{M_P^2}{m}. \quad (135)$$

The TF approximation is valid when

$$\Lambda \gg 1 \quad \text{i.e.} \quad \lambda \gg \left(\frac{m}{M_P}\right)^2. \quad (136)$$

Since $m \ll M_P$, in general, the TF approximation is valid even when $\lambda \sim 1$ or smaller.²⁸ We see that when $\Lambda \gg 1$ the maximum mass $M_{\max, \text{TF}}^{\text{GR}} \sim \sqrt{\Lambda} M_P^2/m$ of self-interacting boson stars is much larger than the maximum mass $M_{\max, \text{NI}}^{\text{GR}} \sim M_P^2/m$ of noninteracting boson stars. They differ by a factor $\sqrt{\Lambda} M_P/m$. Written under the form $M_{\max, \text{TF}}^{\text{GR}} \sim \sqrt{\lambda} M_P^3/m^2$, we see that, when $\lambda \sim 1$, the maximum mass of self-interacting boson stars is on the order of the Chandrasekhar mass $M_{\text{Chandra}} \sim M_P^3/m^2$ for fermion stars. For $m \sim 1 \text{ GeV}/c^2$ (\sim nucleon mass) the maximum mass $M_{\max, \text{TF}}^{\text{GR}} \sim M_\odot$ is on the order of the solar mass (massive boson stars). For $m \sim 1 \text{ MeV}/c^2$ (\sim electron mass) the maximum mass $M_{\max, \text{TF}}^{\text{GR}} \sim 10^6 M_\odot$ is on the order of the mass of SMBHs in AGNs. For $m \sim 100 \text{ GeV}/c^2$ (\sim Higgs mass), we get $M_{\max, \text{TF}}^{\text{GR}} \sim 10^{-4} M_\odot$. In all these examples, the TF approximation is justified because $\lambda \sim 1 \gg (m/M_P)^2 \sim 10^{-38}$, 10^{-44} , and 10^{-34} , respectively.

For boson stars with an arbitrary repulsive self-interaction, we can write the maximum mass [see Eq. (85)] as

$$M_{\max} = 0.633 \frac{M_P^2}{m} \sqrt{1 + 0.117\Lambda}. \quad (137)$$

When $\Lambda = 0$, we recover Eq. (132), and when $\Lambda \gg 1$, we recover Eq. (135). Interestingly, our analytical formula (137) is consistent with the formula $M_{\max} = (2/\pi)\sqrt{1 + \Lambda/8} M_P^2/m$ obtained by Mielke and Schunck [257,258] from different considerations.

For axion stars with an attractive self-interaction, the maximum mass due to the self-interaction can be written, in the nonrelativistic limit, as [see Eq. (39)]

$$M_{\max}^{\text{NR}} = 5.07 \frac{M_P}{\sqrt{|\lambda|}} = 10.1 \left(\frac{f^2 \hbar}{c^3 m^2 G}\right)^{1/2} \quad (138)$$

or, using Eq. (134), as

$$M_{\max}^{\text{NR}} = 1.43 \frac{M_P^2}{m\sqrt{|\Lambda|}}. \quad (139)$$

The nonrelativistic limit is valid when

$$|\Lambda| \gg 1, \quad \text{i.e.,} \quad |\lambda| \gg \left(\frac{m}{M_P}\right)^2. \quad (140)$$

Since $m \ll M_P$, in general, the nonrelativistic approximation is valid even when $|\lambda| \sim 1$ or smaller (see footnote 28 with Λ replaced by $|\Lambda|$). We see that when $|\Lambda| \gg 1$, the maximum mass $M_{\max}^{\text{NR}} \sim M_P^2/m\sqrt{|\Lambda|}$ of dilute axion stars with an attractive self-interaction is much smaller than the mass $M_{\max, \text{NI}}^{\text{GR}} \sim M_P^2/m$ of noninteracting boson stars. They differ by a factor $|\lambda|^{-1/2} m/M_P$. Written under the form $M_{\max}^{\text{NR}} \sim M_P/\sqrt{|\lambda|}$, we see that, when $|\lambda| \sim 1$, the maximum mass of dilute axion stars is on the order of the Planck mass. For QCD axions with $m \sim 10^{-4} \text{ eV}/c^2$ and $a_s \sim -5.8 \times 10^{-53} \text{ m}$ (corresponding to $\lambda \sim -7.39 \times 10^{-49}$ and $f = 5.82 \times 10^{10} \text{ GeV}$), we get $M_{\max}^{\text{NR}} = 6.46 \times 10^{-14} M_\odot$ and $R_{99}^* = 227 \text{ km}$ (asteroids). For ULAs with $m = 2.92 \times 10^{-22} \text{ eV}/c^2$ and $a_s = -3.18 \times 10^{-68} \text{ fm}$ (corresponding to $\lambda = -1.18 \times 10^{-96}$ and $f = 1.34 \times 10^{17} \text{ GeV}$) predicted in [267], we get $M_{\max}^{\text{NR}} = 5.10 \times 10^{10} M_\odot$ and $R_{99}^* = 1.09 \text{ pc}$ (DM cores). In these two examples, the nonrelativistic approximation is justified because $|\lambda| \gg (m/M_P)^2 \sim 10^{-64}$ and 10^{-100} , respectively (the second approximation is marginally valid).

For dilute axion stars with an arbitrary attractive self-interaction, we can write the maximum mass [see Eq. (119)] as

$$M_{\max} = 0.633 \frac{M_P^2}{m} \frac{1}{\sqrt{1 - 0.196\Lambda}}. \quad (141)$$

When $\Lambda = 0$, we recover Eq. (132), and when $|\Lambda| \gg 1$, we recover Eq. (139). We note that the formula of Mielke and Schunck [257,258] quoted above is not valid when $\Lambda < 0$.

B. Transition scales

We introduce the transition scales

$$(a_s)_t = \frac{2Gm}{c^2} = r_s, \quad (142)$$

$$\lambda_t = \frac{Gm^2}{16\pi \hbar c} = \left(\frac{m}{M_P}\right)^2, \quad (143)$$

$$f_t = \frac{M_P c^2}{8\sqrt{\pi}} \sim 10^{18} \text{ GeV}. \quad (144)$$

²⁸Conversely, the self-interaction is negligible if $\Lambda \ll 1$, i.e., $\lambda \ll (m/M_P)^2$. Since $m \ll M_P$, the self-interaction can be neglected only if it is extraordinarily tiny. For example, for a boson mass $m \sim 10^{-22} \text{ eV}/c^2$, the self-interaction can be neglected only if $|\lambda| \ll 10^{-100}$.

We note that $(a_s)_t$ is on the order of the Schwarzschild radius of the boson $r_S = 2Gm/c^2$, λ_t is on the order of the gravitational coupling constant $\alpha_g = Gm^2/\hbar c = (m/M_P)^2$, and f_t is on the order of the Planck mass energy $M_P c^2 \sim 10^{19}$ GeV (note that it is independent of the mass m of the boson).

For a repulsive self-interaction ($a_s \geq 0$), the maximum mass M_{\max}^{GR} is due to general relativity. When $M < M_{\max}^{\text{GR}}$, the boson star is stable, and when $M > M_{\max}^{\text{GR}}$, it collapses toward a black hole. The transition between the non-interacting regime and the TF regime occurs when $M_{\max, \text{NI}}^{\text{GR}} \sim M_{\max, \text{TF}}^{\text{GR}}$, giving $a_s \sim (a_s)_t$ (i.e., $\lambda \sim \lambda_t$). When $a_s \ll (a_s)_t$ (i.e., $\lambda \ll \lambda_t$), we are in the noninteracting regime, and when $a_s \gg (a_s)_t$ (i.e., $\lambda \gg \lambda_t$), we are in the TF regime. In each case, when the mass overcomes M_{\max}^{GR} , a black hole is formed.

For an attractive self-interaction, the instability may be due to general relativity or to the self-interaction of the bosons. When $a_s \simeq 0$, the maximum mass M_{\max}^{GR} is due to general relativity. When $M < M_{\max, \text{NI}}^{\text{GR}}$, the boson star is stable, and when $M > M_{\max, \text{NI}}^{\text{GR}}$, it collapses toward a black hole. When $a_s \rightarrow -\infty$ the maximum mass M_{\max}^{NR} is due to the attractive self-interaction. When $M < M_{\max}^{\text{NR}}$, the dilute axion star is stable, and when $M > M_{\max}^{\text{NR}}$, it collapses and forms a dense axion star (stabilized by, e.g., a $|\phi|^6$ repulsive self-interaction) or explodes in a bosenova. The transition between the noninteracting regime and the nonrelativistic regime occurs when $M_{\max}^{\text{NR}} \sim M_{\max, \text{NI}}^{\text{GR}}$, giving $|a_s| \sim (a_s)_t$ (i.e., $|\lambda| \sim \lambda_t$ and $f \sim f_t$). When $|a_s| \ll (a_s)_t$ (i.e., $|\lambda| \ll \lambda_t$ or $f \gg f_t$), we are in the noninteracting regime. In that case, when the mass overcomes $M_{\max, \text{NI}}^{\text{GR}}$, a black hole is formed. When $|a_s| \gg (a_s)_t$ (i.e., $|\lambda| \gg \lambda_t$ or $f \ll f_t$), we are in the nonrelativistic regime. In that case, when the mass overcomes M_{\max}^{NR} , a dense axion star or a bosenova is formed.

A phase diagram presenting these different possibilities is shown in Fig. 8.

C. Triple point

A repulsive $|\phi|^6$ self-interaction can stabilize a collapsing axion star above the mass M_{\max}^{NR} and allow the formation of a dense axion star. However, a dense axion star can itself undergo a gravitational instability of general relativistic origin above a maximum mass estimated to be [109,110]

$$M_{\max, \text{dense}}^{\text{GR}} = 0.991 \left(\frac{|a_s| \hbar^2 c^4}{G^3 m^3} \right)^{1/2}, \quad (145)$$

i.e.,

$$M_{\max, \text{dense}}^{\text{GR}} = 0.0988 \left(\frac{\hbar^3 c^7}{G^3 f^2 m^2} \right)^{1/2} = 0.198 \sqrt{|\lambda|} \frac{M_P^3}{m^2}. \quad (146)$$

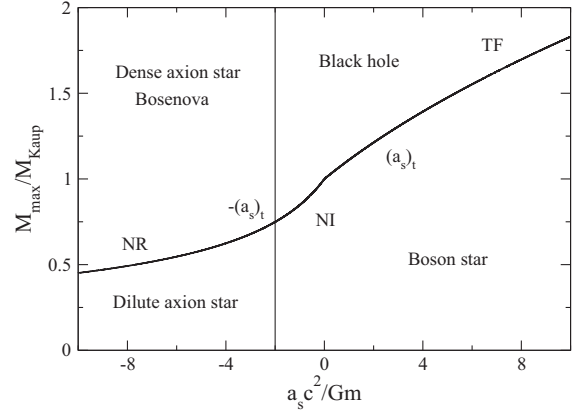


FIG. 8. Phase diagram of boson stars with a $|\phi|^4$ self-interaction (see text for details). We have represented the maximum mass above which the boson star becomes unstable as a function of the scattering length [see Eqs. (85) and (119)]. This maximum mass is $M_{\max, \text{NI}}^{\text{GR}}$ when $a_s = 0$, $M_{\max, \text{TF}}^{\text{GR}}$ when $a_s \gg (a_s)_t$ (repulsive case), and M_{\max}^{NR} when $|a_s| \gg (a_s)_t$ (attractive case).

This mass presents the same scaling as the maximum mass of a boson star in the TF regime [see Eq. (64)], except that, in the present case, $a_s < 0$. We note that $M_{\max, \text{dense}}^{\text{GR}} \sim M_{\max, \text{NI}}^{\text{GR}}$ when $|a_s| \sim (a_s)_t$ (i.e., when $|\lambda| \sim \lambda_t$ and $f \sim f_t$). This leads to a triple point at $\sim [-r_S, M_{\text{Kaup}}]$ separating boson stars, black holes, and dense axion stars or bosenova (see Fig. 9). This triple point was obtained numerically in [309] and reproduced analytically (qualitatively) in [109]. When $a_s > -(a_s)_t$, we expect to observe a boson star for $M < M_{\max}^{\text{GR}}$ and a black hole for $M > M_{\max}^{\text{GR}}$. When

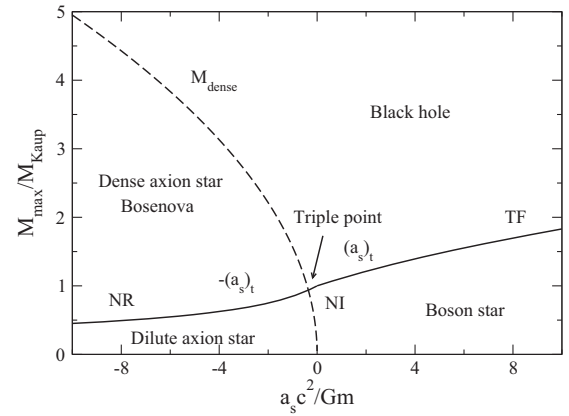


FIG. 9. Phase diagram of boson stars with a $|\phi|^4$ and a $|\phi|^6$ self-interaction (see text for details). It displays a triple point at $\sim [-r_S, M_{\text{Kaup}}]$ separating boson stars, black holes, and dense axion stars or bosenova. With respect to Fig. 8, we have added the mass $M_{\max, \text{dense}}^{\text{GR}}$ above which dense axion stars ($a_s < 0$) become general relativistically unstable and collapse toward a black hole [the corresponding curve is $M_{\max, \text{dense}}^{\text{GR}}/M_{\text{Kaup}} = 1.56(|a_s|c^2/Gm)^{1/2}$]. This figure can be compared to Fig. 31 of [109].

$a_s < -(a_s)_r$, we expect to observe a dilute axion star for $M < M_{\max}^{\text{NR}}$, a dense axion star or a bosonova for $M_{\max}^{\text{NR}} < M < M_{\max}^{\text{GR}}$, and a black hole for $M > M_{\max}^{\text{GR}}$.

X. APPLICATION TO DM HALOS AND INFLATON CLUSTERS: CORE MASS–HALO MASS RELATION

We now apply our results to DM halos and inflaton clusters.

The results of Secs. II–IX describe the ground state of a self-gravitating BEC. In cosmology, they characterize a minimum halo of mass $(M_h)_{\min}$, which is a purely condensed object without atmosphere. Larger DM halos of mass $M_h > (M_h)_{\min}$ have a core-halo structure with a quantum core (soliton) in its ground state and an approximately isothermal atmosphere that arises from the quantum interferences of excited states. This core-halo structure has been explained in Refs. [264,272,320,321] by the process of gravitational cooling [262] and the theory of violent relaxation [263,277]. The results of Secs. II–IX also apply to the quantum core of large DM halos. The mass M_c of the quantum core increases with the halo mass M_h (see Fig. 10). For noninteracting bosons and for bosons with a repulsive self-interaction, we may wonder if the core mass can reach the maximum mass M_{\max}^{GR} [see Eqs. (62) and (64)] set by general relativity and collapse toward a black hole. For bosons with an attractive self-interaction, we may wonder if the core mass can reach the Newtonian maximum mass M_{\max}^{NR} [see Eq. (39)] and collapse toward a dense axion star (soliton) or a black hole, or explode in a bosonova [109,307–313,319].

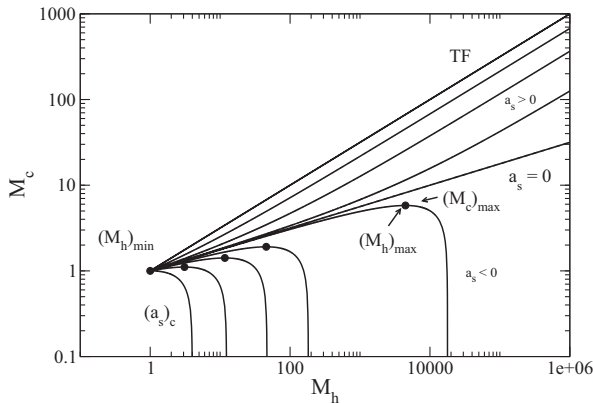


FIG. 10. Core mass M_c as a function of the halo mass M_h for different values of a_s [see Eqs. (155) and (156)]. The mass is normalized by $(M_h)_{\min}$. We have highlighted the curve corresponding to the noninteracting case $a_s = 0$ [see Eq. (157)] and the curve corresponding to the TF limit $a_s/a_* \gg 1$ [see Eq. (159)]. When the self-interaction is attractive ($a_s < 0$), the quantum core becomes unstable when it reaches the maximum mass $(M_c)_{\max}$ [see Eq. (161)]. This occurs in a halo of mass $(M_h)_{\max}$ [see Eq. (162)].

A. General formalism

In Refs. [267,321–323], we have derived the core mass–halo mass relation of DM halos (without or with the presence of a central black hole) from a thermodynamic approach. We have obtained a general relation $M_c(M_h)$ valid for noninteracting bosons as well as for bosons with a repulsive or an attractive self-interaction (and for fermions). To obtain this relation, we have proceeded in three steps:

- (i) We have first shown [321,322] that the maximization of the Lynden-Bell entropy (justified by the theory of violent relaxation [263,264]) at fixed mass and energy leads to the “velocity dispersion tracing” relation according to which the velocity dispersion in the core $v_c^2 \sim GM_c/R_c$ is equal to the velocity dispersion in the halo $v_h^2 \sim GM_h/r_h$. This relation can be written as

$$v_c \sim v_h \Rightarrow \frac{M_c}{R_c} \sim \frac{M_h}{r_h}. \quad (147)$$

- (ii) To determine the core mass-radius relation $M_c(R_c)$, we have used a Gaussian ansatz yielding [265]

$$M_c = \frac{3.76 \frac{\hbar^2}{Gm^2 R_c}}{1 - 3 \frac{a_s \hbar^2}{Gm^3 R_c^2}} \quad (148)$$

or, equivalently,

$$R_c = 1.87 \frac{\hbar^2}{Gm^2 M_c} \left(1 \pm \sqrt{1 + 0.849 \frac{Gma_s M_c^2}{\hbar^2}} \right). \quad (149)$$

- (iii) To determine the halo mass-radius relation $M_h(r_h)$ we have assumed that the atmosphere is isothermal,²⁹ and we have used the fact that the surface density Σ_0 of the DM halos is universal. This leads to the halo mass-radius relation [321]

$$M_h = 1.76 \Sigma_0 r_h^2. \quad (150)$$

Combining Eqs. (147)–(150), we obtain the core mass–halo mass relation $M_c(M_h)$ under the form

$$M_c = 2.23 \frac{\hbar \Sigma_0^{1/4} M_h^{1/4}}{G^{1/2} m} \left(1 + 1.06 \frac{a_s}{m} \Sigma_0^{1/2} M_h^{1/2} \right)^{1/2}. \quad (151)$$

²⁹The fact that the atmosphere should be isothermal is justified in Ref. [264] by the Lynden-Bell [263] theory of violent relaxation. An (approximately) isothermal atmosphere seems to be validated by numerical simulations showing DM density profiles decreasing as r^{-2} [272] and exhibiting a Maxwellian velocity distribution [273,330,347].

As we mentioned above, the minimum halo is a purely condensed object without atmosphere. Writing $M_c = M_h$, meaning that the quantum core contains all the mass (i.e., there is no isothermal halo around it), we obtain

$$(M_h)_{\min}^{3/2} = 4.99 \frac{\hbar^2 \Sigma_0^{1/2}}{Gm^2} \left(1 + 1.06 \frac{a_s}{m} \Sigma_0^{1/2} (M_h)_{\min}^{1/2} \right). \quad (152)$$

This equation determines the mass $(M_h)_{\min}$ of the minimum halo as a function of m and a_s . Alternatively, for a given value of $(M_h)_{\min}$ deduced from the observations, Eq. (152) determines a constraint between m and a_s .

Universal relations can be obtained by introducing an appropriate normalization [267,322,323]. For a given value of the minimum halo mass $(M_h)_{\min}$, we introduce the mass scale

$$m_0 = 2.23 \frac{\hbar \Sigma_0^{1/4}}{G^{1/2} (M_h)_{\min}^{3/4}} \quad (153)$$

and the self-interaction scale

$$a'_* = 2.11 \frac{\hbar}{G^{1/2} \Sigma_0^{1/4} (M_h)_{\min}^{5/4}}. \quad (154)$$

With these scales, the normalized DM particle mass–scattering length relation (152) can be written as

$$\frac{a_s}{a'_*} = \left(\frac{m}{m_0} \right)^3 - \frac{m}{m_0}, \quad (155)$$

and the normalized core mass–halo mass relation (151) can be written as

$$\frac{M_c}{(M_h)_{\min}} = \frac{m_0}{m} \left(\frac{M_h}{(M_h)_{\min}} \right)^{1/4} \sqrt{1 + \frac{m_0 a_s}{m a'_*} \left(\frac{M_h}{(M_h)_{\min}} \right)^{1/2}}. \quad (156)$$

This leads to the universal curves plotted in Fig. 10. The only input is the DM particle mass m or, equivalently, its scattering length a_s [they are related to each other by Eq. (155)]. The minimum halo mass $(M_h)_{\min}$ obtained from the observations determines the scales m_0 and a'_* .

The above relations were derived in the context of DM halos [267,321–323]. In that case, the universal surface density inferred from the observations is $\Sigma_0 = 141 M_\odot / \text{pc}^2$ [348–350]. On the other hand, it is an observational evidence that there is no DM halo with a mass smaller than $M_h \sim 10^7 - 10^8 M_\odot$. Taking a minimum halo mass $(M_h)_{\min} = 10^8 M_\odot$ to fix the ideas, we get $m_0 = 2.25 \times 10^{-22} \text{ eV}/c^2$ and $a'_* = 4.95 \times 10^{-62} \text{ fm}$. Then, for a given value of the scattering length a_s , we obtain the boson mass m from Eq. (155) and the core mass–halo mass relation

$M_c(M_h)$ from Eq. (156). A detailed discussion of the core mass–halo mass relation of DM halos has been given in [267,321–323]. For a repulsive self-interaction (or no self-interaction) it is found that, in realistic DM halos ($M_h < 10^{14} M_\odot$), the quantum core mass M_c is always much smaller than M_{\max}^{GR} . Therefore, it cannot collapse toward a black hole.³⁰ For an attractive self-interaction, and for values of f in the range $10^{16} \leq f \leq 10^{18} \text{ GeV}$ predicted by particle physics and cosmology [266], it is found that the quantum core (soliton) is always stable ($M_c < M_{\max}^{\text{NR}}$) in realistic DM halos of mass $M_h < 10^{14} M_\odot$.³¹ However, we must be careful about observational constraints on a DM particle whose precise nature has not yet been established. If f can be smaller than 10^{15} GeV (a possibility to consider), the soliton can become unstable in sufficiently large realistic DM halos and collapse. For example, for $m \sim 10^{-22} \text{ eV}/c^2$ and $f \sim 10^{14} \text{ GeV}$ (corresponding to $|\lambda| \sim 10^{-91}$), we find a maximum core mass $M_{\max}^{\text{NR}} \sim 10^8 M_\odot$. This value is of the same order as the typical mass of the minimum halo $(M_h)_{\min} \sim 10^8 M_\odot$, implying that the quantum core of all the DM halos [$M_h \geq (M_h)_{\min}$] would be unstable in that case. Since $f \ll M_P c^2 \sim 10^{19} \text{ GeV}$, the collapse of the quantum core leads to a dense soliton or a bosonova, not to a black hole (see Sec. IX).

A similar discussion has been given by Padilla *et al.* [324] in the case of DM halos by using the theoretical formalism described previously [267,321–323]. Recently, Padilla *et al.* [331] applied the same formalism to inflaton clusters [327–330]. In particular, they considered the possibility that the self-interaction between bosons is attractive and that the inflaton stars collapse toward a black hole when they reach the maximum mass M_{\max}^{NR} [see Eq. (39)]. Below, we complement their results and also treat the case of a repulsive self-interaction.

³⁰For noninteracting bosons or for bosons with a repulsive self-interaction, we find that the core mass can reach the critical mass (62) or (64) only in halos of mass larger than $M_h \sim 10^{-2} c^4 / G^2 \Sigma_0 \sim 10^{22} M_\odot$, which are not realistic (the biggest DM halos have a mass $M_h \sim 10^{14} M_\odot$). Remarkably, this result is independent of the characteristics (mass, scattering length, etc.) of the DM particle (see Appendix C of [323]). We conclude that the quantum core is always stable in practice and that it cannot collapse toward a black hole. The fact that $M_c \ll M_{\max}^{\text{GR}}$ also justifies that we use a nonrelativistic approach.

³¹For bosons with an attractive self-interaction, we find that the quantum core mass can reach the critical mass (39) in realistic halos (of mass $M_h \leq 10^{14} M_\odot$) provided that the axion decay constant f is smaller than $f_c = 4.22 \times 10^{15} \text{ GeV}$. Remarkably, this result is independent of the DM particle mass [267,322]. However, such small values of f seem to be excluded by constraints from cosmology and particle physics which place f in the range $10^{16} \leq f \leq 10^{18} \text{ GeV}$. We conclude that the quantum core is always stable in practice and that it cannot collapse toward a dense axion star or a black hole, or explode in a bosonova.

The general results of Eqs. (147)–(156) remain valid in the case of inflaton clusters except for a change of scales. We thus have to determine the relevant scales for this problem. Niemeyer and Easter [328] adopt a boson mass $m = 6.35 \times 10^{-6} M_P$ based on the earlier work of Ref. [351]. In their numerical simulations, Eggemeier *et al.* [329] find that inflaton halos of mass $M_h \sim 20$ kg and radius $r_h \sim 10^{-20}$ m form roughly 10^{-24} s after the big bang. They also observe clusters of mass $M_h \sim 0.01$ kg and size $r_h \sim 10^{-22}$ m. From these values, one obtains the typical surface densities $\Sigma \sim 2 \times 10^{44}$ and $\Sigma \sim 10^{45}$ g/m², respectively. These results are consistent with a constant surface density,³² but its value is considerably larger than in the case of DM halos where $\Sigma_0 = 295$ g/m². To be specific, we shall take $\Sigma_0 = 10^{44}$ g/m². Using Eq. (153) with $m = m_0 = 6.35 \times 10^{-6} M_P = 1.38 \times 10^{-10}$ g, we obtain a minimum halo mass $(M_h)_{\min} = 5.74 \times 10^{-5}$ g. There should be no inflaton cluster below this threshold value. Then, Eq. (154) gives $a'_* = 1.72 \times 10^{-30}$ m (corresponding to $\lambda'_* = 17.0$ and $f'_* = 9.39 \times 10^{12}$ GeV).

B. Noninteracting bosons

For noninteracting bosons, the core mass–halo mass relation (151) reduces to

$$M_c = 2.23 \left(\frac{\hbar^4 \Sigma_0 M_h}{G^2 m^4} \right)^{1/4}. \quad (157)$$

In the noninteracting limit, the boson mass is $m = m_0 = 6.35 \times 10^{-6} M_P$. For an inflaton cluster of mass $M_h = 1$ g and radius $r_h = 7.54 \times 10^{-23}$ m, we obtain a core mass $M_c = 6.59 \times 10^{-4}$ g and a core radius $R_c = 1.32 \times 10^{-25}$ m. This theoretical prediction is consistent with the numerical results of Eggemeier *et al.* [330] who find an inflaton star of mass $M_c \sim 10^{-6}$ kg in a cluster of mass $M_h \sim 10^{-3}$ kg.

The maximum mass and the minimum radius of a noninteracting boson star at $T = 0$ set by general relativity are given by Eqs. (62) and (63). For a boson of mass $m = 6.35 \times 10^{-6} M_P$, we obtain $M_{\max, \text{NI}}^{\text{GR}} = 2.17$ g and $R_{\min, \text{NI}}^{\text{GR}} = 1.53 \times 10^{-29}$ m. The maximum mass is much larger than the typical quantum core mass (inflaton star) of inflaton clusters in the simulations of Eggemeier *et al.* [329,330] ($M_c \ll M_{\max, \text{NI}}^{\text{GR}}$). Therefore, a nonrelativistic approach is justified in most inflaton clusters. According to Eq. (157), the mass of the soliton becomes equal to the maximum mass ($M_c = M_{\max, \text{NI}}^{\text{GR}}$) in an inflaton cluster of mass

³²If the surface density of the inflaton clusters is not constant, we should replace Σ_0 by $M_h/(1.76r_h^2)$ in Eqs. (151) and (152). In that case, the core mass M_c depends on M_h and r_h individually. For simplicity, we will assume below that Σ_0 is constant.

$$(M_h)_{\max}^{\text{NI}} = 6.49 \times 10^{-3} \frac{c^4}{G^2 \Sigma_0} = 1.18 \times 10^{14} \text{ g}. \quad (158)$$

Remarkably, this expression is independent of the boson mass (see Appendix C of [323]). Above that mass, the inflaton star collapses toward a black hole. This may provide a new mechanism for PBH formation during reheating [331].³³ Inflaton stars in less massive inflaton clusters are stable and do not form PBHs.

Remark.—An inflaton cluster would collapse toward a black hole as a whole if $r_h < 2GM_h/c^2$. Using the mass-radius relation from Eq. (150), this criterion gives $M_h > 0.142c^4/(G^2 \Sigma_0) = 2.57 \times 10^{15}$ g. This critical mass is 1 order of magnitude larger than the critical mass $(M_h)_{\max}^{\text{NI}}$ from Eq. (158), above which its core collapses. This suggests that the quantum core (soliton) collapses first.

C. Repulsive self-interaction in the TF limit

For bosons with a repulsive self-interaction in the TF limit, the core mass–halo mass relation (151) reduces to

$$M_c = 2.30 \left(\frac{\hbar^2 \Sigma_0 a_s M_h}{G m^3} \right)^{1/2}. \quad (159)$$

In the TF limit $a_s \gg a'_*$, the ratio a_s/m^3 is given by $a_s/m^3 = a'_*/m_0^3 = 0.654$ m/g³ [see Eq. (155)] (for $m = 6.35 \times 10^{-6} M_P$ this corresponds to $\lambda = 17.0$ and $a_s = 1.73 \times 10^{-30}$ m). For an inflaton cluster of mass $M_h = 1$ g, we obtain a core mass $M_c = 7.60 \times 10^{-3}$ g and a core radius $R_c = 1.04 \times 10^{-24}$ m.

The maximum mass and the minimum radius of a self-interacting boson star at $T = 0$ in the TF limit set by general relativity are given by Eqs. (64) and (65). For a ratio $a_s/m^3 = 0.654$ m/g³, we obtain $M_{\max, \text{TF}}^{\text{GR}} = 1.36 \times 10^5$ g and $R_{\min, \text{TF}}^{\text{GR}} = 6.34 \times 10^{-25}$ m. The maximum mass is much larger than the typical quantum core mass of inflaton clusters ($M_c \ll M_{\max, \text{TF}}^{\text{GR}}$). Therefore, a nonrelativistic approach is justified in most inflaton clusters. According to Eq. (159), the mass of the soliton would be equal to the maximum mass ($M_c = M_{\max, \text{TF}}^{\text{GR}}$) in an inflaton cluster of mass

$$(M_h)_{\max}^{\text{TF}} = 0.0178 \frac{c^4}{G^2 \Sigma_0} = 3.23 \times 10^{14} \text{ g}. \quad (160)$$

³³We note, however, that very massive inflaton clusters are required to form PBHs. Such massive inflaton clusters may not be very numerous (see the much smaller typical masses obtained in the simulations of Eggemeier *et al.* [329,330]). Therefore, the quantity of PBHs produced by this mechanism may be small. Furthermore, PBHs of mass $m \sim 1$ g rapidly evaporate by Hawking [352] radiation on a timescale $t_{\text{evap}} \sim G^2 M^3 / \hbar c^4 \sim 10^{-30}$ s.

Remarkably, this expression is independent of the ratio a_s/m^3 (see Appendix C of [323]). The comments made at the end of Sec. X B also apply to the present situation. There is, however, one important difference. The mass of the PBHs formed by this mechanism is much larger than in the noninteracting case (this is because self-interacting boson stars [58,86] are more massive than noninteracting boson stars [1,2]). As a result, their evaporation time is longer. A PBH of mass $m \sim 10^5$ g evaporates on a timescale $t_{\text{evap}} \sim G^2 M^3 / \hbar c^4 \sim 10^{-15}$ s. This timescale is still short but could be significantly increased (since it depends on the cubic power of M) if the self-interaction is larger.

D. Attractive self-interaction

For bosons with an attractive self-interaction, the core mass–halo mass relation presents a maximum (see Fig. 10) when the core mass reaches the critical value³⁴

$$\begin{aligned} (M_c)_{\text{max}} &= 1.085 \frac{\hbar}{\sqrt{Gm|a_s|}} = 10.9 \left(\frac{f^2 \hbar}{c^3 m^2 G} \right)^{1/2} \\ &= 5.44 \frac{M_P}{\sqrt{|\lambda|}}, \end{aligned} \quad (161)$$

at which it becomes unstable and collapses [265,307]. The collapse of the core, leading to a dense axion star (soliton), a black hole (provided that $M_c > M_{\text{max,dense}}^{\text{GR}}$), or a bosonova [109,307–313,319], occurs in a DM halo of mass

$$(M_h)_{\text{max}} = 0.223 \frac{m^2}{a_s^2 \Sigma_0} = 2255 \frac{f^4}{\hbar^2 c^6 \Sigma_0} = 141 \frac{m^4 c^2}{\Sigma_0 \hbar^2 \lambda^2}. \quad (162)$$

From Eqs. (161) and (162), we obtain the relation

$$(M_c)_{\text{max}} = 1.58 \left(\frac{\hbar^4 \Sigma_0 (M_h)_{\text{max}}}{G^2 m^4} \right)^{1/4}, \quad (163)$$

presenting the same scaling as Eq. (157). Therefore, in Fig. 10, the curve $(M_c)_{\text{max}}[(M_h)_{\text{max}}]$ connecting the bullets is close to the curve $M_c(M_h)$ corresponding to $a_s = 0$. We note that the maximum halo mass $(M_h)_{\text{max}}$ depends only on f , while the maximum core mass $(M_c)_{\text{max}}$ depends on f and m . On the other hand, the maximum core mass $(M_c)_{\text{max}}$ depends only on λ , while the maximum halo mass $(M_h)_{\text{max}}$ depends on λ and m .

According to Eq. (162), the value of f below which the quantum core of an inflaton halo of mass $M_h = 1$ g collapses is $f_{\text{crit}} = 1.53 \times 10^{14}$ GeV (for $m = 6.35 \times 10^{-6} M_P$, this corresponds to $\lambda_{\text{crit}} = -6.42 \times 10^{-2}$

³⁴Recall that we use here the values of the Gaussian ansatz in order to be consistent with the general formalism of Sec. X A.

and $(a_s)_{\text{crit}} = -6.50 \times 10^{-33}$ m). In that case, the critical core mass is $(M_c)_{\text{max}} = 4.68 \times 10^{-4}$ g.³⁵ Since $f_{\text{crit}} \ll f_t \sim M_P c^2 \sim 10^{19}$ GeV [i.e., $|\lambda_{\text{crit}}| \gg \lambda_t \sim (m/M_P)^2 \sim 4.03 \times 10^{-11}$ and $|(a_s)_{\text{crit}}| \gg 2Gm/c^2 \sim 2.05 \times 10^{-40}$ m] and $(M_c)_{\text{max}} \ll M_{\text{max,dense}}^{\text{GR}} = 2.71 \times 10^4$ g, the collapse of the quantum core leads to a dense axion star (soliton) [109,311,312] or a bosonova [308], not to a black hole [309,310] (see Sec. IX). The possibility to form dense inflation stars and bosonova has not been considered by Padilla *et al.* [331]. The critical decay constant f_{crit} becomes on the order of the Planck scale $M_P c^2$ [or $|\lambda_{\text{crit}}| \sim (m/M_P)^2$ and $|(a_s)_{\text{crit}}| \sim 2Gm/c^2$], allowing the formation of PBHs [331], in much more massive inflaton clusters of mass $M_h \sim 10^{14}$ g or larger. This essentially returns the results of Sec. X B because for $f \sim M_P c^2$ we are in the noninteracting limit. For $f \lesssim M_P c^2$, the attractive self-interaction may facilitate the formation of PBHs in sufficiently massive inflaton clusters.

Remark.— Equations (147)–(156) are valid in the non-relativistic limit. When $a_s \leq 0$, we can easily extend our results to the relativistic regime by making the substitution $a_s \rightarrow a_s - \kappa Gm/c^2$ [see Eq. (96)] with $\kappa_G = 2.50$. In that case, the maximum mass $(M_c)_{\text{max}}$ in Fig. 10 is given by Eq. (119). It returns $M_{\text{max}}^{\text{NR}}$ [see Eq. (39)] when $|a_s| \gg (a_s)_t$ and $M_{\text{max,NL}}^{\text{GR}}$ [see Eq. (62)] when $|a_s| \ll (a_s)_t$. If we make the substitution from Eq. (96) in Eq. (162) and take $a_s = 0$ [which is equivalent to directly taking $a_s = -\kappa Gm/c^2$ in Eq. (162)], we get $(M_h)_{\text{max}} = 0.0357 c^4 / (G^2 \Sigma_0) = 6.47 \times 10^{14}$ g (we have used $\kappa_G = 2.50$). This value can be compared to the value $M_h = 6.49 \times 10^{-3} c^4 / (G^2 \Sigma_0) = 1.18 \times 10^{14}$ g obtained in Sec. X B. On the other hand, for $f \sim f_t \sim M_P c^2 / 8\sqrt{\pi}$ (see Sec. IX), we find that $(M_h)_{\text{max}} \sim 0.0558 c^4 / (G^2 \Sigma_0)$. This result qualitatively agrees with the value obtained in the noninteracting case.

E. Virial mass

Following our previous works [267,321–323], we have defined the halo mass M_h and the halo radius r_h such that r_h represents the distance at which the central density is divided by 4. However, some authors [269,324,331] use another definition of the halo mass and halo radius. They introduce the virial mass M_v and the virial radius r_v through the relation

$$M_v = \frac{4}{3} \pi \rho_{200} r_v^3, \quad (164)$$

³⁵It is comparable to the core mass corresponding to $a_s = 0$ on account of the remark following Eq. (163). On the other hand, for $m = 6.35 \times 10^{-6} M_P$ and $|\lambda| \sim 1$, we have $f \sim 3.17 \times 10^{-6} M_P c^2$ [see Eq. (131)]. According to Eq. (162), the quantum core becomes unstable in a halo of mass $(M_h)_{\text{max}} = 4.13 \times 10^{-3}$ g. The critical core mass is then $(M_c)_{\text{max}} = 5.44 M_P = 1.18 \times 10^{-4}$ g.

where $\rho_{200} = 200\rho_b$ is 200 times the background density. Using

$$\frac{GM_v}{r_v} \sim \frac{GM_h}{r_h}, \quad (165)$$

in consistency with Eq. (147), and combining this relation with Eqs. (150) and (164), we obtain

$$M_h \sim \frac{1}{1.76\Sigma_0} \left(\frac{4}{3} \pi \rho_{200} \right)^{2/3} M_v^{4/3}. \quad (166)$$

The relation between the halo mass M_h and the virial mass M_v exhibits the scaling $M_h \propto M_v^{4/3}$ [321]. We can use this relation to express the previous results in terms of M_v instead of M_h . In particular, we find $M_c \propto M_v^{1/3}$ for noninteracting bosons (in agreement with [269]) and $M_c \propto M_v^{2/3}$ for bosons with a repulsive self-interaction in the TF limit [322].

XI. CONCLUSION

In this paper, by using simple considerations, we have obtained general approximate analytical expressions for the maximum mass and the minimum radius of relativistic self-gravitating Bose-Einstein condensates at $T = 0$ with repulsive or attractive $|\varphi|^4$ self-interaction (see Sec. VIII for a summary).

For boson stars with a repulsive self-interaction, our analytical expressions [see Eqs. (122)–(125)] interpolate between the maximum mass and minimum radius [see Eq. (62)] of noninteracting bosons stars [1,2] and the maximum mass and minimum radius [see Eq. (64)] of bosons stars with a strong self-interaction (TF limit) [58,86]. The noninteracting regime is valid for $a_s \ll r_s = 2Gm/c^2$ or $\lambda \ll (m/M_P)^2$ and the TF regime is valid for $a_s \gg r_s = 2Gm/c^2$ or $\lambda \gg (m/M_P)^2$. In all cases, the maximum mass has a general relativistic origin, i.e., it is due to the fact that the radius of the star approaches the Schwarzschild radius (strong gravity). Above the maximum mass, there is no equilibrium state and the boson star collapses toward a black hole.

For boson stars with an attractive self-interaction (axion stars), our analytical expressions [see Eqs. (126)–(129)] interpolate between the general relativistic maximum mass and minimum radius [see Eq. (62)] of noninteracting bosons stars [1,2] and the nonrelativistic maximum mass and minimum radius [see Eqs. (39) and (40)] of boson stars with a strong self-interaction [265]. When $|a_s| \ll r_s = 2Gm/c^2$, $|\lambda| \ll (m/M_P)^2$, or $f \gg M_P c^2$ (noninteracting regime), the maximum mass has a general relativistic origin (strong gravity). Above that mass, the boson star collapses toward a black hole. When $|a_s| \gg r_s = 2Gm/c^2$, $|\lambda| \gg (m/M_P)^2$, or $f \ll M_P c^2$ (nonrelativistic regime), the maximum mass is essentially

due to the attractive self-interaction of the bosons and to relativistic corrections in the kinetic energy (or quantum potential) of the BEC (weak gravity). Above that mass, the dilute axion star collapses toward a dense axion star or explodes in a bosenova [it can collapse toward a black hole only if it has a very large mass $M > M_{\text{max,dense}}^{\text{GR}}$ given by Eqs. (145) and (146)].

We have confirmed the existence of a triple point at $(a_s, M) \sim (-r_s, M_{\text{Kaup}})$ separating boson stars, black holes, and dense axion stars or bosenova. We have considered applications of these results to DM halos and inflaton clusters. We have shown that the quantum core of DM halos is stable, in general (it would collapse toward a black hole in DM halos of mass $M_h > 10^{14} M_\odot$, which are not realistic and it would form a dense axion star or a bosenova in realistic halos of mass $M_h < 10^{14} M_\odot$ provided that $f < 10^{15}$ GeV, which seems to be excluded by constraints from cosmology and particle physics).³⁶ We have also discussed the possibility to form PBHs in inflaton clusters [331]. We have shown that, for noninteracting bosons of mass $m \sim 10^{-5} M_P$, the quantum core (inflaton star) of an inflaton cluster can collapse toward a black hole only if the inflaton cluster is sufficiently massive, on the order of $M_h \sim 10^{14}$ g. In that case, we form a PBH of mass ~ 1 g. In less massive inflaton clusters, the quantum core is stable and no black hole can form. We have mentioned that the amount of PBHs formed by this mechanism may not be very large and that PBHs of mass ~ 1 g quickly evaporate ($t_{\text{evap}} \sim 10^{-30}$ s). For bosons with a repulsive self-interaction, the mass of the PBHs is larger and their evaporation time longer (but still short). For bosons with an attractive self-interaction, we have shown similarly that PBHs of mass ~ 1 g can form only in sufficiently massive inflaton clusters of mass $M_h \sim 10^{14}$ g or larger. The attractive self-interaction facilitates the collapse of the quantum core (inflaton star). On the other hand, we have suggested that, in smaller inflaton clusters, for a sufficiently strong attractive self-interaction, the inflaton star could become unstable and collapse toward a dense inflaton star or explode in a bosenova (for $f \sim 10^{14}$ GeV the quantum core of an inflaton cluster of mass $M_h \sim 1$ g collapses toward a dense axion star of mass $M_c \sim 10^{-4}$ g). The collapse of the core cannot lead to a PBH in that case because the core is not massive enough. The possibility to form dense inflaton stars and bosenova was not considered by Padilla *et al.* [331] and deserves a specific study [353].

Our analytical results have been obtained from a Gaussian ansatz. This Gaussian ansatz provides a good approximation of the exact maximum mass of nonrelativistic boson stars with an attractive self-interaction [265,290]. It also provides

³⁶We have, however, considered the possibility that these constraints may be bypassed and that the quantum core of DM halos may be unstable.

a good approximation of the exact maximum mass of noninteracting relativistic boson stars (see the Remarks at the end of Secs. VII B and VII C). It is expected to provide relatively accurate results in more general cases.

Fermion stars, such as white dwarfs and neutron stars also possess a maximum mass due to special or general relativity. The study of DM halos made of fermions (like sterile neutrinos) is also of interest and can be investigated with methods similar to those exposed in this paper (see, e.g., [264,265,322,323,354] for the development of the analogy between bosonic and fermionic DM).

APPENDIX A: GAUSSIAN ANSATZ TO EVALUATE THE RELATIVISTIC CORRECTION TO THE QUANTUM KINETIC ENERGY

For spherically symmetric density profiles, the relativistic correction to the quantum kinetic energy of self-gravitating BECs can be written as [see Eq. (90)]

$$E_R = \frac{\hbar^2}{m^2 c^2} \int_0^{+\infty} \left(\frac{d\sqrt{\rho}}{dr} \right)^2 \Phi(r) 4\pi r^2 dr. \quad (\text{A1})$$

Making a Gaussian ansatz for the density profile

$$\rho(r) = \frac{M}{R^3} \frac{1}{\pi^{3/2}} e^{-r^2/R^2}, \quad (\text{A2})$$

we get

$$E_R = \frac{\hbar^2 M}{m^2 c^2 R^7} \frac{4}{\sqrt{\pi}} \int_0^{+\infty} e^{-r^2/R^2} \Phi(r) r^4 dr. \quad (\text{A3})$$

We will evaluate $\Phi(r)$ in two different manners.

1. First approach

Following [343,345], we make the approximation

$$\Phi(r) = -\frac{GM(r)}{r}, \quad (\text{A4})$$

where

$$M(r) = \int_0^r \rho(r') 4\pi r'^2 dr' \quad (\text{A5})$$

is the mass contained within the sphere of radius r . In that case, Eq. (A3) becomes

$$E_R = -\frac{\hbar^2 GM}{m^2 c^2 R^7} \frac{4}{\sqrt{\pi}} \int_0^{+\infty} e^{-r^2/R^2} M(r) r^3 dr. \quad (\text{A6})$$

With the Gaussian ansatz from Eq. (A2), we have

$$M(r) = \frac{4M}{\sqrt{\pi}} \mathcal{M}\left(\frac{r}{R}\right), \quad (\text{A7})$$

where

$$\mathcal{M}(x) = \int_0^x e^{-y^2} y^2 dy = \frac{\sqrt{\pi}}{4} \text{erf}(x) - \frac{1}{2} x e^{-x^2}. \quad (\text{A8})$$

Substituting Eqs. (A7) and (A8) into Eq. (A6), we obtain

$$E_R = -\frac{16 G \hbar^2 M^2}{\pi m^2 c^2 R^3} \int_0^{+\infty} e^{-x^2} \mathcal{M}(x) x^3 dx. \quad (\text{A9})$$

This leads to the expression from Eq. (92) with the coefficient

$$\chi_G = \frac{16}{\pi} \int_0^{+\infty} e^{-x^2} \mathcal{M}(x) x^3 dx = \frac{7}{4\sqrt{2\pi}} \simeq 0.698. \quad (\text{A10})$$

2. Second approach

For spherically symmetric systems, the gravitational potential can be determined (without approximation at that stage) from Newton's law

$$\frac{d\Phi}{dr}(r) = \frac{GM(r)}{r^2}. \quad (\text{A11})$$

Using Eq. (A7) and integrating Eq. (A11) with the condition $\Phi(r) \sim -GM/r$ at infinity, we obtain

$$\Phi(r) = -\frac{4GM}{\sqrt{\pi}R} \int_{r/R}^{+\infty} \frac{\mathcal{M}(x)}{x^2} dx = -\frac{GM}{r} \text{erf}\left(\frac{r}{R}\right). \quad (\text{A12})$$

In that case, Eq. (A3) becomes

$$E_R = -\frac{\hbar^2 GM^2}{m^2 c^2 R^3} \frac{4}{\sqrt{\pi}} \int_0^{+\infty} e^{-x^2} \text{erf}(x) x^3 dx. \quad (\text{A13})$$

This leads to the expression from Eq. (92) with the coefficient

$$\chi_G = \frac{4}{\sqrt{\pi}} \int_0^{+\infty} e^{-x^2} \text{erf}(x) x^3 dx = \frac{5}{2\sqrt{2\pi}} \simeq 0.997. \quad (\text{A14})$$

APPENDIX B: RELATIVISTIC COMPLEX SF

In this appendix, we discuss the main properties of a relativistic complex self-interacting SF, establish its hydrodynamic representation, make the TF approximation, and determine its equation of state $P(\epsilon)$ for an arbitrary self-interaction potential $V(|\varphi|^2)$. For a $|\varphi|^4$ self-interaction, we justify the equation of state introduced by Colpi *et al.* [58]. We also justify the GPP equations (1) and (2) in the nonrelativistic limit $c \rightarrow +\infty$.

1. Klein-Gordon-Einstein equations

We consider a relativistic complex SF $\varphi(x^\mu) = \varphi(x, y, z, t)$, which is a continuous function of space and time. It can represent the wave function of a relativistic BEC [20,87]. The total action of the system, which is the sum of the Einstein-Hilbert action of general relativity plus the action of the SF, can be written as

$$S = \int \left(\frac{c^4}{16\pi G} R + \mathcal{L} \right) \sqrt{-g} d^4x, \quad (\text{B1})$$

where R is the Ricci scalar curvature, $\mathcal{L} = \mathcal{L}(\varphi, \varphi^*, \partial_\mu \varphi, \partial_\mu \varphi^*)$ is the Lagrangian density of the SF, and $g = \det(g_{\mu\nu})$ is the determinant of the metric tensor. We consider a canonical Lagrangian density of the form

$$\mathcal{L} = \frac{1}{2} g^{\mu\nu} \partial_\mu \varphi^* \partial_\nu \varphi - V_{\text{tot}}(|\varphi|^2), \quad (\text{B2})$$

where the first term is the kinetic energy and the second term is minus the potential energy. The potential energy can be decomposed into a rest-mass energy term and a self-interaction energy term,

$$V_{\text{tot}}(|\varphi|^2) = \frac{m^2 c^2}{2\hbar^2} |\varphi|^2 + V(|\varphi|^2). \quad (\text{B3})$$

The least action principle $\delta S = 0$ with respect to variations $\delta\varphi$ (or $\delta\varphi^*$), which is equivalent to the Euler-Lagrange equation

$$D_\mu \left[\frac{\partial \mathcal{L}}{\partial(\partial_\mu \varphi)^*} \right] - \frac{\partial \mathcal{L}}{\partial \varphi^*} = 0, \quad (\text{B4})$$

yields the KG equation

$$\square \varphi + 2 \frac{dV_{\text{tot}}}{d|\varphi|^2} \varphi = 0, \quad (\text{B5})$$

where $\square = D_\mu \partial^\mu = \frac{1}{\sqrt{-g}} \partial_\mu (\sqrt{-g} g^{\mu\nu} \partial_\nu)$ is the d'Alembertian operator. For a free massless SF ($V_{\text{tot}} = 0$), the KG equation reduces to $\square \varphi = 0$. On the other hand, using the decomposition from Eq. (B3) we can rewrite the KG equation (B5) as

$$\square \varphi + \frac{m^2 c^2}{\hbar^2} \varphi + 2 \frac{dV}{d|\varphi|^2} \varphi = 0. \quad (\text{B6})$$

The least action principle $\delta S = 0$ with respect to variations $\delta g^{\mu\nu}$ yields the Einstein field equations

$$R_{\mu\nu} - \frac{1}{2} g_{\mu\nu} R = \frac{8\pi G}{c^4} T_{\mu\nu}, \quad (\text{B7})$$

where $R_{\mu\nu}$ is the Ricci tensor and $T_{\mu\nu}$ is the energy-momentum (stress) tensor given by

$$T_{\mu\nu} = \frac{2}{\sqrt{-g}} \frac{\delta S}{\delta g^{\mu\nu}} = \frac{2}{\sqrt{-g}} \frac{\partial(\sqrt{-g}\mathcal{L})}{\partial g^{\mu\nu}} = 2 \frac{\partial \mathcal{L}}{\partial g^{\mu\nu}} - g_{\mu\nu} \mathcal{L}. \quad (\text{B8})$$

For a complex SF, the energy-momentum tensor takes the form

$$T_\mu^\nu = \frac{\partial \mathcal{L}}{\partial(\partial_\nu \varphi)} \partial_\mu \varphi + \frac{\partial \mathcal{L}}{\partial(\partial_\nu \varphi^*)} \partial_\mu \varphi^* - g_\mu^\nu \mathcal{L}. \quad (\text{B9})$$

For the Lagrangian (B2), we get

$$T_{\mu\nu} = \frac{1}{2} (\partial_\mu \varphi^* \partial_\nu \varphi + \partial_\nu \varphi^* \partial_\mu \varphi) - g_{\mu\nu} \mathcal{L}. \quad (\text{B10})$$

Equations (B5) and (B7) with Eq. (B10) form the KGE equations.

The conservation of the energy-momentum tensor, which results from the invariance of the Lagrangian density under continuous translations in space and time (Noether theorem), reads

$$D_\nu T^{\mu\nu} = 0. \quad (\text{B11})$$

The conservation of the energy-momentum tensor is automatically included in the Einstein equations through the contracted Bianchi identities. The energy-momentum four-vector is $P^\mu = \int T^{\mu 0} \sqrt{-g} d^3x$. Its time component P^0 is the energy, while (P^1, P^2, P^3) are the components of the impulse \mathbf{P} . Each component of P^μ is conserved in time, i.e., it is a constant of the motion. Indeed,

$$\begin{aligned} \dot{P}^\mu &= \frac{d}{dt} \int T^{\mu 0} \sqrt{-g} d^3x = c \int \partial_0 (T^{\mu 0} \sqrt{-g}) d^3x \\ &= -c \int \partial_i (T^{\mu i} \sqrt{-g}) d^3x = 0, \end{aligned} \quad (\text{B12})$$

where we have used Eq. (B11) with $D_\mu V^\mu = \frac{1}{\sqrt{-g}} \partial_\mu (\sqrt{-g} V^\mu)$ to get the third equality.

The current of charge of a complex SF is given by

$$J^\mu = \frac{m}{i\hbar} \left[\varphi \frac{\partial \mathcal{L}}{\partial(\partial_\mu \varphi)} - \varphi^* \frac{\partial \mathcal{L}}{\partial(\partial_\mu \varphi^*)} \right]. \quad (\text{B13})$$

For the Lagrangian (B2), we obtain

$$J_\mu = -\frac{m}{2i\hbar} (\varphi^* \partial_\mu \varphi - \varphi \partial_\mu \varphi^*). \quad (\text{B14})$$

Using the KG equation (B5), one can show that

$$D_\mu J^\mu = 0. \quad (\text{B15})$$

This equation expresses the local conservation of the charge. The total charge of the SF is $Q = \frac{e}{mc} \int J^0 \sqrt{-g} d^3x$. Proceeding as above, we easily find that $\dot{Q} = 0$. The charge Q is proportional to the number N of bosons provided that antibosons are counted negatively [355]. Therefore, Eq. (B15) also expresses the local conservation of the boson number ($Q = Ne$). This conservation law results via the Noether theorem from the global $U(1)$ symmetry of the Lagrangian, i.e., from the invariance of the Lagrangian density under a global phase transformation $\varphi \rightarrow \varphi e^{-i\theta}$ (rotation) of the complex SF. Note that J_μ vanishes for a real SF so that the charge and the particle number are not conserved in that case.

2. Hydrodynamic representation

We can write the KG equation (B5) under the form of hydrodynamic equations by using the de Broglie transformation [356–358]. To that purpose, we write the SF as

$$\varphi = \frac{\hbar}{m} \sqrt{\rho} e^{im\theta/\hbar}, \quad (\text{B16})$$

where ρ is the pseudo-rest-mass density³⁷ and $\theta = S_{\text{tot}}/m$ (\sim phase) is the action by unit of mass. They satisfy

$$\rho = \frac{m^2}{\hbar^2} |\varphi|^2 \quad \text{and} \quad \theta = \frac{\hbar}{2mi} \ln\left(\frac{\varphi}{\varphi^*}\right). \quad (\text{B17})$$

Substituting Eq. (B16) into the Lagrangian density (B2), we obtain

$$\mathcal{L} = \frac{1}{2} g^{\mu\nu} \rho \partial_\mu \theta \partial_\nu \theta + \frac{\hbar^2}{8m^2 \rho} g^{\mu\nu} \partial_\mu \rho \partial_\nu \rho - V_{\text{tot}}(\rho) \quad (\text{B18})$$

with

$$V_{\text{tot}}(\rho) = \frac{1}{2} \rho c^2 + V(\rho). \quad (\text{B19})$$

The Euler-Lagrange equations for θ and ρ , resulting from the least action principle, are

$$D_\mu \left[\frac{\partial \mathcal{L}}{\partial(\partial_\mu \theta)} \right] - \frac{\partial \mathcal{L}}{\partial \theta} = 0, \quad D_\mu \left[\frac{\partial \mathcal{L}}{\partial(\partial_\mu \rho)} \right] - \frac{\partial \mathcal{L}}{\partial \rho} = 0. \quad (\text{B20})$$

They yield the equations of motion [20,87]

$$D_\mu(\rho \partial^\mu \theta) = 0, \quad (\text{B21})$$

$$\frac{1}{2} \partial_\mu \theta \partial^\mu \theta - \frac{\hbar^2}{2m^2} \frac{\square \sqrt{\rho}}{\sqrt{\rho}} - V'_{\text{tot}}(\rho) = 0. \quad (\text{B22})$$

³⁷We stress that ρ is *not* the rest-mass density. It is only in the nonrelativistic regime $c \rightarrow +\infty$ that ρ coincides with the rest-mass density.

The same equations are obtained by substituting the de Broglie transformation from Eq. (B16) into the KG equation (B5) and separating the real and the imaginary parts.³⁸ Equation (B21) can be interpreted as a continuity equation and Eq. (B22) can be interpreted as a quantum relativistic Hamilton-Jacobi (or Bernoulli) equation with a relativistic covariant quantum potential

$$Q_{\text{dB}} = \frac{\hbar^2}{2m} \frac{\square \sqrt{\rho}}{\sqrt{\rho}}. \quad (\text{B23})$$

The energy-momentum tensor is given, in the hydrodynamic representation, by

$$T_\mu^\nu = \frac{\partial \mathcal{L}}{\partial(\partial_\nu \theta)} \partial_\mu \theta + \frac{\partial \mathcal{L}}{\partial(\partial_\nu \rho)} \partial_\mu \rho - g_\mu^\nu \mathcal{L}. \quad (\text{B24})$$

For the Lagrangian (B18), we obtain

$$T_{\mu\nu} = \rho \partial_\mu \theta \partial_\nu \theta + \frac{\hbar^2}{4m^2 \rho} \partial_\mu \rho \partial_\nu \rho - g_{\mu\nu} \mathcal{L}. \quad (\text{B25})$$

This result can also be obtained from Eq. (B10) by using Eq. (B16).

The current of charge of a complex SF is given, in the hydrodynamic representation, by

$$J^\mu = -\frac{\partial \mathcal{L}}{\partial(\partial_\mu \theta)}. \quad (\text{B26})$$

For the Lagrangian (B18), we obtain

$$J_\mu = -\rho \partial_\mu \theta. \quad (\text{B27})$$

This result can also be obtained from Eq. (B14) by using Eq. (B16). We then see that the continuity equation (B21) is equivalent to Eq. (B15). It expresses the local conservation of the charge Q of the SF (or the local conservation of the boson number N): $Q = Ne = -\frac{e}{mc} \int \rho \partial^0 \theta \sqrt{-g} d^3x$.

3. TF approximation

In the classical limit or in the TF approximation ($\hbar \rightarrow 0$), the Lagrangian from Eq. (B18) reduces to

$$\mathcal{L} = \frac{1}{2} g^{\mu\nu} \rho \partial_\mu \theta \partial_\nu \theta - V_{\text{tot}}(\rho). \quad (\text{B28})$$

The Euler-Lagrange equations (B20) yield the equations of motion

$$D_\mu(\rho \partial^\mu \theta) = 0, \quad (\text{B29})$$

$$\frac{1}{2} \partial_\mu \theta \partial^\mu \theta - V'_{\text{tot}}(\rho) = 0. \quad (\text{B30})$$

³⁸The quantity $v_\mu = \partial_\mu \theta$ could be interpreted as a pseudoquadrivelocity but it does not satisfy the identity $v_\mu v^\mu = c^2$ [20,87].

The same equations are obtained by making the TF approximation in Eq. (B22), i.e., by neglecting the quantum potential. Equation (B29) can be interpreted as a continuity equation and Eq. (B30) can be interpreted as a classical relativistic Hamilton-Jacobi (or Bernoulli) equation. We note that the continuity equation is not affected by the TF approximation.

Assuming $V'_{\text{tot}} > 0$, and using Eq. (B30), we introduce the fluid quadrivelocity

$$u_\mu = -\frac{\partial_\mu \theta}{\sqrt{2V'_{\text{tot}}(\rho)}} c, \quad (\text{B31})$$

which satisfies the identity $u_\mu u^\mu = c^2$. The energy-momentum tensor is given by Eq. (B24). For the Lagrangian (B28), we obtain

$$T_{\mu\nu} = \rho \partial_\mu \theta \partial_\nu \theta - g_{\mu\nu} \mathcal{L}. \quad (\text{B32})$$

This expression can also be obtained from Eq. (B25) by making the TF approximation. Using Eq. (B31), we get

$$T_{\mu\nu} = 2\rho V'_{\text{tot}}(\rho) \frac{u_\mu u_\nu}{c^2} - g_{\mu\nu} \mathcal{L}. \quad (\text{B33})$$

The energy-momentum tensor (B33) can be written under the perfect fluid form

$$T_{\mu\nu} = (\epsilon + P) \frac{u_\mu u_\nu}{c^2} - P g_{\mu\nu}, \quad (\text{B34})$$

where ϵ is the energy density and P is the pressure, provided that we make the identifications

$$P = \mathcal{L}, \quad \epsilon + P = 2\rho V'_{\text{tot}}(\rho). \quad (\text{B35})$$

Therefore, the Lagrangian plays the role of the pressure of the fluid. Combining Eq. (B28) with the Bernoulli equation (B30), we get

$$\mathcal{L} = \rho V'_{\text{tot}}(\rho) - V_{\text{tot}}(\rho). \quad (\text{B36})$$

Therefore, according to Eqs. (B35) and (B36), the energy density and the pressure derived from the Lagrangian (B28) are given by [87,346]

$$\epsilon = \rho V'_{\text{tot}}(\rho) + V_{\text{tot}}(\rho) = \rho c^2 + \rho V'(\rho) + V(\rho), \quad (\text{B37})$$

$$P = \rho V'_{\text{tot}}(\rho) - V_{\text{tot}}(\rho) = \rho V'(\rho) - V(\rho), \quad (\text{B38})$$

where we have used Eq. (B19) to get the second equalities.³⁹ Eliminating ρ between Eqs. (B37) and (B38), we obtain the

³⁹Equations (B37) and (B38) can also be derived for a cosmological homogeneous SF from its hydrodynamic representation or from the virial theorem in the fast oscillation regime [346].

equation of state $P(\epsilon)$. On the other hand, Eq. (B38) can be integrated into [87]

$$V(\rho) = \rho \int \frac{P(\rho)}{\rho^2} d\rho. \quad (\text{B39})$$

Equation (B38) determines $P(\rho)$ as a function of $V(\rho)$, while Eq. (B39) determines $V(\rho)$ as a function of $P(\rho)$.

4. Rest-mass density

In the TF approximation, using Eqs. (B27) and (B31), we can write the current as

$$J_\mu = \rho \sqrt{\frac{2}{c^2} V'_{\text{tot}}(\rho)} u_\mu. \quad (\text{B40})$$

The rest-mass density $\rho_m = nm$, which is related to the charge density $\rho_e = ne$ by $\rho_m = (m/e)\rho_e$, is such that

$$J_\mu = \rho_m u_\mu. \quad (\text{B41})$$

The continuity equation (B15) can then be written as

$$D_\mu(\rho_m u^\mu) = 0. \quad (\text{B42})$$

Comparing Eq. (B40) with Eq. (B41), we find that the rest-mass density of the SF is related to the pseudo-rest-mass density ρ by

$$\rho_m = \rho \sqrt{\frac{2}{c^2} V'_{\text{tot}}(\rho)} = \rho \sqrt{1 + \frac{2}{c^2} V'(\rho)}. \quad (\text{B43})$$

In general, $\rho_m \neq \rho$ except (i) for a noninteracting SF ($V = 0$), (ii) when V is constant, corresponding to the Λ FDM model (see Appendix E of [359]), (iii) and in the nonrelativistic limit $c \rightarrow +\infty$.

Remark.—More general results valid beyond the TF approximation are given in [87,360].

5. Gross-Pitaevskii-Einstein equations

In order to recover the GPP equations in the non-relativistic limit $c \rightarrow +\infty$, we make the Klein transformation (see, e.g., [20])

$$\varphi(\mathbf{r}, t) = \frac{\hbar}{m} e^{-imc^2 t/\hbar} \psi(\mathbf{r}, t), \quad (\text{B44})$$

where ψ is the pseudo-wave-function. The pseudo-rest-mass density [see Eq. (B17)] is related to the pseudo-wave-function by

$$\rho = |\psi|^2. \quad (\text{B45})$$

Mathematically, we can always make the change of variables from Eq. (B44). However, we emphasize that it

is only in the nonrelativistic limit $c \rightarrow +\infty$ that ψ has the interpretation of a wave function and that $\rho = |\psi|^2$ has the interpretation of a mass density.

Substituting Eq. (B44) into the KG equation (B5), we obtain after simplification the general relativistic GP equation [20,361]

$$i\hbar c \partial^0 \psi - \frac{\hbar^2}{2m} \square \psi + \frac{1}{2} m c^2 (g^{00} - 1) \psi + i \frac{\hbar c^2}{2} \square t \psi - m \frac{dV}{d|\psi|^2} \psi = 0. \quad (\text{B46})$$

We note that $\square t$ can be written as $\square t = -\frac{1}{c} g^{\mu\nu} \Gamma_{\mu\nu}^0$, where $\Gamma_{\mu\nu}^\sigma$ are the Christoffel symbols [20]. We can similarly express the energy-momentum tensor (B10) of the SF that appears in the Einstein equations (B7) in terms of the pseudo-wave-function ψ . This leads to the Gross-Pitaevskii-Einstein (GPE) equations.

6. Weak gravity limit

In the weak gravity limit of general relativity $\Phi/c^2 \ll 1$, using the simplest form of the conformal Newtonian gauge, the line element is given by

$$ds^2 = c^2 \left(1 + 2 \frac{\Phi}{c^2} \right) dt^2 - \left(1 - 2 \frac{\Phi}{c^2} \right) \delta_{ij} dx^i dx^j, \quad (\text{B47})$$

where $\Phi(\mathbf{r}, t)$ is the Newtonian potential.⁴⁰ In that limit, the Lagrangian of the SF is

$$\mathcal{L} = \frac{1}{2c^2} \left(1 - \frac{2\Phi}{c^2} \right) \left| \frac{\partial \varphi}{\partial t} \right|^2 - \frac{1}{2} \left(1 + \frac{2\Phi}{c^2} \right) |\nabla \varphi|^2 - \frac{m^2 c^2}{2\hbar^2} |\varphi|^2 - V(|\varphi|^2) \quad (\text{B48})$$

and the KGE equations reduce to [20,287,288]

$$\frac{1}{c^2} \frac{\partial^2 \varphi}{\partial t^2} - \left(1 + \frac{4\Phi}{c^2} \right) \Delta \varphi - \frac{4}{c^4} \frac{\partial \Phi}{\partial t} \frac{\partial \varphi}{\partial t} + \left(1 + \frac{2\Phi}{c^2} \right) \frac{m^2 c^2}{\hbar^2} \varphi + 2 \left(1 + 2 \frac{\Phi}{c^2} \right) \frac{dV}{d|\varphi|^2} \varphi = 0, \quad (\text{B49})$$

$$\begin{aligned} \frac{\Delta \Phi}{4\pi G} &= \frac{T_0^0}{c^2} \\ &= \frac{1}{2c^4} \left(1 - \frac{2\Phi}{c^2} \right) \left| \frac{\partial \varphi}{\partial t} \right|^2 \\ &\quad + \frac{1}{2c^2} \left(1 + \frac{2\Phi}{c^2} \right) |\nabla \varphi|^2 + \frac{m^2}{2\hbar^2} |\varphi|^2 + \frac{1}{c^2} V(|\varphi|^2). \end{aligned} \quad (\text{B50})$$

⁴⁰As in Refs. [20,287,288] we have neglected anisotropic stresses and assumed that the lapse function Ψ is equal to the Newtonian potential Φ . See [362,363] for a more general treatment.

Making the Klein transformation from Eq. (B44) into Eqs. (B48)–(B50), we obtain [20,287,288]

$$\begin{aligned} \mathcal{L} &= \frac{\hbar^2}{2m^2 c^2} \left(1 - \frac{2\Phi}{c^2} \right) \left| \frac{\partial \psi}{\partial t} \right|^2 \\ &\quad + \frac{i\hbar}{2m} \left(1 - \frac{2\Phi}{c^2} \right) \left(\psi^* \frac{\partial \psi}{\partial t} - \psi \frac{\partial \psi^*}{\partial t} \right) \\ &\quad - \frac{\hbar^2}{2m^2} \left(1 + \frac{2\Phi}{c^2} \right) |\nabla \psi|^2 - \Phi |\psi|^2 - V(|\psi|^2), \end{aligned} \quad (\text{B51})$$

$$\begin{aligned} i\hbar \frac{\partial \psi}{\partial t} - \frac{\hbar^2}{2m c^2} \frac{\partial^2 \psi}{\partial t^2} + \frac{\hbar^2}{2m} \left(1 + \frac{4\Phi}{c^2} \right) \Delta \psi - m \Phi \psi \\ - \left(1 + \frac{2\Phi}{c^2} \right) m \frac{dV}{d|\psi|^2} \psi + \frac{2\hbar^2}{m c^4} \frac{\partial \Phi}{\partial t} \left(\frac{\partial \psi}{\partial t} - \frac{i m c^2}{\hbar} \psi \right) = 0, \end{aligned} \quad (\text{B52})$$

$$\begin{aligned} \frac{\Delta \Phi}{4\pi G} &= \frac{T_0^0}{c^2} \\ &= \left(1 - \frac{\Phi}{c^2} \right) |\psi|^2 + \frac{1}{c^2} V(|\psi|^2) \\ &\quad + \frac{\hbar^2}{2m^2 c^4} \left(1 - \frac{2\Phi}{c^2} \right) \left| \frac{\partial \psi}{\partial t} \right|^2 + \frac{\hbar^2}{2m^2 c^2} \left(1 + \frac{2\Phi}{c^2} \right) |\nabla \psi|^2 \\ &\quad - \frac{\hbar}{m c^2} \left(1 - \frac{2\Phi}{c^2} \right) \text{Im} \left(\frac{\partial \psi}{\partial t} \psi^* \right). \end{aligned} \quad (\text{B53})$$

We note the identity

$$\text{Im} \left(\frac{\partial \psi}{\partial t} \psi^* \right) = \frac{1}{2i} \left(\psi^* \frac{\partial \psi}{\partial t} - \psi \frac{\partial \psi^*}{\partial t} \right). \quad (\text{B54})$$

Equations (B52) and (B53) form the GPE equations in the weak gravity limit. In the nonrelativistic limit $c \rightarrow +\infty$, they reduce to the GPP equations [20,287,288]

$$i\hbar \frac{\partial \psi}{\partial t} = -\frac{\hbar^2}{2m} \Delta \psi + m \Phi \psi + m \frac{dV}{d|\psi|^2} \psi, \quad (\text{B55})$$

$$\Delta \Phi = 4\pi G |\psi|^2. \quad (\text{B56})$$

In that case, the Lagrangian of the SF is

$$\begin{aligned} \mathcal{L} &= \frac{i\hbar}{2m} \left(\psi^* \frac{\partial \psi}{\partial t} - \psi \frac{\partial \psi^*}{\partial t} \right) \\ &\quad - \frac{\hbar^2}{2m^2} |\nabla \psi|^2 - \Phi |\psi|^2 - V(|\psi|^2). \end{aligned} \quad (\text{B57})$$

The GPP equations (B55) and (B56) can also be rewritten as a single equation

$$\begin{aligned} i\hbar \frac{\partial \psi}{\partial t} &= -\frac{\hbar^2}{2m} \Delta \psi + m \frac{dV}{d|\psi|^2} \psi \\ &\quad - \psi \int \frac{Gm}{|\mathbf{r} - \mathbf{r}'|} |\psi|^2(\mathbf{r}', t) d\mathbf{r}'. \end{aligned} \quad (\text{B58})$$

Remark.—We note that, for a complex SF, the potential $V(|\psi|^2)$, which occurs in the GP equation (B55), is equal to the potential $V(|\varphi|^2)$, which occurs in the KG equation (B6) up to the change of function from Eq. (B44), leading to

$$|\varphi|^2 = \frac{\hbar^2}{m^2} |\psi|^2. \quad (\text{B59})$$

This equivalence is no more true for a real SF (see [109] and Appendix C).

7. Hydrodynamic representation of the GPE equations in the weak gravity limit

We can write the GPE equations (B52) and (B53) in the form of hydrodynamic equations by making the Madelung transformation [289]

$$\psi(\mathbf{r}, t) = \sqrt{\rho(\mathbf{r}, t)} e^{iS(\mathbf{r}, t)/\hbar}, \quad (\text{B60})$$

$$\rho = |\psi|^2, \quad \mathbf{u}(\mathbf{r}, t) = \frac{\nabla S}{m}, \quad (\text{B61})$$

where ρ is the pseudo-rest-mass density, S is the pseudoaction, and \mathbf{u} is the pseudovelocity field (they coincide with the mass density, the action, and the velocity field in the nonrelativistic limit $c \rightarrow +\infty$).

Substituting Eqs. (B60) and (B61) into the GPE equations (B52) and (B53) and separating the real and the imaginary parts, we obtain the system of hydrodynamic equations [20,287,288]

$$\begin{aligned} \frac{\partial \rho}{\partial t} + \nabla \cdot (\rho \mathbf{u}) &= \frac{1}{mc^2} \frac{\partial}{\partial t} \left(\rho \frac{\partial S}{\partial t} \right) + \frac{4\rho}{mc^4} \frac{\partial \Phi}{\partial t} \left(mc^2 - \frac{\partial S}{\partial t} \right) \\ &\quad - \frac{4\Phi}{c^2} \nabla \cdot (\rho \mathbf{u}), \end{aligned} \quad (\text{B62})$$

$$\begin{aligned} \frac{\partial S}{\partial t} + \frac{(\nabla S)^2}{2m} &= -\frac{\hbar^2}{2mc^2} \frac{\partial^2 \sqrt{\rho}}{\partial t^2} + \left(1 + \frac{4\Phi}{c^2} \right) \frac{\hbar^2}{2m} \frac{\Delta \sqrt{\rho}}{\sqrt{\rho}} \\ &\quad - \frac{2\Phi}{mc^2} (\nabla S)^2 - m\Phi - \left(1 + \frac{2\Phi}{c^2} \right) mh(\rho) \\ &\quad + \frac{1}{2mc^2} \left(\frac{\partial S}{\partial t} \right)^2 + \frac{\partial \Phi}{\partial t} \frac{\hbar^2}{mc^4 \rho} \frac{\partial \rho}{\partial t}, \end{aligned} \quad (\text{B63})$$

$$\begin{aligned} \frac{\partial \mathbf{u}}{\partial t} + (\mathbf{u} \cdot \nabla) \mathbf{u} &= -\frac{\hbar^2}{2m^2 c^2} \nabla \left(\frac{\partial^2 \sqrt{\rho}}{\partial t^2} \right) \\ &\quad + \frac{\hbar^2}{2m^2} \nabla \left[\left(1 + \frac{4\Phi}{c^2} \right) \frac{\Delta \sqrt{\rho}}{\sqrt{\rho}} \right] - \nabla \Phi - \frac{1}{\rho} \nabla P \\ &\quad - \frac{2}{c^2} \nabla (h\Phi) - \frac{2}{c^2} \nabla (\Phi \mathbf{u}^2) + \frac{1}{2m^2 c^2} \nabla \left[\left(\frac{\partial S}{\partial t} \right)^2 \right] \\ &\quad + \frac{\hbar^2}{m^2 c^4} \nabla \left(\frac{\partial \Phi}{\partial t} \frac{1}{\rho} \frac{\partial \rho}{\partial t} \right), \end{aligned} \quad (\text{B64})$$

$$\begin{aligned} \frac{\Delta \Phi}{4\pi G} &= \frac{\hbar^2}{2m^2 c^4} \left(1 - \frac{2\Phi}{c^2} \right) \left[\frac{1}{4\rho} \left(\frac{\partial \rho}{\partial t} \right)^2 + \frac{\rho}{\hbar^2} \left(\frac{\partial S}{\partial t} \right)^2 \right] \\ &\quad + \frac{\hbar^2}{2m^2 c^2} \left(1 + \frac{2\Phi}{c^2} \right) \left[\frac{1}{4\rho} (\nabla \rho)^2 + \frac{\rho}{\hbar^2} (\nabla S)^2 \right] \\ &\quad - \left(1 - \frac{2\Phi}{c^2} \right) \frac{\rho}{mc^2} \frac{\partial S}{\partial t} + \left(1 - \frac{\Phi}{c^2} \right) \rho + \frac{1}{c^2} V(\rho), \end{aligned} \quad (\text{B65})$$

where $h(\rho)$ is the pseudoenthalpy defined by

$$h(\rho) = V'(\rho), \quad (\text{B66})$$

and $P(\rho)$ is the pseudopressure defined by the relation $h'(\rho) = P'(\rho)/\rho$, which can be integrated into $P(\rho) = \rho h(\rho) - \int h(\rho) d\rho$, yielding

$$P(\rho) = \rho V'(\rho) - V(\rho) = \rho^2 \left[\frac{V(\rho)}{\rho} \right]'. \quad (\text{B67})$$

Equation (B67) determines the equation of state $P(\rho)$ for a given self-interaction potential $V(\rho)$. Inversely, for a given equation of state, the self-interaction potential reads

$$V(\rho) = \rho \int \frac{P(\rho)}{\rho^2} d\rho. \quad (\text{B68})$$

The pseudo squared speed of sound is $c_s^2 = P'(\rho) = \rho V''(\rho)$. The hydrodynamic equations (B62)–(B65) have a clear physical interpretation. Equation (B62), corresponding to the imaginary part of the GPE equations, is the continuity equation expressing the conservation of the charge of the SF $Q = -(e/m^2 c^2) \int \rho (\partial S / \partial t - mc^2) (1 - 4\Phi/c^2) d\mathbf{r}$. Equation (B63), corresponding to the real part of the GPE equations, is the Hamilton-Jacobi (or Bernoulli) equation. Equation (B64), obtained by taking the gradient of Eq. (B63), is the momentum equation. Equation (B65) is the Einstein equation. We stress that the hydrodynamic equations (B62)–(B65) are equivalent to the GPE equations (B52) and (B53), which are themselves equivalent to the KGE equations (B49) and (B50).⁴¹ The corresponding Lagrangian is

$$\begin{aligned} \mathcal{L} &= \frac{\hbar^2}{2m^2 c^2} \left(1 - \frac{2\Phi}{c^2} \right) \left[\frac{1}{4\rho} \left(\frac{\partial \rho}{\partial t} \right)^2 + \frac{\rho}{\hbar^2} \left(\frac{\partial S}{\partial t} \right)^2 \right] \\ &\quad - \frac{\hbar^2}{2m^2} \left(1 + \frac{2\Phi}{c^2} \right) \left[\frac{1}{4\rho} (\nabla \rho)^2 + \frac{\rho}{\hbar^2} (\nabla S)^2 \right] \\ &\quad - \left(1 - \frac{2\Phi}{c^2} \right) \frac{\rho}{m} \frac{\partial S}{\partial t} - \Phi \rho - V(\rho). \end{aligned} \quad (\text{B69})$$

⁴¹We note that the Bernoulli equation (B63) is a second degree equation in $E = -\partial S / \partial t$, which can be solved easily. We can then substitute the solution into Eqs. (B62), (B64), and (B65) to get a closed reduced system of equations (see Ref. [20]).

In the nonrelativistic limit $c \rightarrow +\infty$, the Lagrangian reduces to

$$\mathcal{L} = -\frac{\rho}{m} \frac{\partial S}{\partial t} - \frac{\rho}{2m^2} (\nabla S)^2 - \frac{\hbar^2}{8m^2} \frac{(\nabla \rho)^2}{\rho} - \Phi \rho - V(\rho), \quad (\text{B70})$$

and we obtain the quantum Euler-Poisson equations [20,287,288]

$$\frac{\partial \rho}{\partial t} + \nabla \cdot (\rho \mathbf{u}) = 0, \quad (\text{B71})$$

$$\frac{\partial S}{\partial t} + \frac{(\nabla S)^2}{2m} = \frac{\hbar^2}{2m} \frac{\Delta \sqrt{\rho}}{\sqrt{\rho}} - m\Phi - mh(\rho), \quad (\text{B72})$$

$$\frac{\partial \mathbf{u}}{\partial t} + (\mathbf{u} \cdot \nabla) \mathbf{u} = \frac{\hbar^2}{2m^2} \nabla \left(\frac{\Delta \sqrt{\rho}}{\sqrt{\rho}} \right) - \nabla \Phi - \frac{1}{\rho} \nabla P, \quad (\text{B73})$$

$$\Delta \Phi = 4\pi G \rho, \quad (\text{B74})$$

where $h(\rho)$ and $P(\rho)$ are given by Eqs. (B66) and (B67) as before.

Remark.—In the TF approximation, we can neglect the terms containing \hbar . In that case, we have seen that the energy density ϵ and the pressure P are given by Eqs. (B37) and (B38). We note that Eq. (B38) coincides with Eq. (B67). By contrast, $\epsilon \neq T_0^0$ even if we use the Bernoulli equation to eliminate $\partial S / \partial t$.

8. $|\varphi|^4$ potential

We now consider a $|\varphi|^4$ (quartic) potential of the form

$$V(|\varphi|^2) = \frac{\lambda}{4\hbar c} |\varphi|^4, \quad (\text{B75})$$

where λ is the dimensionless self-interaction constant. For nonrelativistic BECs, the potential that occurs in the GP equation (1) is usually written as in Eq. (3). Substituting Eq. (B59) into Eq. (3), we get

$$V(|\varphi|^2) = \frac{2\pi a_s m}{\hbar^2} |\varphi|^4. \quad (\text{B76})$$

Comparing Eqs. (B75) and (B76), we obtain [307]

$$\frac{\lambda}{8\pi} = \frac{a_s m c}{\hbar} = \frac{a_s}{\lambda_C}, \quad (\text{B77})$$

where $\lambda_C = \hbar/mc$ is the Compton wavelength of the bosons. For the $|\varphi|^4$ model, the KG and GP equations take the form

$$\square \varphi + \frac{m^2 c^2}{\hbar^2} \varphi + \frac{8\pi a_s m}{\hbar^2} |\varphi|^2 \varphi = 0, \quad (\text{B78})$$

$$i\hbar \frac{\partial \psi}{\partial t} = -\frac{\hbar^2}{2m} \Delta \psi + m\Phi \psi + \frac{4\pi a_s \hbar^2}{m^2} |\psi|^2 \psi = 0. \quad (\text{B79})$$

In terms of the pseudo-rest-mass density [see Eqs. (B16) and (B17)], the potential (B76) can be written as

$$V(\rho) = \frac{2\pi a_s \hbar^2}{m^3} \rho^2. \quad (\text{B80})$$

Substituting Eq. (B80) into Eqs. (B37) and (B38), we obtain

$$\epsilon = \rho c^2 \left(1 + \frac{6\pi a_s \hbar^2}{m^3 c^2} \rho \right), \quad (\text{B81})$$

$$P = \frac{2\pi a_s \hbar^2}{m^3} \rho^2. \quad (\text{B82})$$

Eliminating ρ between these two equations, we get

$$P = \frac{m^3 c^4}{72\pi a_s \hbar^2} \left(\sqrt{1 + \frac{24\pi a_s \hbar^2}{m^3 c^4} \epsilon} \mp 1 \right)^2. \quad (\text{B83})$$

This relativistic equation of state $P(\epsilon)$ was first obtained by Colpi *et al.* [58] in the context of boson stars. It was studied in detail by Chavanis and Harko [86] in connection to general relativistic BEC stars and by Li *et al.* [364] and Suárez and Chavanis [346] in a BECDM cosmology (see also [87,298,360,365,366] for related studies). This equation of state reduces to that of an $n = 1$ polytrope [see Eq. (B82) with $\epsilon \sim \rho c^2$] at low densities $\rho \ll m^3 c^2 / |a_s| \hbar^2$ (nonrelativistic limit) and to the linear law $P \sim \epsilon/3$ similar to the equation of state of the radiation at high densities (ultrarelativistic limit).

Remark.—Sometimes, a $|\varphi|^4$ self-interaction potential is written as

$$V(|\varphi|^2) = \frac{m^2}{2\hbar^4} \lambda_s |\varphi|^4, \quad (\text{B84})$$

where λ_s is the dimensional self-interaction constant. Comparing Eq. (B84) with Eqs. (B75) and (B76), we get

$$\lambda_s = \frac{4\pi a_s \hbar^2}{m} = \frac{\lambda \hbar^3}{2m^2 c}. \quad (\text{B85})$$

APPENDIX C: RELATIVISTIC REAL SF

In this Appendix, we discuss the main properties of a relativistic real SF, consider the instantonic potential of axions, take the nonrelativistic limit, and justify the GPP equations (1)–(3) with $a_s < 0$.

1. Klein-Gordon-Einstein equations

For a real SF described by a canonical Lagrangian,

$$\mathcal{L} = \frac{1}{2} g^{\mu\nu} \partial_\mu \varphi \partial_\nu \varphi - \frac{m^2 c^2}{2\hbar^2} \varphi^2 - V(\varphi), \quad (\text{C1})$$

the KGE equations read

$$\square\varphi + \frac{m^2 c^2}{\hbar^2} \varphi + \frac{dV}{d\varphi} = 0, \quad (\text{C2})$$

$$R_{\mu\nu} - \frac{1}{2} g_{\mu\nu} R = \frac{8\pi G}{c^4} T_{\mu\nu}, \quad (\text{C3})$$

with the energy-momentum tensor

$$T_{\mu\nu} = \partial_\mu \varphi \partial_\nu \varphi - g_{\mu\nu} \mathcal{L}. \quad (\text{C4})$$

2. The nonrelativistic limit

In the nonrelativistic limit $c \rightarrow +\infty$, where the SF displays rapid oscillations, the KGE equations can be simplified by averaging over the oscillations. To that purpose, we write

$$\varphi(\mathbf{r}, t) = \frac{1}{\sqrt{2}} \frac{\hbar}{m} [\psi(\mathbf{r}, t) e^{-imc^2 t/\hbar} + \psi^*(\mathbf{r}, t) e^{imc^2 t/\hbar}], \quad (\text{C5})$$

where the complex wave function $\psi(\mathbf{r}, t)$ is a slowly varying function of time (the fast oscillations $e^{imc^2 t/\hbar}$ of the SF have been factored out). This transformation (which is the counterpart of the Klein transformation for a real SF) allows us to separate the fast oscillations of the SF with pulsation $\omega = mc^2/\hbar$ caused by its rest mass from the slow evolution of $\psi(\mathbf{r}, t)$. Using the simplest form of the Newtonian gauge [see Eq. (B47)], substituting Eq. (C5) into the KGE equations (C2)–(C4) and averaging over the oscillations, we obtain the GPE equations (B52) and (B53) with an effective potential $V_{\text{eff}}(|\psi|^2)$ [see Secs. II and III of Ref. [109] and Appendix A of Ref. [110] for the details of the derivation]. In the nonrelativistic limit $c \rightarrow +\infty$, we obtain the GPP equations (B55) and (B56) with $V_{\text{eff}}(|\psi|^2)$ instead of $V(|\psi|^2)$. For a real SF, the effective potential $V_{\text{eff}}(|\psi|^2)$ that occurs in the GP equations (B52) and (B55) is obtained from the potential $V(\varphi)$ that occurs in the KG equation (C2) by first substituting Eq. (C5) into $V(\varphi)$, then averaging over the oscillations. It is different from the potential that one would obtain by directly replacing φ^2 by $(\hbar/m)^2 |\psi|^2$ in the potential $V(\varphi)$.

Remark.—General relativistic boson stars described by a real SF have a naked singularity at the origin and are always unstable [92,93]. It is possible to construct regular solutions that are periodic in time provided that $M < M_{\text{max}}^{\text{GR}} = 0.606 M_P^2/m$ [111,112] but, on a long timescale (which can nevertheless exceed the age of the Universe), these oscillations are unstable and disperse to infinity or form a black hole. Their instability is basically due to the fact that the charge (boson number) is not conserved for a real SF. However, in the nonrelativistic limit, particle number conservation is approximately restored and Newtonian boson stars (like axion stars) can be stable (see Sec. III).

3. The instantonic potential of axions

Axions are hypothetical pseudo-Nambu-Goldstone bosons of the Peccei-Quinn phase transition associated with a $U(1)$ symmetry that solves the strong CP problem of QCD. The axion is a spin-0 particle with a very small mass $m = 10^{-4} \text{ eV}/c^2$ and an extremely weak self-interaction (with a decay constant $f = 5.82 \times 10^{10} \text{ GeV}$) arising from nonperturbative effects in QCD. Axions have huge occupation numbers, so they can be described by a classical relativistic quantum field theory with a real SF $\varphi(\mathbf{r}, t)$ whose evolution is governed by the KGE equations. The instantonic potential of axions is [300,367,368]

$$V(\varphi) = \frac{m^2 c f^2}{\hbar^3} \left[1 - \cos\left(\frac{\hbar^{1/2} c^{1/2} \varphi}{f}\right) \right] - \frac{m^2 c^2}{2\hbar^2} \varphi^2, \quad (\text{C6})$$

where m is the mass of the axion and f is the axion decay constant. For this potential, the KG equation (C2) takes the form

$$\square\varphi + \frac{m^2 c^{3/2} f}{\hbar^{5/2}} \sin\left(\frac{\hbar^{1/2} c^{1/2} \varphi}{f}\right) = 0. \quad (\text{C7})$$

This is the general relativistic sine-Gordon equation. Considering the dilute regime $\varphi \ll f/\sqrt{\hbar c}$ (which is valid, in particular, in the nonrelativistic limit $c \rightarrow +\infty$)⁴² and expanding the cosine term of Eq. (C6) in Taylor series, we obtain at leading order the φ^4 potential,

$$V(\varphi) = -\frac{m^2 c^3}{24 f^2 \hbar} \varphi^4. \quad (\text{C8})$$

In that case, the KG equation (C2) takes the form

$$\square\varphi + \frac{m^2 c^2}{\hbar^2} \varphi - \frac{m^2 c^3}{6 f^2 \hbar} \varphi^3 = 0. \quad (\text{C9})$$

In the nonrelativistic limit, the effective potential $V(|\psi|^2)$ appearing in the GP equation (B55) is given by [109,312]

$$V(|\psi|^2) = \frac{m^2 c f^2}{\hbar^3} \left[1 - \frac{\hbar^3 c}{2 f^2 m^2} |\psi|^2 - J_0\left(\sqrt{\frac{2 \hbar^3 c |\psi|^2}{f^2 m^2}}\right) \right], \quad (\text{C10})$$

where J_0 is the Bessel function of zeroth order.⁴³ If we keep only the first term in the expansion of Eq. (C10), we obtain the $|\psi|^4$ potential,

$$V(|\psi|^2) = -\frac{\hbar^3 c^3}{16 f^2 m^2} |\psi|^4. \quad (\text{C11})$$

⁴²According to Eq. (C11), the axion decay constant f scales as $c^{3/2}$.

⁴³For convenience, we write $V(|\psi|^2)$ instead of $V_{\text{eff}}(|\psi|^2)$ now that we have explained the meaning of the effective potential in Appendix C 2.

This approximation is valid for dilute axion stars satisfying $|\psi|^2 \ll f^2 m^2 / \hbar^3 c$. We note that $V(|\psi|^2) \equiv \overline{V(\varphi)}$ is different from the expression that one would have naively obtained by directly substituting $\varphi^2 = (\hbar/m)^2 |\psi|^2$ into Eq. (C6). The difference is already apparent in the first term of the expansion of the potential, which involves a coefficient $-1/16$ [see Eq. (C11)] instead of $-1/24$ [see Eq. (C8)]. They differ by a factor $2/3$. This is because φ is a real SF. Therefore, substituting φ (exact) from Eq. (C5) into $V(\varphi)$, then averaging over the oscillations, is different from substituting $\varphi^2 = (\hbar/m)^2 |\psi|^2$ (already averaged over the oscillations) into $V(\varphi)$.

In general, a quartic potential is written as

$$V(\varphi) = \frac{\lambda}{4\hbar c} \varphi^4, \quad (\text{C12})$$

where λ is the dimensionless self-interaction constant. Comparing Eqs. (C8) and (C12), we find that

$$\lambda = -\frac{m^2 c^4}{6f^2}. \quad (\text{C13})$$

On the other hand, comparing Eq. (C11) with Eq. (3), we obtain

$$a_s = -\frac{\hbar c^3 m}{32\pi f^2}. \quad (\text{C14})$$

Equations (C13) and (C14) then yield

$$\frac{\lambda}{8\pi} = \frac{2a_s mc}{3\hbar}. \quad (\text{C15})$$

The relation between λ and a_s is different for a real SF and for a complex SF (see Appendix B). They differ by a factor $2/3$ for the reason indicated previously.

We note that the self-interaction constant λ or the scattering length a_s is negative, so that the φ^4 self-interaction term for axions is “attractive.” This attraction is responsible for the collapse of dilute axion stars above the maximum mass $M_{\text{max}}^{\text{NR}}$ from Eq. (39) obtained in Refs. [265,307]. The next order φ^6 term in the expansion of the potential (C6) has been considered in Refs. [109,312] and turns out to be repulsive. This repulsion, which occurs at high densities and which has a relativistic origin, may stop the collapse of dilute axion stars and lead to the formation of dense axion stars [311] (see, however, footnote 18 concerning their possible instability with respect to relativistic decay).

APPENDIX D: SIMPLE MODEL OF EXTENDED ELEMENTARY PARTICLE

In the main text, we have considered a self-gravitating BEC made of N bosons of individual mass m . In the

nonrelativistic limit, the mass-radius relation of the BEC is given by Eq. (53). Using Eq. (130), this relation can be rewritten as

$$M = \frac{a \frac{\hbar^2}{Gm^2 R}}{1 - b^2 \frac{\lambda \hbar^3}{8\pi Gm^4 c R^2}}. \quad (\text{D1})$$

We now introduce a simple model of extended elementary particle.⁴⁴ We consider a quantum particle of mass m and we assume that it is confined by the gravitational potential created by its own wave function. More specifically, we assume that the wave function $\psi(\mathbf{r}, t)$ governed by the GP equation (1) determines the density profile $\rho(\mathbf{r}, t)$ of the particle through the relation $\rho = |\psi|^2$. The corresponding density $\rho(\mathbf{r}, t)$ creates, via the Poisson equation (2), a gravitational potential $\Phi(\mathbf{r}, t)$, which enters into the GP equation (1). Finally, we identify the mass $M = \int \rho d\mathbf{r}$ produced by ρ with the mass m of the particle. This model is similar to the model introduced by Diósi [369] who proposed that the spreading of the wave packet of a free particle is prevented by the gravitational potential created by its own wave function ψ . This interpretation gives to the Schrödinger-Poisson equation the status of a fundamental equation of physics (i.e., more than the Schrödinger equation alone). For the sake of generality, we complete this model by taking into account a possible self-interaction of the particle and consider the GPP equations (1) and (2) with an arbitrary value of a_s (or λ).

In this model, the mass-radius relation of the particle is obtained by setting $M = m$ in Eq. (D1), yielding

$$R^2 - a \frac{\hbar^2}{Gm^3} R - b^2 \frac{\lambda \hbar^3}{8\pi Gm^4 c} = 0. \quad (\text{D2})$$

The solution of this second degree equation is

$$R = \frac{a\hbar^2}{2Gm^3} \pm \sqrt{\frac{a^2 \hbar^4}{4G^2 m^6} + \frac{b^2 \lambda \hbar^3}{8\pi Gm^4 c}}. \quad (\text{D3})$$

We must select the sign $+$ when $\lambda \geq 0$, while the two signs are allowed when $\lambda < 0$.

1. No self-interaction

For a noninteracting particle ($\lambda = 0$), we obtain the mass-radius relation

$$R = a \frac{\hbar^2}{Gm^3}. \quad (\text{D4})$$

The exact prefactor is 9.95. This returns the result obtained in [210,234,369].⁴⁵

⁴⁴This model can be related to the models of extended particles listed in footnote 13.

⁴⁵These authors did not give the value of the prefactor.

Remark.—If we apply this model to the electron of mass $m = m_e = 9.11 \times 10^{-28}$ g, we obtain a radius

$$R \sim \frac{\hbar^2}{Gm_e^3} \sim \left(\frac{M_P}{m_e}\right)^2 \frac{\hbar}{m_e c} = 2.20 \times 10^{32} \text{ m}. \quad (\text{D5})$$

Since $M_P/m_e \sim 10^{20} \gg 1$, this radius is much larger than the Compton wavelength of the electron $\lambda_e = \hbar/(m_e c) = 3.86 \times 10^{-13}$ m, which provides an estimate of its typical size (see Appendix F for more details). Therefore, this model cannot describe the electron. This is because self-gravity is negligible at the scale of the electron (see Appendix D 6).

2. Repulsive self-interaction

For a repulsive self-interaction ($\lambda > 0$), the mass-radius relation is given by Eq. (D3) with the sign $+$. The radius R of the particle decreases with its mass m (see Fig. 11). For $m \rightarrow 0$ (noninteracting limit), we recover Eq. (D4). For $m \rightarrow +\infty$ (TF limit), we find that

$$R \sim b \sqrt{\frac{\lambda}{8\pi}} \left(\frac{\hbar^3}{Gm^4 c}\right)^{1/2}. \quad (\text{D6})$$

The exact prefactor is π . Therefore, the radius R behaves like m^{-3} when $m \ll m_a = (8\pi\hbar c/\lambda G)^{1/2}$ and like m^{-2} when $m \gg m_a = (8\pi\hbar c/\lambda G)^{1/2}$.

Actually, in the TF approximation, we can solve the problem exactly. Using Eq. (130), we can rewrite Eq. (33) as

$$\Delta\rho + \frac{8\pi Gm^4 c}{\lambda\hbar^3} \rho = 0. \quad (\text{D7})$$

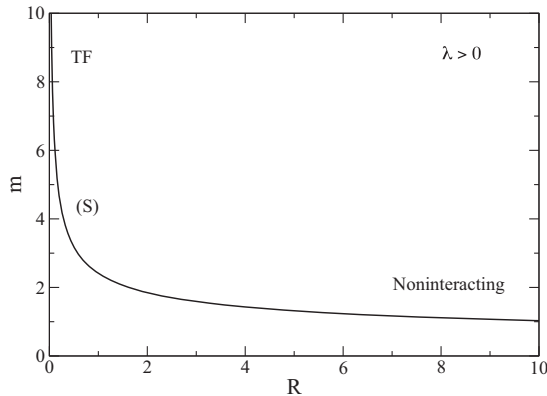


FIG. 11. Mass-radius relation of an extended elementary particle with $\lambda > 0$. The mass is normalized by $m_a = (8\pi/\lambda)^{1/2} M_P$ and the radius by $R_a = (\lambda/8\pi)^{3/2} l_P$ (this amounts to setting $\hbar = c = G = \lambda/8\pi = 1$ in the dimensional equations). We have taken $a = 9.946$ and $b = \pi$.

The density profile of the extended particle, which is determined by Eq. (D7), is given by [see Eq. (34)]

$$\rho(r) = \frac{\rho_0 R}{\pi r} \sin\left(\frac{\pi r}{R}\right). \quad (\text{D8})$$

Its radius is given by [see Eq. (35)]

$$R \sim \pi \sqrt{\frac{\lambda}{8\pi}} \left(\frac{\hbar^3}{Gm^4 c}\right)^{1/2} \quad (\text{D9})$$

and its central density is given by [see Eq. (36)]

$$\rho_0 = \frac{\pi m}{4R^3}. \quad (\text{D10})$$

On the other hand, according to Eq. (37), the total energy (gravitational + internal) of the particle is

$$E_{\text{tot}} = -\frac{Gm^2}{2R}. \quad (\text{D11})$$

Finally, its pulsation is on the order of the inverse dynamical time [see Eq. (38)]

$$t_D \sim \frac{1}{\sqrt{G\rho_0}} \sim \left(\frac{R^3}{Gm}\right)^{1/2}. \quad (\text{D12})$$

Remark.—If we apply this model to the electron of mass $m_e = 9.11 \times 10^{-28}$ g and radius $r_e = e^2/(m_e c^2) = 2.82 \times 10^{-15}$ m (see Appendix F), we find that the self-interaction constant must be equal to

$$\frac{\lambda}{8\pi} = \frac{\alpha^2}{\pi^2} \left(\frac{m_e}{M_P}\right)^2 = 9.45 \times 10^{-51}, \quad (\text{D13})$$

where α is the fine-structure constant (F4). However, the TF approximation is valid when $\lambda \gg (M_P/m_e)^2 = 5.71 \times 10^{44}$, so we see that this condition is not satisfied for a particle of mass $m_e \ll M_P$. Therefore, this model cannot describe the electron. This is because self-gravity is negligible at the scale of the electron (see Appendix D 6).

3. Attractive self-interaction

For an attractive self-interaction ($\lambda < 0$), the two signs are allowed in the mass-radius relation from Eq. (D3). This determines two branches of solutions. These two branches merge at the maximum mass (see Fig. 12)

$$m_{\text{max}} = \frac{a}{2b} \sqrt{\frac{8\pi}{|\lambda|}} \left(\frac{\hbar c}{G}\right)^{1/2}, \quad (\text{D14})$$

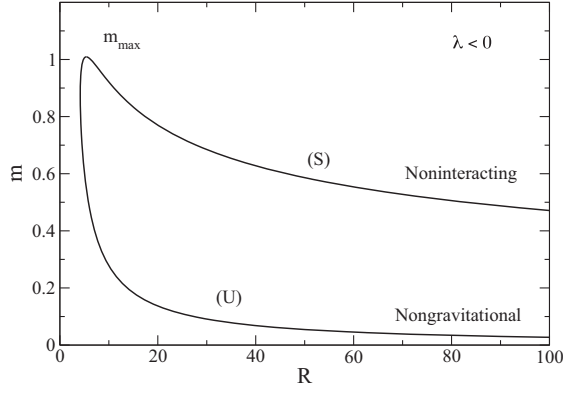


FIG. 12. Mass-radius relation of an extended elementary particle with $\lambda < 0$. The mass is normalized by $m_a = (8\pi/|\lambda|)^{1/2}M_P$ and the radius by $R_a = (|\lambda|/8\pi)^{3/2}l_P$ (this amounts to setting $\hbar = c = G = |\lambda|/8\pi = 1$ in the dimensional equations). We have taken $a = 11.1$ and $b = 5.5$.

corresponding to the radius

$$R_* = \frac{4b^3}{a^2} \left(\frac{|\lambda|}{8\pi} \right)^{3/2} \left(\frac{G\hbar}{c^3} \right)^{1/2}. \quad (\text{D15})$$

The exact prefactors are 1.012 and 5.5. The branch associated with the sign + corresponds to stable solutions. For $R \rightarrow +\infty$ and $m \rightarrow 0$ (noninteracting limit), we recover Eq. (D4). The branch associated with the sign - corresponds to unstable solutions. For $R \rightarrow +\infty$ and $m \rightarrow 0$ (nongravitational limit), we obtain

$$R \sim \frac{b^2 |\lambda| \hbar}{a 8\pi mc}, \quad (\text{D16})$$

where $\hbar/(mc)$ is the Compton wavelength of the particle. The exact prefactor is 3.64.

For $\lambda \sim 1$, the maximum mass is on the order of the Planck mass $M_P = (\hbar c/G)^{1/2} = 2.18 \times 10^{-5}$ g and the corresponding radius is on the order of the Planck length $l_P = (G\hbar/c^3)^{1/2} = 1.62 \times 10^{-35}$ m, which is also the semi-Schwarzschild radius GM_P/c^2 corresponding to the Planck mass. It is interesting to see that the Schwarzschild radius enters into the problem although we have used a nonrelativistic approach. This is due to the definition of λ in Eq. (130). Actually, our nonrelativistic approach is valid for $|\lambda| \gg 1$. Therefore, the maximum mass is much smaller than the Planck mass and its radius is much larger than the Planck length (or Schwarzschild radius). This is relevant to describe an elementary particle. However, in that case, we have to take into account electrostatic forces (see Appendix D6), except if the particle is uncharged.

Remark.—Eliminating $|\lambda|$ between Eqs. (D14) and (D15), we find that

$$R_* = \frac{a \hbar^2}{2 G m_{\max}^3}. \quad (\text{D17})$$

This is the same scaling as in Eq. (D4). Therefore, as in Appendix D1, this model cannot describe the electron because it would yield a too large radius. Actually, substituting $m = m_e$ and $R = r_e = e^2/(m_e c^2)$ (see Appendix F) in Eq. (D2) and introducing the fine-structure constant (F4), we get

$$\frac{\lambda}{8\pi} = \frac{1}{b^2} \alpha^2 \left(\frac{m_e}{M_P} \right)^2 - \frac{a}{b^2} \alpha. \quad (\text{D18})$$

Since $m_e \ll M_P$, this formula reduces to

$$\frac{\lambda}{8\pi} = -\frac{a}{b^2} \alpha, \quad (\text{D19})$$

corresponding to the nongravitational limit ($m \ll m_{\max}$ and $R \gg R_*$). Interestingly, in this limit, the mass-radius relation from Eq. (D16) is consistent with the mass-radius relation of the electron [see Eq. (F2) with $R = r_e$] provided that λ is given by Eq. (D19), which is a pure number $\lambda = -0.275\alpha = -2.00 \times 10^{-3}$. Unfortunately, this equilibrium state is unstable (see Sec. III C).

4. Tunnel effect

For an attractive self-interaction ($\lambda < 0$), since the stable equilibrium state with $m < m_{\max}$ is only metastable, the particle can overcome the barrier of potential by tunnel effect and collapse (possibly becoming a black hole). It has therefore a finite lifetime. The lifetime of a self-gravitating BEC with an attractive self-interaction has been calculated in [110] by using the instanton theory. It is found that $t_{\text{life}} \sim e^{Nb(M)}$, where N is the number of particles in the BEC and $b(M)$ is a function related to the barrier of potential which tends to zero when $M \rightarrow M_{\max}$. Since the number of bosons in a boson star is huge, on the order of $N \sim 10^{50} - 10^{100}$, the probability of a boson star to collapse by tunnel effect is completely negligible, being of order e^{-N} (except when $M = M_{\max}$, where it scales as $N^{-1/5}$) [110]. However, in the case of an elementary particle, we have $N = 1$, so the tunneling probability is determined by the function $b(m)$.

When $m \rightarrow m_{\max}$, we can obtain the lifetime $t_{\text{life}} \sim 1/\Gamma$ of the particle by taking $N = 1$ in Eq. (86) of [110]. This yields

$$\Gamma \sim 12 \left(\frac{8}{\pi^2} \right)^{1/4} \left[2 \left(1 - \frac{m}{m_{\max}} \right) \right]^{7/8} (\alpha\sigma)^{1/4} \times e^{-\frac{24}{5}\sqrt{2} \left[2 \left(1 - \frac{m}{m_{\max}} \right) \right]^{5/4} \sqrt{\alpha\sigma}} t_D^{-1}, \quad (\text{D20})$$

where

$$t_D = \left(\frac{\alpha}{\nu} \right)^{1/2} \frac{1}{\sqrt{G\rho_0}} = \frac{6\pi\zeta}{\nu} \left(\frac{\alpha}{\nu} \right)^{1/2} \frac{|a_s| \hbar}{Gm^2} \quad (\text{D21})$$

is the dynamical time. Within the Gaussian ansatz, the values of the coefficients are $\alpha_G = 3/2$, $\sigma_G = 3/4$, $\zeta_G = 1/(2\pi)^{3/2}$, and $\nu_G = 1/\sqrt{2\pi}$ [110,265]. Using Eq. (130), we can rewrite the dynamical time as

$$t_D \sim \frac{|\lambda|\hbar^2}{Gm^3c}. \quad (\text{D22})$$

For $m \sim m_{\max}$ and $R \sim R_*$ with [see Eqs. (D14) and (D15)]

$$m_{\max} \sim \frac{M_P}{\sqrt{|\lambda|}} \quad \text{and} \quad R_* \sim |\lambda|^{3/2}l_P, \quad (\text{D23})$$

we obtain

$$t_D \sim |\lambda|^{5/2}t_P, \quad (\text{D24})$$

where $t_P = (\hbar G/c^5)^{1/2} = 5.39 \times 10^{-44}$ s is the Planck time.

In order to have a long lifetime, we need $|\lambda| \gg 1$, hence $m \ll M_P$ (this condition is actually required by the validity of the nonrelativistic approximation). Therefore, in this model, elementary particles with a mass $m \sim m_{\max} \ll M_P$ have a long lifetime. However, when $m \ll M_P$, it is generally necessary to take into account electrostatic interactions (see Appendix D 6), except if the particles are neutral.

Alternatively, for a particle of mass $m \sim m_{\max} \sim M_P$, corresponding to $|\lambda| \sim 1$, electrostatic interactions may be neglected (at least marginally), but the lifetime of the particle is on the order of the Planck time t_P . In that case, we have an elementary particle of mass M_P and radius l_P (on the order of the Schwarzschild radius). This ‘‘Planck particle’’ (planckion) may be destabilized by tunnel effect and collapse quasi-immediately toward a Planck black hole of mass M_P on a timescale $\sim t_P$. This scenario should be confirmed by a general relativistic calculation.

5. Relativistic effects

In the main text, we have determined general equations giving the maximum mass M_{\max} of a relativistic self-gravitating gas of bosons of individual mass m at $T = 0$. Taking $M = m$ in these equations, we obtain the maximum mass m_{\max} of an elementary particle described by the KGE equations (B6) and (B7), in which the gravitational field is produced by the wave function φ of the particle itself.

For a noninteracting particle, using Eq. (132), we get

$$m_{\max} = 0.796M_P. \quad (\text{D25})$$

The maximum mass of the elementary particle is on the order of the Planck mass. This result may be connected to the result of Rosen [178].

For a particle with a repulsive self-interaction in the TF approximation ($\lambda \gg 1$), using Eq. (133), we get

$$m_{\max} = 0.394\lambda^{1/6}M_P. \quad (\text{D26})$$

The maximum mass of the elementary particle is larger than the Planck mass.

For a particle with an attractive self-interaction in the nonrelativistic limit ($|\lambda| \gg 1$), using Eq. (138), we get

$$m_{\max} = 5.07 \frac{M_P}{\sqrt{|\lambda|}}. \quad (\text{D27})$$

The maximum mass of the elementary particle is smaller than the Planck mass (see Appendix D 4).

More generally, for a particle with an arbitrary repulsive self-interaction, using the interpolation formula (137), we obtain the relation $m_{\max}(\lambda)$ under the inverse form

$$\frac{\lambda}{8\pi} = \frac{2.50\left(\frac{m_{\max}}{M_P}\right)^4 - 1}{0.235\left(\frac{M_P}{m_{\max}}\right)^2}. \quad (\text{D28})$$

On the other hand, for a particle with an arbitrary attractive self-interaction, using the interpolation formula (122), we obtain the relation $m_{\max}(\lambda)$ under the inverse form

$$\frac{\lambda}{8\pi} = \frac{1 - 0.401\left(\frac{M_P}{m_{\max}}\right)^4}{0.391\left(\frac{M_P}{m_{\max}}\right)^2}. \quad (\text{D29})$$

Equation (D28) is a third degree equation for $(m_{\max}/M_P)^2$, while Eq. (D29) is a second degree equation for $(M_P/m_{\max})^2$. The function $m_{\max}(\lambda)$ is plotted in Fig. 13.

Remark.—For an attractive self-interaction, the relativistic mass-radius relation of the particle can be obtained from Eq. (D3) by making the substitution (see Sec. VII)

$$\lambda \rightarrow \lambda \left(1 - \kappa \frac{8\pi Gm^2}{\lambda c\hbar}\right), \quad (\text{D30})$$

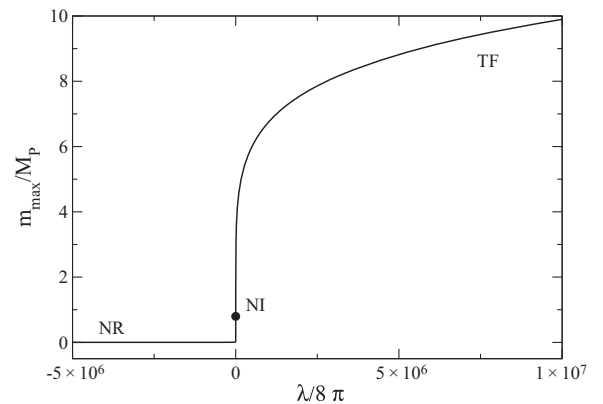


FIG. 13. Maximum mass m_{\max} of a relativistic extended elementary particle as a function of the self-interaction parameter λ .

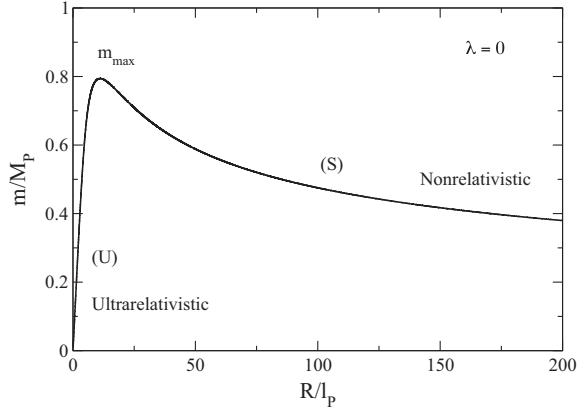


FIG. 14. Mass-radius relation of a relativistic extended elementary particle without self-interaction ($\lambda = 0$).

yielding

$$R = \frac{a\hbar^2}{2Gm^3} \pm \sqrt{\frac{a^2\hbar^4}{4G^2m^6} + \frac{b^2\lambda\hbar^3}{8\pi Gm^4c} \left(1 - \kappa \frac{8\pi Gm^2}{\lambda c\hbar}\right)}. \quad (\text{D31})$$

For $\lambda < 0$, the mass-radius relation has a shape similar to that of Fig. 12. For a noninteracting ($\lambda = 0$) relativistic particle, the mass-radius relation reduces to

$$R = \frac{a\hbar^2}{2Gm^3} \pm \sqrt{\frac{a^2\hbar^4}{4G^2m^6} - \frac{\kappa b^2\hbar^2}{m^2c^2}}. \quad (\text{D32})$$

It is plotted in Fig. 14. From this relation, we recover the maximum mass (D25) and the nonrelativistic mass-radius relation (D4) for $m \ll m_{\max}$ and $R \gg R_*$ (or $c \rightarrow +\infty$). In the ultrarelativistic limit $m \ll m_{\max}$ and $R \ll R_*$, we have $m \sim ac^2R/\kappa b^2G$, but these configurations are unstable.

6. Planck mass

Let us introduce the ratio between the electrostatic force and the gravitational force $F = e^2/Gm^2$, where e is the elementary charge (the charge of the electron) and m is the mass of the particle under consideration. Electrostatic and gravitational forces are comparable ($F \sim 1$) when $m \sim e/\sqrt{G}$. Introducing the fine-structure constant (F4) and treating α as a dimensionless number of order unity, the condition $F \sim 1$ can be rewritten as $m \sim M_P$, where $M_P = (\hbar c/G)^{1/2} = 2.18 \times 10^{-5}$ g is the Planck mass. When $m \ll M_P$ (i.e., $e^2 \gg Gm^2$), the electrostatic forces overcome the gravitational forces. For example, for the electron of mass $m_e = 9.11 \times 10^{-28}$ g, we have $F \sim 10^{40}$ (Weyl number). Therefore, self-gravity is completely negligible at the scale of the electron. When $m \gg M_P$ (i.e., $Gm^2 \gg e^2$), the gravitational forces overcome the electrostatic forces. When $m \sim M_P$ (i.e., $e^2 \sim Gm^2$),

corresponding to the Planck scale or the grand unification energy scale, the gravitational and the electrostatic forces are comparable. Therefore, models of extended elementary charged particles that include gravitational and electrostatic forces have masses on the order of the Planck mass M_P (up to a factor α) [210].

APPENDIX E: CHARGED BOSONS

In this Appendix, we consider the case of BECs made of charged bosons. We assume that the bosons have a mass m and carry a charge e . We stress that e is not necessarily equal to the elementary charge of the electron.

1. Without self-gravity

We first ignore the gravitational interaction between bosons and consider the electrostatic GPP equations

$$i\hbar \frac{\partial \psi}{\partial t} = -\frac{\hbar^2}{2m} \Delta \psi + \frac{4\pi a_s \hbar^2}{m^2} |\psi|^2 \psi + m\Phi \psi, \quad (\text{E1})$$

$$\Delta \Phi = -\frac{4\pi e^2}{m^2} |\psi|^2. \quad (\text{E2})$$

Since the electrostatic interaction e^2/r between two charges is similar to the gravitational interaction $-Gm^2/r$ between two masses (except for the change of sign), the results of Sec. IV remain valid provided that we make the substitution $Gm^2 \rightarrow -e^2$ in the equations. Since the electrostatic force between two charges is repulsive, and since the quantum potential also has a repulsive nature, equilibrium states can exist only if the self-interaction between bosons is attractive. Therefore, in the following, we assume $a_s < 0$.

In that case, the mass-radius relation from Eq. (53) becomes

$$M = \frac{a \frac{\hbar^2}{e^2 R}}{b^2 \frac{|a_s| \hbar^2}{e^2 m R^2} - 1}. \quad (\text{E3})$$

The radius increases monotonically with the mass (see Fig. 15) and tends to the asymptotic value

$$R_{\max} = b \left(\frac{|a_s| \hbar^2}{e^2 m} \right)^{1/2} \quad (\text{E4})$$

when $M \rightarrow +\infty$ (TF limit). This corresponds to the result from Eq. (56) with the above substitution. For $M \rightarrow 0$ (nonelectrostatic limit), we have

$$R \sim \frac{b^2 |a_s| M}{a m}, \quad (\text{E5})$$

returning the result from Eq. (61). From these asymptotic results, we obtain $b = \pi$ and $a/b^2 = 0.275$, yielding $a = 2.71$.

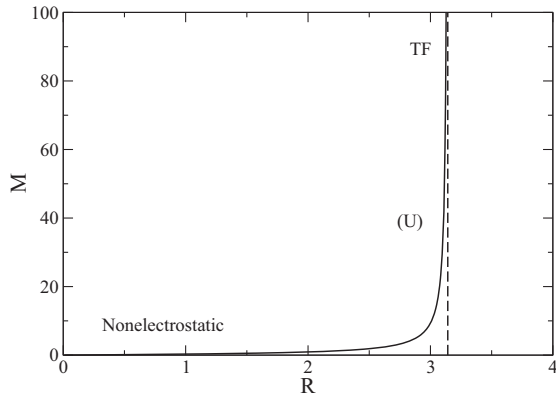


FIG. 15. Mass-radius relation of charged BECs with $a_s < 0$ [for illustration we have used Eq. (E3) with $a = 2.71$ and $b = \pi$]. The mass is normalized by $M_a = (m\hbar^2/e^2|a_s|)^{1/2}$ and the radius by $R_a = (|a_s|\hbar^2/e^2m)^{1/2}$.

The total energy of the BEC [see Eq. (50)] is

$$E_{\text{tot}}(R) = \sigma \frac{\hbar^2 M}{m^2 R^2} + \nu \frac{e^2 M^2}{m^2 R} - \zeta \frac{2\pi |a_s| \hbar^2 M^2}{m^3 R^3}. \quad (\text{E6})$$

We see that the equilibrium state is always unstable (it is a maximum of energy at fixed mass). This probably precludes physical applications of this model.

Remark.—In the nonelectrostatic limit ($e = 0$ and $a_s < 0$), we can use the exact results from Sec. III C valid for nongravitational BECs with an attractive self-interaction ($G = 0$ and $a_s < 0$). In the TF limit ($\hbar = 0$), we can use the exact results from Sec. III B provided that we make the substitutions $Gm^2 \rightarrow -e^2$ and $a_s \rightarrow -|a_s|$. The density profile of the BEC is given by Eq. (34), its radius by Eq. (E4) with $b = \pi$, its central density by Eq. (36), its energy by $E_{\text{tot}} = M^2 e^2 / 2m^2 R_{\text{max}}$, and the instability time by $t_D \sim (m^2 R_{\text{max}}^3 / M e^2)^{1/2}$. Therefore, in the TF limit, a gas of charged bosons with an attractive self-interaction ($-e^2 < 0$ and $a_s < 0$) has the same structure as a boson star with a repulsive self-interaction ($G > 0$ and $a_s > 0$). However, a boson star with a repulsive self-interaction is stable, while a gas of charged bosons with an attractive self-interaction is unstable. In this connection, we note that the total energy E_{tot} is negative in the gravitational case and positive in the electrostatic case.

2. With self-gravity

If we take into account the gravitational force and the electrostatic force between bosons, we just have to make the substitution $Gm^2 \rightarrow Gm^2 - e^2$ or, equivalently, $G \rightarrow G(1 - e^2/Gm^2)$ in the equations of Sec. IV. The effect of the electrostatic repulsion is to decrease the value of the gravitational constant. Introducing the dimensionless parameter

$$\alpha = \frac{e^2}{\hbar c}, \quad (\text{E7})$$

coinciding with the fine-structure constant only when e is the charge of the electron, this transformation can be rewritten as

$$G \rightarrow G \left(1 - \alpha \frac{M_P^2}{m^2} \right), \quad (\text{E8})$$

where $M_P = (\hbar c/G)^{1/2}$ is the Planck mass. The gravitational attraction prevails over the electric repulsion (allowing stable equilibrium states) provided that $e^2 < e_c^2 \equiv Gm^2$, i.e., $\alpha < \alpha_c \equiv m^2/M_P^2$. When this condition is fulfilled, the mass-radius relation (53) becomes

$$M = \frac{a \frac{\hbar^2}{(Gm^2 - e^2)R}}{1 - b^2 \frac{a_s \hbar^2}{m(Gm^2 - e^2)R^2}}. \quad (\text{E9})$$

Figures 1 and 2 remain valid with the new scales M_a and R_a obtained by using the transformation (E8). There is always an equilibrium state (for any mass M) when $a_s \geq 0$, while an equilibrium state exists only below the maximum mass [see Eq. (58) with Eq. (E8)],

$$M_{\text{max}} = \frac{a}{2b} \frac{\hbar}{\sqrt{\frac{|a_s|}{m} (Gm^2 - e^2)}} \quad (\text{E10})$$

when $a_s < 0$. When $e^2 > e_c^2 = Gm^2$, the equilibrium states are unstable.⁴⁶

For relativistic bosons with a repulsive self-interaction ($a_s \geq 0$), substituting $R = kGM/c^2$ into Eq. (E9), we obtain⁴⁷

$$M_{\text{max}} = \left(\frac{a}{k} \right)^{1/2} \frac{\hbar c}{Gm} \left(\frac{Gm^2}{Gm^2 - e^2} \right)^{1/2} \sqrt{1 + \frac{b^2 a_s c^2}{ak Gm}}. \quad (\text{E11})$$

This is the general relativistic maximum mass of a charged boson star arising from the fact that its radius approaches the Schwarzschild radius (see Sec. VI). The electrostatic corrections are encapsulated in the factor

$$\left(\frac{Gm^2}{Gm^2 - e^2} \right)^{1/2}. \quad (\text{E12})$$

⁴⁶The results of Appendix E 1 can be generalized by making the substitution $e^2 \rightarrow e^2 - Gm^2$.

⁴⁷In principle, we should take into account the electrostatic correction to the Schwarzschild radius. This correction will be considered in a future work.

Therefore, using the interpolation formulas of Sec. VIII and including the electrostatic corrections, we get

$$M_{\max} = 0.633 \frac{\hbar c}{Gm} \left(\frac{Gm^2}{Gm^2 - e^2} \right)^{1/2} \sqrt{1 + 0.235 \frac{a_s c^2}{Gm}} \quad (\text{E13})$$

and

$$R_* = 6.03 \frac{\hbar}{mc} \left(\frac{Gm^2}{Gm^2 - e^2} \right)^{1/2} \sqrt{1 + 0.101 \frac{a_s c^2}{Gm}}. \quad (\text{E14})$$

For relativistic bosons with an attractive self-interaction ($a_s \leq 0$), making the transformation from Eq. (96) into Eq. (E9), we obtain the mass-radius relation⁴⁸

$$M = \frac{a \frac{\hbar^2}{(Gm^2 - e^2)R}}{1 + b^2 \frac{|a_s - \kappa \frac{Gm}{c^2}| \hbar^2}{m(Gm^2 - e^2)R^2}}. \quad (\text{E15})$$

This mass-radius relation displays a maximum mass. Using the interpolation formulas of Sec. VIII and including the electrostatic corrections, we get

$$M_{\max} = 1.012 \frac{\hbar}{\sqrt{Gm|a_s - 2.56 \frac{Gm}{c^2}|}} \left(\frac{Gm^2}{Gm^2 - e^2} \right)^{1/2} \quad (\text{E16})$$

and

$$R_* = 5.5 \left(\frac{|a_s - 1.20 \frac{Gm}{c^2}| \hbar^2}{Gm^3} \right)^{1/2} \left(\frac{Gm^2}{Gm^2 - e^2} \right)^{1/2}. \quad (\text{E17})$$

In the noninteracting limit ($a_s = 0$), using Eqs. (E13) and (E14) or Eqs. (E16) and (E17), we obtain

$$M_{\max} = 0.633 \frac{\hbar c}{Gm} \left(\frac{Gm^2}{Gm^2 - e^2} \right)^{1/2}, \quad (\text{E18})$$

$$R_* = 6.03 \frac{\hbar}{mc} \left(\frac{Gm^2}{Gm^2 - e^2} \right)^{1/2}. \quad (\text{E19})$$

For $e \rightarrow e_c = Gm^2$, taking $G = \hbar = c = m = 1$ for convenience (we adopt the same convention below), we find that $M_{\max} \sim 0.448(1 - e)^{-1/2}$ and $R_* \sim 4.26(1 - e)^{-1/2}$.

In the TF limit (when $a_s > 0$ with $a_s \gg Gm/c^2$), using Eqs. (E13) and (E14), we obtain

$$M_{\max} = 0.307 \left(\frac{a_s \hbar^2 c^4}{G^3 m^3} \right)^{1/2} \left(\frac{Gm^2}{Gm^2 - e^2} \right)^{1/2}, \quad (\text{E20})$$

⁴⁸In principle, we should take into account the electrostatic correction in the relativistic quantum potential. This correction will be considered in a future work.

$$R_* = 1.92 \left(\frac{a_s \hbar^2}{Gm^3} \right)^{1/2} \left(\frac{Gm^2}{Gm^2 - e^2} \right)^{1/2}. \quad (\text{E21})$$

For $e \rightarrow e_c = Gm^2$, we find that $M_{\max} \sim 0.217(1 - e)^{-1/2}$ and $R_* \sim 1.36(1 - e)^{-1/2}$.

In the nonrelativistic limit (when $a_s < 0$ with $|a_s| \gg Gm/c^2$), using Eqs. (E16) and (E17), we obtain

$$M_{\max} = 1.012 \frac{\hbar}{\sqrt{Gm|a_s|}} \left(\frac{Gm^2}{Gm^2 - e^2} \right)^{1/2}, \quad (\text{E22})$$

$$R_* = 5.5 \left(\frac{|a_s| \hbar^2}{Gm^3} \right)^{1/2} \left(\frac{Gm^2}{Gm^2 - e^2} \right)^{1/2}. \quad (\text{E23})$$

For $e \rightarrow e_c = Gm^2$, we find that $M_{\max} \sim 0.716(1 - e)^{-1/2}$ and $R_* \sim 3.89(1 - e)^{-1/2}$.

Charged boson stars in general relativity have been studied numerically by Jetzer and van der Bij in Refs. [370,371] by solving the Klein-Gordon-Maxwell-Einstein equations numerically. Their asymptotic results for $e \rightarrow e_c = 1$, displaying the scalings $M_{\max} \propto (1 - e)^{-1/2}$ and $R_* \propto (1 - e)^{-1/2}$, are recovered by our analytical approach.⁴⁹ For the maximum mass M_{\max} , they obtained the prefactors $0.44 \times 2^{1/4} = 0.523$ and $0.226 \times 2^{1/4} = 0.269$ in the noninteracting and TF limits, respectively. These numerical results are reasonably close to our approximate analytical results 0.448 and 0.217.

3. Model of extended particles with electrostatic interactions

We can use the foregoing results to take into account electrostatic interactions in the models of relativistic elementary particles considered in Appendix D 5. We focus on the case where the gravitational forces are more important than the electrostatic forces (i.e., $m > e/\sqrt{G} = \sqrt{\alpha} M_P$).

a. Nonrelativistic mass-radius relation

We can easily generalize the nonrelativistic mass-radius relation $m(R)$ from Eq. (D3) to a charged particle by making the substitution from Eq. (E8). The general formula is a bit cumbersome but it takes a simple form in appropriate limits. In the noninteracting case, we get [see Eq. (D4) with (E8)]

$$R = a \frac{\hbar^2}{Gm^3 \left(1 - \alpha \frac{M_P^2}{m^2} \right)}. \quad (\text{E24})$$

⁴⁹These scalings do not amount to naively making the substitution $Gm^2 \rightarrow Gm^2 - e^2$ in the relativistic formulas of uncharged boson stars.

In the TF limit when $\lambda > 0$, we get [see Eq. (D6) with (E8)]

$$R \sim b \sqrt{\frac{\lambda}{8\pi}} \left[\frac{\hbar^3}{Gm^4 \left(1 - \alpha \frac{M_p^2}{m^2}\right) c} \right]^{1/2}. \quad (\text{E25})$$

The radius diverges when $m \rightarrow \sqrt{\alpha} M_p$. We recover the nonelectrostatic case when $m \gg \sqrt{\alpha} M_p$.

b. Relativistic mass-radius relation when $\lambda \leq 0$

For an attractive self-interaction $\lambda \leq 0$, we can easily generalize the relativistic mass-radius relation $m(R)$ from Eq. (D31) to a charged particle by making the substitution from Eq. (E8), except in the term that is proportional to κ , since we have assumed that it is not affected by electrostatic corrections (see footnote 48). The general formula is a bit cumbersome, but for a noninteracting ($\lambda = 0$) particle, it reduces to

$$R = \frac{a\hbar^2}{2G \left(1 - \alpha \frac{M_p^2}{m^2}\right) m^3} \pm \sqrt{\frac{a^2 \hbar^4}{4G^2 \left(1 - \alpha \frac{M_p^2}{m^2}\right)^2 m^6} - \frac{\kappa b^2 \hbar^2}{m^2 c^2 \left(1 - \alpha \frac{M_p^2}{m^2}\right)}}. \quad (\text{E26})$$

c. Maximum mass

We now determine how electrostatic corrections affect the maximum mass of the particle calculated in Appendix D.

For a repulsive self-interaction, using Eqs. (130) and (E7) and making $M = m$ in Eq. (E13), we find that the relation between the maximum particle mass m_{\max} and the dimensionless self-interaction constant λ can be expressed under the inverse form as

$$\frac{\lambda}{8\pi} = \frac{2.50 \frac{m_{\max}^2}{M_p^2} \left(\frac{m_{\max}^2}{M_p^2} - \alpha\right) - 1}{0.235 \frac{M_p^2}{m_{\max}^2}}. \quad (\text{E27})$$

When $\alpha = 0$ (i.e., $e = 0$), we recover Eq. (D28).

For an attractive self-interaction, using Eqs. (130) and (E7) and making $M = m$ in Eq. (E16), we find that

$$\frac{|\lambda|}{8\pi} = \frac{1.02}{\frac{m_{\max}^2}{M_p^2} - \alpha} - 2.56 \frac{m_{\max}^2}{M_p^2}. \quad (\text{E28})$$

When $\alpha = 0$, we recover Eq. (D29).

In the noninteracting case, making $M = m$ in Eq. (E18), we obtain

$$m_{\max} = M_p \left[\frac{\alpha}{2} + \sqrt{\frac{\alpha^2}{4} + 0.401} \right]^{1/2}. \quad (\text{E29})$$

When $\alpha = 0$, we recover Eq. (D25). When $\alpha \gg 1$, we get $m \sim \sqrt{\alpha} M_p$.⁵⁰

In the TF limit (when $\lambda > 0$ and $\lambda \gg 1$), making $M = m$ in Eq. (E20), we obtain

$$\frac{\lambda}{8\pi} = 10.6 \frac{m_{\max}^4}{M_p^4} \left(\frac{m_{\max}^2}{M_p^2} - \alpha \right). \quad (\text{E30})$$

When $\alpha = 0$, or when $\lambda \rightarrow +\infty$, we recover Eq. (D26).

In the nonrelativistic limit (when $\lambda < 0$ with $|\lambda| \gg 1$), making $M = m$ in Eq. (E22), we obtain

$$m_{\max} = M_p \sqrt{1.02 \frac{8\pi}{|\lambda|} + \alpha}. \quad (\text{E31})$$

When $\alpha = 0$, we recover Eq. (D27). When $|\lambda| \rightarrow +\infty$, we find $m_{\max} \rightarrow \sqrt{\alpha} M_p$.

4. A simple model of extended electron

We can use the results of Appendix E 1 to construct a simple model of extended electron.⁵¹ We assume that the wave function $\psi(\mathbf{r}, t)$ governed by the Schrödinger equation (E1) determines the density profile $\rho(\mathbf{r}, t)$ of the electron through the relation $\rho = |\psi|^2$. The corresponding density of charge $-\rho e/m$ creates, via the Poisson equation (E2), an electric potential $(m/e)\Phi$ that enters into the Schrödinger equation (E1). Finally, we identify the mass m appearing in the Schrödinger equation (E1) and the mass $M = \int \rho d\mathbf{r}$ produced by ρ with the mass m_e of the electron, following an argument similar to the one given by Diósi [369] for the gravitational interaction (see Appendix D).⁵² Of course, since the electrostatic interaction and the quantum potential are both repulsive, this model does not yield any equilibrium state (contrary to the gravitational model of Diósi [369], where the gravitational attraction compensates the repulsion of the quantum potential). Therefore, we add an attractive $|\psi|^4$ self-interaction ($\lambda < 0$) that opposes itself to the electrostatic repulsion. This attractive term is similar in spirit to the Poincaré stress [183,374] introduced in the Abraham-Lorentz [182,184] electromagnetic model of the electron to stabilize the particle (see Appendix F 2). Using Eqs. (E3) and (130), introducing

⁵⁰Recall that e is not necessarily the charge of the electron, so α can take large values.

⁵¹This model can be related to the models of extended particles listed in footnote 13. Unfortunately, the particle of our model appears to be unstable.

⁵²Vlasov [372] argued that this system of coupled Schrödinger-Poisson equations was imagined by Schrödinger himself, but Pitaevskii [373] contested that claim.

the fine-structure constant (F4), and taking $M = m_e$, we obtain the electron mass-radius relation

$$m_e^2 + \frac{ae^2}{\alpha^2 R c^2} m_e - \frac{b^2 |\lambda| e^4}{8\pi \alpha^3 c^4 R^2} = 0, \quad (\text{E32})$$

where $a = 2.71$ and $b = \pi$. The solution of this second degree equation is

$$m_e c^2 = \frac{e^2}{R} \left\{ \sqrt{\frac{a^2}{4\alpha^4} + \frac{b^2 |\lambda|}{8\pi \alpha^3}} - \frac{a}{2\alpha^2} \right\}. \quad (\text{E33})$$

It can be written as

$$m_e c^2 = \chi(\lambda) \frac{e^2}{R}, \quad (\text{E34})$$

with the dimensionless constant

$$\chi(\lambda) = \left\{ \sqrt{\frac{a^2}{4\alpha^4} + \frac{b^2 |\lambda|}{8\pi \alpha^3}} - \frac{a}{2\alpha^2} \right\}. \quad (\text{E35})$$

Interestingly, this relation is similar to the relation appearing in the Abraham-Lorentz [182,184] model of the electron and in the Born-Infeld [188,189] theory (see Appendix F). Comparing Eq. (E34) with Eq. (F1), we get

$$R = \chi(\lambda) r_e, \quad (\text{E36})$$

where r_e is the classical electron radius (F2).

a. TF approximation

In the TF approximation $|\lambda|/8\pi \gg a^2/(4b^2\alpha)$, the term proportional to m_e in Eq. (E32) can be neglected and Eq. (E33) reduces to

$$m_e c^2 = \frac{b}{\alpha^{3/2}} \sqrt{\frac{|\lambda|}{8\pi}} \frac{e^2}{R}. \quad (\text{E37})$$

In that case, the equilibrium state results from the balance between the repulsive electrostatic interaction and the attractive self-interaction. Actually, in the TF approximation, we can solve the problem exactly. Making the substitutions $Gm^2 \rightarrow -e^2$ and $a_s \rightarrow -|a_s|$ in Eq. (33), using Eq. (130) and introducing the fine-structure constant (F4), we obtain⁵³

⁵³This equation is equivalent to the Lane-Emden equation for a polytrope of index $n = 1$, which describes the balance between the gravitational attraction and the repulsive self-interaction. In the present case, it describes the balance between the electrostatic repulsion and the attractive self-interaction. However, in the gravitational case (boson stars), the equilibrium is stable, while in the electrostatic case (electron), it is unstable.

$$\Delta\rho + \frac{8\pi m_e^2 c^4 \alpha^3}{|\lambda| e^4} \rho = 0. \quad (\text{E38})$$

The density profile of the extended electron, which is determined by Eq. (E38), is given by [see Eq. (34)]

$$\rho(r) = \frac{\rho_0 R}{\pi r} \sin\left(\frac{\pi r}{R}\right). \quad (\text{E39})$$

Its radius is [see Eq. (35)]

$$R = \frac{\pi}{\alpha^{3/2}} \sqrt{\frac{|\lambda|}{8\pi}} \frac{e^2}{m_e c^2}. \quad (\text{E40})$$

It can be written as Eq. (E36) with

$$\chi_{\text{TF}}(\lambda) = \frac{\pi}{\alpha^{3/2}} \sqrt{\frac{|\lambda|}{8\pi}}. \quad (\text{E41})$$

Its central density is [see Eq. (36)]

$$\rho_0 = \frac{\pi m_e}{4R^3}. \quad (\text{E42})$$

The timescale of the instability is of order [see Eq. (38)]

$$t_D \sim \left(\frac{m^2}{\rho_0 e^2}\right)^{1/2} \sim \left(\frac{m_e R^3}{e^2}\right)^{1/2}. \quad (\text{E43})$$

Finally, according to Eq. (37), the total energy (electrostatic + internal) of the electron is⁵⁴

$$E_{\text{tot}} = \frac{e^2}{2R}. \quad (\text{E44})$$

Combining Eq. (E44) with Eq. (E34), we find that

$$E_{\text{tot}} = \frac{m_e c^2}{2\chi_{\text{TF}}(\lambda)}. \quad (\text{E45})$$

If we impose that $R = r_e$, we get $\chi_{\text{TF}}(\lambda) = 1$. In that case, the total energy of the electron is⁵⁵

$$E_{\text{tot}} = \frac{1}{2} m_e c^2, \quad (\text{E46})$$

⁵⁴The energy of the electron is positive, implying that this configuration is unstable. By contrast, the gravitational energy of a boson star is negative, consistent with the fact that these objects are stable.

⁵⁵We note that $E_{\text{tot}} \neq m_e c^2$. Alternatively, we could impose $E_{\text{tot}} = m_e c^2$ and deduce that the radius of the electron is given by $m_e c^2 = e^2/(2R)$ [see Eq. (E44)], i.e., $R = e^2/(2m_e c^2) = r_e/2$. The relation $E = mc^2$ (sometimes with a prefactor 3/4) has a long history in physics even before Einstein's theory of relativity. It appeared at the end of the 19th century when some researchers like Thomson noticed that the electromagnetic energy is equivalent to mass. It was also used by Born and Infeld in their nonlinear electrodynamics (see Appendix F).

where $m_e c^2$ is its rest-mass energy. On the other hand, its central density is

$$\rho_0 = \frac{\pi}{4} \rho_e, \quad (\text{E47})$$

where ρ_e is the classical electron density (F5). The timescale of the instability is of order

$$t_D \sim t_e, \quad (\text{E48})$$

where t_e is the chronon (F6).

The condition $\chi_{\text{TF}}(\lambda) = 1$ implies that the self-interaction constant is given by

$$\frac{\lambda}{8\pi} = -\frac{\alpha^3}{\pi^2} = -3.94 \times 10^{-8}. \quad (\text{E49})$$

This result shows that the TF approximation $|\lambda|/8\pi \gg a^2/(4b^2\alpha) = 25.5$ is not justified. One has to take into account the contribution of the quantum potential and use the more general mass-radius relation from Eq. (E33).

b. Nonelectrostatic limit

In the nonelectrostatic limit $|\lambda|/8\pi \ll a^2/(4b^2\alpha) = 25.5$, the term proportional to m_e^2 in Eq. (E32) can be neglected and Eq. (E33) reduces to

$$m_e c^2 = \frac{b^2 |\lambda| e^2}{a 8\pi \alpha R}. \quad (\text{E50})$$

In that case, the equilibrium state results from the balance between the repulsive quantum potential and the attractive self-interaction (see Appendix D 3). The total energy is of order $E_{\text{tot}} = 0.393 m_e c^2 / (\lambda/8\pi)^2$ [see Eq. (54) of [290] with Eq. (130)]. If we impose that $R = r_e$ [i.e., $\chi_{\text{NE}}(\lambda) = 1$], we get⁵⁶

$$\frac{|\lambda|}{8\pi} = \frac{a}{b^2} \alpha = 2.00 \times 10^{-3}. \quad (\text{E51})$$

This result is consistent with the condition of validity of the nonelectrostatic limit. However, the equilibrium state is unstable.

c. General case

In the general case, if we impose that $R = r_e$ [i.e., $\chi(\lambda) = 1$], we get

⁵⁶This yields $E_{\text{tot}} = 9.82 \times 10^4 m_e c^2$. Alternatively, we could impose $E_{\text{tot}} = m_e c^2$ and get $|\lambda|/8\pi = 0.627$ and $R = 313 r_e = 8.82 \times 10^{-13}$ m. In that case, the electron radius is on the order of its Compton wavelength $\lambda_e = \hbar/(m_e c) = 3.86 \times 10^{-13}$ m (see Appendix F), which is sensible since we are using a quantum model.

$$\frac{|\lambda|}{8\pi} = \frac{a\alpha + \alpha^3}{b^2}. \quad (\text{E52})$$

Since $\alpha \ll 1$, we have in good approximation

$$\frac{|\lambda|}{8\pi} \simeq \frac{a}{b^2} \alpha = 2.00 \times 10^{-3}, \quad (\text{E53})$$

corresponding to the nonelectrostatic limit that we have discussed previously. This is also a regime of weak self-interaction since $|\lambda|/8\pi \ll a^2/(4b^2\alpha)$.

In conclusion, our simple model of extended electron determines its density profile [it can be obtained by solving the electrostatic Gross-Pitaevskii-Poisson equations (E1) and (E2) or, in good approximation, by solving the non-electrostatic Gross-Pitaevskii equation alone], as well as its radius and central density. Equation (E33) with $\chi(\lambda) = 1$ is consistent with the relation $m_e c^2 = e^2/r_e$ usually introduced from qualitative considerations, but it is obtained here from the solution of the electrostatic GPP equations. Unfortunately, this equilibrium state is unstable. The timescale of the instability is [see Eq. (112) in [265]]

$$t_u \sim \frac{m_e r_e^2}{\hbar} = 6.87 \times 10^{-26} \text{ s}. \quad (\text{E54})$$

In this model, the electron would have a very short lifetime. Therefore, although this model correctly reproduces the relation between the mass and the radius of the electron, it cannot account for its stability unless a particular mechanism to increase its lifetime is found. Maybe this model could describe another elementary particle, different from the electron. In that case, e does not need to represent the elementary charge and the lifetime of the particle may be enhanced.

APPENDIX F: MODELS OF EXTENDED ELECTRON

In this appendix we present basic equations applying to the electron and we briefly recall the historical background.

1. Basic equations

The classical radius r_e of the electron is defined through the relation

$$E = m_e c^2 = \frac{e^2}{r_e}. \quad (\text{F1})$$

This equation expresses the equality (in order of magnitude) between the rest-mass energy of the electron and its electrostatic energy. This is a convenient manner to define the ‘‘radius’’ of the electron. This relation first appeared in the Abraham-Lorentz [182,184] model of the extended electron with electromagnetic mass and later in the Born-Infeld [188,189] theory of nonlinear electrodynamics.

Recalling the value of the charge of the electron $e = 4.80 \times 10^{-13} \text{ g}^{1/2} \text{ m}^{3/2} \text{ s}^{-1}$ and its mass $m_e = 9.11 \times 10^{-28} \text{ g} = 0.511 \text{ MeV}/c^2$, we obtain

$$r_e = \frac{e^2}{m_e c^2} = 2.82 \times 10^{-15} \text{ m}. \quad (\text{F2})$$

The Compton wavelength of the electron is $\lambda_e = \hbar/(m_e c) = 3.86 \times 10^{-13} \text{ m}$. It is related to the classical radius of the electron by

$$\lambda_e = \frac{r_e}{\alpha} \simeq 137 r_e, \quad (\text{F3})$$

where

$$\alpha = \frac{e^2}{\hbar c} \simeq \frac{1}{137} \simeq 7.30 \times 10^{-3} \quad (\text{F4})$$

is Sommerfeld's fine-structure constant.⁵⁷ In comparison, the Bohr (atomic) radius is $a_B = \hbar^2/(m_e e^2) = r_e/\alpha^2 = 5.29 \times 10^{-11} \text{ m}$. We have $r_e \ll \lambda_e \ll a_B$. The typical electron density is

$$\rho_e = \frac{m_e}{r_e^3} = 4.07 \times 10^{16} \text{ g m}^{-3}. \quad (\text{F5})$$

The dynamical time associated with the electron is

$$t_e = \left(\frac{m_e r_e^3}{e^2} \right)^{1/2} = \frac{e^2}{m_e c^3} = \frac{r_e}{c} = 3.32 \times 10^{-24} \text{ s}. \quad (\text{F6})$$

This is the time it takes for a light wave to travel across the “size” of an electron. This time first appeared in the Abraham-Lorentz [182,184] theory of the extended electron when they tried to calculate the recoil force on an accelerated charged particle caused by the particle emitting electromagnetic radiation. This is also what Caldirola [375] called the “chronon,” which is a sort of “quantum of time.”

2. Abraham-Lorentz model

In the model of extended electron developed by Abraham [182] and Lorentz [184], the electron is considered as a spherical charge of radius R (which must be nonzero to avoid infinite energy accumulation) with a charge e uniformly distributed on its surface. It was originally believed that the mass of the electron had a purely electromagnetic nature. The electromagnetic energy of the electron at rest (reducing to its electrostatic energy) is

$$E = \frac{1}{2} \frac{e^2}{R}. \quad (\text{F7})$$

On the other hand, the electromagnetic impulse (Poynting vector) of the electron in slow motion ($v \ll c$) is

$$\mathbf{p} = \frac{2}{3} \frac{e^2}{R c^2} \mathbf{v}. \quad (\text{F8})$$

It is proportional to the velocity like in the classical mechanical relation $\mathbf{p} = m\mathbf{v}$. This suggests introducing the “electromagnetic mass” of the electron

$$m_e = \frac{2}{3} \frac{e^2}{R c^2}. \quad (\text{F9})$$

This relation can also be written as

$$m_e c^2 = \frac{2}{3} \frac{e^2}{R}. \quad (\text{F10})$$

Comparing Eq. (F10) with Eq. (F1), we get

$$R = \frac{2}{3} r_e = 1.88 \times 10^{-15} \text{ m}. \quad (\text{F11})$$

This is the radius of the electron in the Abraham-Lorentz theory. In this sense, the Abraham-Lorentz theory *justifies* the relation from Eq. (F1) defining the classical radius of the electron.

For an arbitrary velocity, Lorentz [376] understood that the charged sphere had to contract itself into an ellipsoid. Therefore, the electrons undergo length contraction in the line of motion. In his famous 1904 paper [377], he obtained the relation

$$\mathbf{p} = \frac{2}{3} \frac{e^2}{R c^2} \frac{\mathbf{v}}{\sqrt{1 - v^2/c^2}}. \quad (\text{F12})$$

In that case, the mass of the electron depends on the velocity as

$$m = \frac{m_e}{\sqrt{1 - v^2/c^2}}, \quad (\text{F13})$$

where the rest mass m_e is given by Eq. (F9). This relation was discovered before Einstein's theory of relativity. It shows that the velocity cannot be larger than the speed of light. On the other hand, if we combine Eqs. (F7) and (F10), we get

$$E = \frac{3}{4} m_e c^2, \quad (\text{F14})$$

⁵⁷Since quantum effects enter at a distance of the order λ_e , which is much larger than r_e , a purely classical electromagnetic model of the electron is not relevant.

instead of $E = m_e c^2$. Abraham [182,378] understood that a purely charged sphere is unstable since the electric forces are all repulsive. Poincaré [183,374] solved these problems by introducing additional forces of nonelectromagnetic origin (Poincaré stresses) that maintain the charges in the sphere. These stresses prevent the electron from exploding and contribute to 1/4 of the total energy restoring the expected relation $E = m_e c^2$. Poincaré stresses were also thought of as a dynamical explanation of Lorentz length contraction. In this theory, the mass of the electron has an electromagnetic part and a part due to Poincaré stresses. It is impossible that all the mass is electromagnetic in origin. The result of Einstein's relativity theory [379] then showed that the dependence of mass on velocity is not characteristic of electromagnetic mass, but can be derived very generally from the transformation law. After Einstein's theory of relativity, several authors pointed out that the electron's stability and the 4/3 problem are two different things [380]. However, binding forces (or confining pressure) like the Poincaré stresses are still necessary to prevent the electron from exploding due to Coulomb repulsion.

Remark.—The concept of electromagnetic mass was introduced by Thomson [381] in 1881 (he discovered the electron in 1897). He realized that the apparent mass of a charged body in motion is larger than the mass it would have if it were uncharged (similar considerations were already made by Stokes [382] in hydrodynamics). The electromagnetic mass was initially considered as a dynamical explanation of the inertial mass of an object. This idea was further developed by Heaviside [383], Thomson [384], Searle [385], Abraham [386], and Lorentz [377,387] and was incorporated in the Abraham-Lorentz theory of the electron. Even before the work of Lorentz [376], Heaviside [383], Thompson [384], and Searle [385] understood that the mass of a charged body depends on its velocity and becomes infinite when $v \rightarrow c$. They concluded that no body can move at a speed greater than the speed of light. Heaviside [383] and Thompson [384] seem to be the first to have isolated the factor

$$\frac{1}{\sqrt{1 - v^2/c^2}} \quad (\text{F15})$$

in the energy (mass) of a charged body in motion. Searle [385] obtained a different formula

$$E = E_0 \left[\frac{c}{v} \ln \left(\frac{1 + v/c}{1 - v/c} \right) - 1 \right], \quad (\text{F16})$$

where $E_0 = e^2/2R$ is the rest-mass energy. For $v \ll c$, this formula becomes

$$E = E_0 \left(1 + \frac{2}{3} \frac{v^2}{c^2} + \dots \right). \quad (\text{F17})$$

Using this result, and identifying the second term of the expansion $\frac{2}{3} E_0 \frac{v^2}{c^2}$ with the kinetic energy $\frac{1}{2} m v^2$, Wien [388] obtained the relation

$$m = \frac{4}{3} \frac{E_0}{c^2} \quad (\text{F18})$$

between the (electromagnetic) mass m and the energy of the body at rest E_0 . It is apparently the first time that the famous formula $E = m c^2$ appeared in the literature (under the form $m = \frac{4}{3} \mathcal{E} A^2$) with, however, the wrong prefactor 3/4.

3. Born-Infeld model

The Maxwell equations of classical electrodynamics lead to the description of an elementary charged particle like an electron as a singular point in the electromagnetic field. It was initially thought that the mass of the electron was entirely due to its electromagnetic self-energy. However, the self-energy of a point charge ("point electron") in Maxwell's electrodynamics is infinite. Abraham [182] and Lorentz [184], respectively, introduced the notion of rigid and contracting electron with a finite size, but models of extended electron need cohesive forces of nonelectromagnetic origin (Poincaré stresses [183,374]) to stabilize the structure (see Appendix F 2). Therefore, modifications of the Maxwell equations were suggested first by Mie [187], then by Born and Infeld [188,189]. Using an analogy with special relativity, Born and Infeld developed a theory of nonlinear electrodynamics that prevents the divergence of the electric field produced by a point charge. They introduced an electromagnetic Lagrangian of the form

$$\mathcal{L}_{\text{BI}} = -b^2 \sqrt{1 - \frac{E^2 - B^2}{b^2}}, \quad (\text{F19})$$

which reduces to the Lagrangian of Maxwell electrodynamics in the weak field limit. This Lagrangian contains a fundamental constant b ("absolute field"), which plays the role of the speed of light c in special relativity. In the electrostatic case, the universal constant b is simply the upper limit of the field strength \mathbf{E} . As a result, the Born-Infeld equations that replace the Maxwell equations have a solution for the point electron with the field everywhere finite and with a finite self-energy. Born and Infeld computed the electrostatic energy of the electron (which is now finite) and obtained the formula

$$E = 1.24 \frac{4\pi e^2}{r_*}, \quad (\text{F20})$$

where $r_* = (e/b)^{1/2}$. They proposed to identify the electric energy with the mass of the electron via the relation $E = m_e c^2$. This yields

$$m_e c^2 = 1.24 \frac{4\pi e^2}{r_*}. \quad (\text{F21})$$

Comparing Eq. (F21) with Eq. (F1), we get

$$r_* = 1.24 \times 4\pi r_e = 4.39 \times 10^{-14} \text{ m}, \quad (\text{F22})$$

which may be interpreted as the effective radius of the electron in the Born-Infeld theory. In this sense, the Born-Infeld theory justifies the relation from Eq. (F1) defining the

classical radius of the electron. In the Born-Infeld electrodynamics, the electron has a finite radius because the electric field and the electrostatic energy of a point charge are finite. Their theory of the electron can be considered as a revival of the old idea of the electromagnetic origin of mass; namely, that the electron is a singularity in the electromagnetic field and that its mass is purely electromagnetic.

-
- [1] D. J. Kaup, *Phys. Rev.* **172**, 1331 (1968).
 [2] R. Ruffini and S. Bonazzola, *Phys. Rev.* **187**, 1767 (1969).
 [3] A. Das, *J. Math. Phys. (N.Y.)* **4**, 45 (1963).
 [4] S. Bonazzola and F. Pacini, *Phys. Rev.* **148**, 1269 (1966).
 [5] D. A. Feinblum and W. A. McKinley, *Phys. Rev.* **168**, 1445 (1968).
 [6] J. A. Wheeler, *Phys. Rev.* **97**, 511 (1955).
 [7] A. Einstein, *Sitz. König. Preu. Akad. Wiss.*, 349 (1919).
 [8] A. Einstein and N. Rosen, *Phys. Rev.* **48**, 73 (1935).
 [9] N. Rosen, *Phys. Rev.* **55**, 94 (1939).
 [10] A. C. Menius and N. Rosen, *Phys. Rev.* **62**, 436 (1942).
 [11] R. J. Finkelstein, *Phys. Rev.* **75**, 1079 (1949).
 [12] R. J. Finkelstein, R. LeLevier, and M. Ruderman, *Phys. Rev.* **83**, 326 (1951).
 [13] N. Rosen and H. B. Rosenstock, *Phys. Rev.* **85**, 257 (1952).
 [14] H. B. Rosenstock, *Phys. Rev.* **93**, 331 (1954).
 [15] R. J. Finkelstein, C. Fronsdal, and P. Kaus, *Phys. Rev.* **103**, 1571 (1956).
 [16] E. A. Power and J. A. Wheeler, *Rev. Mod. Phys.* **29**, 480 (1957).
 [17] T. Regge and J. A. Wheeler, *Phys. Rev.* **108**, 1063 (1957).
 [18] C. W. Misner, *Phys. Rev.* **118**, 1110 (1960).
 [19] R. W. Fuller and J. A. Wheeler, *Phys. Rev.* **128**, 919 (1962).
 [20] P. H. Chavanis and T. Matos, *Eur. Phys. J. Plus* **132**, 30 (2017).
 [21] M. R. Baldeschi, G. B. Gelmini, and R. Ruffini, *Phys. Lett.* **122B**, 221 (1983).
 [22] W. Thirring, *Phys. Lett.* **127B**, 27 (1983).
 [23] J. D. Breit, S. Gupta, and A. Zaks, *Phys. Lett.* **140B**, 329 (1984).
 [24] E. Takasugi and M. Yoshimura, *Z. Phys. C* **26**, 241 (1984).
 [25] T. D. Lee, *Phys. Rev. D* **35**, 3637 (1987).
 [26] R. Friedberg, T. D. Lee, and Y. Pang, *Phys. Rev. D* **35**, 3640 (1987).
 [27] T. D. Lee and Y. Pang, *Nucl. Phys.* **B315**, 477 (1989).
 [28] S. Chandrasekhar, *Astrophys. J.* **74**, 81 (1931).
 [29] J. R. Oppenheimer and G. M. Volkoff, *Phys. Rev.* **55**, 374 (1939).
 [30] B. K. Harrison, K. S. Thorne, M. Wakano, and J. A. Wheeler, *Gravitation Theory and Gravitational Collapse* (University of Chicago Press, Chicago, 1965).
 [31] J. J. van der Bij and M. Gleiser, *Phys. Lett. B* **194**, 482 (1987).
 [32] M. Gleiser, *Phys. Rev. D* **38**, 2376 (1988).
 [33] P. Jetzer, *Nucl. Phys.* **B316**, 411 (1989).
 [34] M. Gleiser and R. Watkins, *Nucl. Phys.* **B319**, 733 (1989).
 [35] E. Seidel and W.-M. Suen, *Phys. Rev. D* **42**, 384 (1990).
 [36] F. V. Kusmartsev, E. W. Mielke, and F. E. Schunck, *Phys. Rev. D* **43**, 3895 (1991).
 [37] F. V. Kusmartsev, E. W. Mielke, and F. E. Schunck, *Phys. Lett.* **157A**, 465 (1991).
 [38] F. V. Kusmartsev and F. E. Schunck, *Physica (Amsterdam)* **178A**, 24 (1992).
 [39] M. Gleiser, *Phys. Rev. D* **39**, 1257 (1989).
 [40] P. Jetzer, *Phys. Lett. B* **222**, 447 (1989).
 [41] S. Chandrasekhar, *Astrophys. J.* **140**, 417 (1964).
 [42] T. Poston and I. Stewart, *Catastrophe Theory and its Applications* (Pitman, London, 1978).
 [43] V. I. Arnold, S. M. Gusein-Zade, and A. N. Varchenko, *Singularities of Differentiable Maps* (Birkhäuser, Boston, 1985).
 [44] H. Whitney, *Ann. Math.* **62**, 374 (1955).
 [45] F. V. Kusmartsev, *Phys. Rep.* **183**, 1 (1989).
 [46] H. Poincaré, *Acta Math.* **7**, 259 (1885).
 [47] J. Katz, *Mon. Not. R. Astron. Soc.* **183**, 765 (1978).
 [48] G. Alberti and P. H. Chavanis, *Eur. Phys. J. B* **93**, 208 (2020).
 [49] P. H. Chavanis, *Int. J. Mod. Phys. B* **20**, 3113 (2006).
 [50] J. Katz, *Found. Phys.* **33**, 223 (2003).
 [51] F. S. Guzmán, *Phys. Rev. D* **70**, 044033 (2004).
 [52] F. S. Guzmán, *Rev. Mex. Fís.* **55**, 321 (2009).
 [53] E. W. Mielke and R. Scherzer, *Phys. Rev. D* **24**, 2111 (1981).
 [54] W. Deppert and E. W. Mielke, *Phys. Rev. D* **20**, 1303 (1979).
 [55] E. W. Mielke, *J. Math. Phys. (N.Y.)* **21**, 543 (1979).
 [56] T. D. Lee, *Comments Nucl. Part. Phys.* **17**, 225 (1987).
 [57] R. Ferrell and M. Gleiser, *Phys. Rev. D* **40**, 2524 (1989).
 [58] M. Colpi, S. L. Shapiro, and I. Wasserman, *Phys. Rev. Lett.* **57**, 2485 (1986).
 [59] E. W. Mielke, *Phys. Rev. Lett.* **39**, 530 (1977).
 [60] E. W. Mielke, *Phys. Rev. D* **18**, 4525 (1978).
 [61] E. W. Mielke, *Int. J. Theor. Phys.* **19**, 189 (1980).
 [62] W. Heisenberg, *Introduction to the Unified Field Theory of Elementary Particles* (Wiley, London, 1966).
 [63] H. Weyl, *Proc. Natl. Acad. Sci. U.S.A.* **15**, 323 (1929).
 [64] H. Weyl, *Phys. Rev.* **77**, 699 (1950).
 [65] C. J. Isham, A. Salam, and J. Strathdee, *Phys. Rev. D* **3**, 867 (1971).
 [66] K. Tennakone, *Phys. Rev. D* **10**, 1722 (1974).

- [67] C. Sivaram and K. P. Sinha, *Phys. Lett.* **60B**, 181 (1976).
- [68] A. Salam and J. Strathdee, *Phys. Lett.* **61B**, 375 (1976).
- [69] A. Salam and J. Strathdee, *Phys. Lett.* **66B**, 143 (1977).
- [70] C. Sivaram and K. P. Sinha, *Phys. Rev. D* **16**, 1975 (1977).
- [71] A. Salam and J. Strathdee, *Phys. Rev. D* **16**, 2668 (1977).
- [72] A. Salam and J. Strathdee, *Phys. Rev. D* **18**, 4596 (1978).
- [73] P. Caldirola, M. Pavisic, and E. Recami, *Nuovo Cimento B* **48**, 205 (1978).
- [74] C. Sivaram and K. P. Sinha, *Phys. Rep.* **51**, 111 (1979).
- [75] D. R. Brill and J. A. Wheeler, *Rev. Mod. Phys.* **29**, 465 (1957).
- [76] R. Friedberg, T. D. Lee, and Y. Pang, *Phys. Rev. D* **35**, 3658 (1987).
- [77] T. D. Lee and Y. Pang, *Phys. Rev. D* **35**, 3678 (1987).
- [78] P. Higgs, *Phys. Rev.* **145**, 1156 (1966).
- [79] A. Nishimura and Y. Yamaguchi, *Prog. Theor. Phys.* **53**, 891 (1975).
- [80] C. Rhoades and R. Ruffini, *Phys. Rev. Lett.* **32**, 324 (1974).
- [81] I. I. Tkachev, *Sov. Astron. Lett.* **12**, 305 (1986).
- [82] F. E. Schunck and A. R. Liddle, *Phys. Lett. B* **404**, 25 (1997).
- [83] J. Balakrishna, E. Seidel, and W.-M. Suen, *Phys. Rev. D* **58**, 104004 (1998).
- [84] F. E. Schunck and D. F. Torres, *Int. J. Mod. Phys. D* **09**, 601 (2000).
- [85] F. S. Guzmán and J. M. Rueda-Becerril, *Phys. Rev. D* **80**, 084023 (2009).
- [86] P. H. Chavanis and T. Harko, *Phys. Rev. D* **86**, 064011 (2012).
- [87] P. H. Chavanis, *Astronomy* **1**, 126 (2022).
- [88] A. B. Henriques, A. R. Liddle, and R. G. Moorhouse, *Phys. Lett. B* **233**, 99 (1989).
- [89] A. B. Henriques, A. R. Liddle, and R. G. Moorhouse, *Nucl. Phys.* **B337**, 737 (1990).
- [90] A. B. Henriques, A. R. Liddle, and R. G. Moorhouse, *Phys. Lett. B* **251**, 511 (1990).
- [91] P. Jetzer, *Phys. Lett. B* **243**, 36 (1990).
- [92] P. Jetzer and D. Scialom, *Phys. Lett.* **169A**, 12 (1992).
- [93] P. Jetzer and D. Scialom, *arXiv:gr-qc/9709056*.
- [94] R. Penrose, *Riv. Nuovo Cimento* **1**, 252 (1969).
- [95] O. Bergmann and R. Leipnik, *Phys. Rev.* **107**, 1157 (1957).
- [96] H. Yilmaz, *Phys. Rev.* **111**, 1417 (1958).
- [97] H. Treder, *Phys. Rev.* **112**, 2127 (1958).
- [98] H. A. Buchdahl, *Phys. Rev.* **115**, 1325 (1959).
- [99] J. Ehlers, *Z. Phys.* **143**, 239 (1955).
- [100] S. D. Majumdar, *Phys. Rev.* **72**, 390 (1947).
- [101] M. Wyman, *Phys. Rev. D* **24**, 839 (1981).
- [102] P. Baekler, E. W. Mielke, R. Hecht, and F. W. Hehl, *Nucl. Phys.* **B288**, 800 (1987).
- [103] K. Schmoltzi and Th. Schücker, *Phys. Lett.* **161A**, 212 (1991).
- [104] B. C. Xanthopoulos and Th. Zannias, *Phys. Rev. D* **40**, 2564 (1989).
- [105] D. Christodoulou, *Commun. Math. Phys.* **105**, 337 (1986).
- [106] D. Christodoulou, *Commun. Math. Phys.* **109**, 613 (1987).
- [107] D. S. Goldwirth and T. Piran, *Phys. Rev. D* **36**, 3575 (1987).
- [108] M. W. Choptuik, *Phys. Rev. Lett.* **70**, 9 (1993).
- [109] P. H. Chavanis, *Phys. Rev. D* **98**, 023009 (2018).
- [110] P. H. Chavanis, *Phys. Rev. D* **102**, 083531 (2020).
- [111] E. Seidel and W.-M. Suen, *Phys. Rev. Lett.* **66**, 1659 (1991).
- [112] M. Alcubierre, R. Becerril, F. S. Guzmán, T. Matos, D. Núñez, and L. A. Ureña-López, *Classical Quantum Gravity* **20**, 2883 (2003).
- [113] D. Ivanenko, *Nuovo Cimento Suppl.* **6**, 349 (1957).
- [114] G. Petiau, *Nuovo Cimento* **9**, 542 (1958).
- [115] T. H. R. Skyrme, *Proc. R. Soc. A* **262**, 237 (1961).
- [116] J. K. Perring and T. H. R. Skyrme, *Nucl. Phys.* **31**, 550 (1962).
- [117] U. Enz, *Phys. Rev.* **131**, 1392 (1963).
- [118] G. H. Derrick, *J. Math. Phys. (N.Y.)* **5**, 1252 (1964).
- [119] G. Rosen, *J. Math. Phys. (N.Y.)* **6**, 1269 (1965).
- [120] G. Rosen, *J. Math. Phys. (N.Y.)* **7**, 2066 (1966).
- [121] G. Rosen, *J. Math. Phys. (N.Y.)* **7**, 2071 (1966).
- [122] G. Rosen, *J. Math. Phys. (N.Y.)* **8**, 573 (1967).
- [123] G. H. Derrick and W. Kay-Kong, *J. Math. Phys. (N.Y.)* **9**, 232 (1968).
- [124] G. Rosen, *J. Math. Phys. (N.Y.)* **9**, 996 (1968).
- [125] G. Rosen, *Phys. Rev.* **183**, 1186 (1969).
- [126] A. C. Scott, *Am. J. Phys.* **37**, 52 (1969).
- [127] J. Rubinstein, *J. Math. Phys. (N.Y.)* **11**, 258 (1970).
- [128] M. Soler, *Phys. Rev. D* **1**, 2766 (1970).
- [129] A. Barone, F. Esposito, J. Magee, and A. C. Scott, *Riv. Nuovo Cimento* **1**, 227 (1971).
- [130] D. L. T. Anderson, *J. Math. Phys. (N.Y.)* **12**, 945 (1971).
- [131] T. D. Lee and G. C. Wick, *Phys. Rev. D* **9**, 2291 (1974).
- [132] R. F. Dashen, B. Hasslacher, and A. Neveu, *Phys. Rev. D* **10**, 4130 (1974).
- [133] J. Goldstone and R. Jackiw, *Phys. Rev. D* **11**, 1486 (1975).
- [134] R. F. Dashen, B. Hasslacher, and A. Neveu, *Phys. Rev. D* **11**, 3424 (1975).
- [135] N. H. Christ and T. D. Lee, *Phys. Rev. D* **12**, 1606 (1975).
- [136] R. Friedberg, T. D. Lee, and A. Sirlin, *Phys. Rev. D* **13**, 2739 (1976).
- [137] R. Jackiw, *Rev. Mod. Phys.* **49**, 681 (1977).
- [138] L. I. Schiff, *Phys. Rev.* **84**, 1 (1951).
- [139] L. I. Schiff, *Phys. Rev.* **84**, 10 (1951).
- [140] B. J. Malenka, *Phys. Rev.* **85**, 686 (1952).
- [141] J. Goldstone, *Nuovo Cimento* **19**, 154 (1961).
- [142] H. B. Nielsen and P. Olesen, *Nucl. Phys.* **B61**, 45 (1973).
- [143] W. Döring, *Z. Naturforsch.* **3**, 373 (1948).
- [144] F. Frenkel and T. Kontorova, *J. Phys. USSR* **1**, 137 (1939).
- [145] A. Kochendörfer and A. Seeger, *Z. Phys.* **127**, 533 (1950).
- [146] A. Seeger and A. Kochendörfer, *Z. Phys.* **130**, 321 (1951).
- [147] A. Seeger, H. Donth, and A. Kochendörfer, *Z. Phys.* **134**, 173 (1953).
- [148] N. J. Zabusky and M. D. Kruskal, *Phys. Rev. Lett.* **15**, 240 (1965).
- [149] D. J. Korteweg and G. de Vries, *Philos. Mag. Ser. 5* **39**, 422 (1895).
- [150] P. A. M. Dirac, *Proc. R. Soc. A* **209**, 291 (1951).
- [151] P. A. M. Dirac, *Proc. R. Soc.* **212**, 330 (1952).
- [152] P. A. M. Dirac, *Proc. R. Soc.* **223**, 438 (1954).
- [153] P. A. M. Dirac, *Proc. R. Soc.* **268**, 57 (1962).
- [154] L. de Broglie, *Une tentative d'interprétation causale et nonlinéaire de la mécanique ondulatoire (la théorie de la double solution)* (Gauthier-Villars, Paris, 1956).
- [155] S. Coleman, *Nucl. Phys.* **B262**, 263 (1985).

- [156] B. W. Lynn, *Nucl. Phys.* **B321**, 465 (1989).
 [157] S. Bahcall, B. W. Lynn, and S. Selipsky, *Nucl. Phys.* **B325**, 606 (1989).
 [158] S. Bahcall, B. W. Lynn, and S. Selipsky, *Nucl. Phys.* **B331**, 67 (1990).
 [159] S. Bahcall, B. W. Lynn, and S. Selipsky, *Astrophys. J.* **362**, 251 (1990).
 [160] B. Holdon, *Phys. Rev. D* **36**, 1000 (1987).
 [161] E. Witten, *Phys. Rev. D* **30**, 272 (1984).
 [162] C. J. Hogan and M. J. Rees, *Phys. Lett. B* **205**, 228 (1988).
 [163] E. W. Kolb and I. I. Tkachev, *Phys. Rev. Lett.* **71**, 3051 (1993).
 [164] E. W. Kolb and I. I. Tkachev, *Phys. Rev. D* **49**, 5040 (1994).
 [165] E. W. Kolb and I. I. Tkachev, *Phys. Rev. D* **50**, 769 (1994).
 [166] E. W. Kolb and I. I. Tkachev, *Astrophys. J.* **460**, L25 (1996).
 [167] B. Gradwohl and G. Kälbermann, *Nucl. Phys.* **B324**, 215 (1989).
 [168] I. I. Tkachev, *Phys. Lett. B* **261**, 289 (1991).
 [169] Z.-j. Tao and X. Xue, *Phys. Rev. D* **45**, 1878 (1992).
 [170] I. L. Bogolubsky and V. G. Makhankov, *JETP Lett.* **24**, 12 (1976).
 [171] I. L. Bogolubsky and V. G. Makhankov, *JETP Lett.* **25**, 107 (1977).
 [172] M. Gleiser, *Phys. Rev. D* **49**, 2978 (1994).
 [173] E. J. Copeland, M. Gleiser, and H. R. Müller, *Phys. Rev. D* **52**, 1920 (1995).
 [174] J. A. Okolowski, *J. Math. Phys. (N.Y.)* **19**, 2253 (1978).
 [175] E. Elizalde and R. Tarrach, *Nuovo Cimento B* **100**, 371 (1987).
 [176] E. Elizalde, *Phys. Rev. D* **36**, 1269 (1987).
 [177] E. Elizalde, *Phys. Rev. D* **37**, 2127 (1988).
 [178] G. Rosen, *Found. Phys.* **24**, 1563 (1994).
 [179] G. Rosen, *Found. Phys.* **24**, 1689 (1994).
 [180] R. Brito, V. Cardoso, C. A. R. Herdeiro, and E. Radu, *Phys. Lett. B* **752**, 291 (2016).
 [181] C. A. R. Herdeiro, A. M. Pombo, and E. Radu, *Phys. Lett. B* **773**, 654 (2017).
 [182] M. Abraham, *Theorie der Elektrizität* (Teubner, Leipzig, 1905).
 [183] H. Poincaré, *Rend. Circ. Mat. Palermo* **21**, 129 (1906).
 [184] H. A. Lorentz, *The Theory of Electrons* (Teubner, Leipzig, 1909).
 [185] G. Horwitz and J. Katz, *Nuovo Cimento* **3**, 245 (1971).
 [186] G. Horwitz and J. Katz, *Nuovo Cimento* **5**, 59 (1971).
 [187] G. Mie, *Ann. Phys. (Berlin)* **342**, 511 (1912).
 [188] M. Born, *Proc. R. Soc. A* **143**, 410 (1933).
 [189] M. Born and L. Infeld, *Proc. R. Soc.* **144**, 425 (1934).
 [190] H. Schiff, *Proc. R. Soc.* **269**, 277 (1962).
 [191] A. Burinskii, *Sov. Phys. JETP* **39**, 193 (1974).
 [192] H. Weyl, *Phys. Rev.* **77**, 699 (1950).
 [193] W. Thirring, *Z. Naturforschg.* **7**, 63 (1952).
 [194] W. Heisenberg, *Physica* **19**, 897 (1953).
 [195] W. Heisenberg, *Z. Naturforsch.* **9**, 292 (1954).
 [196] F. Gürsey, *Nuovo Cimento* **3**, 988 (1956).
 [197] W. Heisenberg, *Rev. Mod. Phys.* **29**, 269 (1957).
 [198] W. Thirring, *Ann. Phys. (N.Y.)* **3**, 91 (1958).
 [199] A. Das, *Nuovo Cimento* **27**, 1175 (1963).
 [200] A. Rañada and M. Soler, *J. Math. Phys. (N.Y.)* **13**, 671 (1972).
 [201] A. Rañada, *J. Phys. A* **11**, 341 (1978).
 [202] E. W. Mielke, *J. Math. Phys. (N.Y.)* **22**, 2034 (1980).
 [203] F. A. Kaempffer, *Phys. Rev.* **99**, 1614 (1955).
 [204] M. Wakano, *Prog. Theor. Phys.* **35**, 1117 (1965).
 [205] A. G. Lisi, *J. Phys. A* **28**, 5385 (1995).
 [206] C. S. Bohun and F. I. Cooperstock, *Phys. Rev. A* **60**, 4291 (1999).
 [207] L. V. Biguaa and V. V. Kassandrov, *Phys. Part. Nucl.* **51**, 965 (2020).
 [208] F. Edjo Ovono and Ya. P. Terletskii, *Sov. Phys. J.* **26**, 304 (1983).
 [209] F. I. Cooperstock and N. Rosen, *Int. J. Theor. Phys.* **28**, 423 (1989).
 [210] A. Alharthy and V. V. Kassandrov, *Universe* **6**, 193 (2020).
 [211] G. Rosen, *J. Math. Phys. (N.Y.)* **9**, 999 (1968).
 [212] F. I. Cooperstock, *Fund. Phys. Lett.* **2**, 553 (1989).
 [213] Yu. P. Rybakov and B. Saha, *Phys. Lett. A* **222**, 5 (1996).
 [214] M. Soler, *Phys. Rev. D* **8**, 3424 (1973).
 [215] A. Rañada and M. Soler, *Phys. Rev. D* **8**, 3430 (1973).
 [216] A. Rañada, M. Rañada, M. Soler, and L. Vázquez, *Phys. Rev. D* **10**, 517 (1974).
 [217] W. A. Bardeen, M. S. Chanowitz, S. D. Drell, M. Weinstein, and T. M. Yan, *Phys. Rev. D* **11**, 1094 (1975).
 [218] A. Rañada and L. Vázquez, *Prog. Theor. Phys.* **56**, 311 (1976).
 [219] T. Kodama, K. C. Chung, and F. Teixeira, *Nuovo Cimento* **46**, 206 (1978).
 [220] T. Kodama, *Phys. Rev. D* **18**, 3529 (1978).
 [221] T. Kodama, L. C. S. de Oliveira, and F. C. Santos, *Phys. Rev. D* **19**, 3576 (1979).
 [222] R. N. Tiwari, J. R. Rao, and R. R. Kanakamedala, *Phys. Rev. D* **30**, 489 (1984).
 [223] R. Gautreau, *Phys. Rev. D* **31**, 1860 (1985).
 [224] O. Gron, *Phys. Rev. D* **31**, 2129 (1985).
 [225] M. Israelit and N. Rosen, *Found. Phys.* **21**, 1237 (1991).
 [226] M. Israelit and N. Rosen, *Found. Phys.* **22**, 549 (1992).
 [227] R. Bartnik and J. McKinnon, *Phys. Rev. Lett.* **61**, 141 (1988).
 [228] N. Straumann and Z. H. Zhou, *Phys. Lett. B* **237**, 353 (1990).
 [229] M. Israelit and N. Rosen, *Found. Phys.* **26**, 585 (1996).
 [230] F. Finster, J. Smoller, and S. T. Yau, *Phys. Rev. D* **59**, 104020 (1999).
 [231] F. Finster, J. Smoller, and S. T. Yau, *Phys. Lett. A* **259**, 431 (1999).
 [232] F. Finster, J. Smoller, and S. T. Yau, *Mod. Phys. Lett. A* **14**, 1053 (1999).
 [233] A. Burinskii, *J. Phys. A* **43**, 392001 (2010).
 [234] V. V. Kassandrov and N. V. Markova, *Int. J. Mod. Phys. A* **35**, 2040017 (2020).
 [235] A. Einstein and L. Infeld, *The Evolution of Physics* (Simon and Schuster, New York, 1938), pp. 257–258.
 [236] C. A. López, *Phys. Rev. D* **30**, 313 (1984).
 [237] C. A. López, *Gen. Relativ. Gravit.* **24**, 285 (1992).
 [238] M. Israelit and N. Rosen, *Gen. Relativ. Gravit.* **27**, 153 (1995).
 [239] A. Burinskii, *Gravitation Cosmol.* **14**, 109 (2008).
 [240] A. Burinskii, *Gravitation Cosmol.* **26**, 87 (2020).
 [241] K. Schwarzschild, *Berliner Sitzungsbesichte*, 189 (1916).
 [242] K. Schwarzschild, *Berliner Sitzungsbesichte*, 424 (1916).

- [243] R. P. Kerr, *Phys. Rev. Lett.* **11**, 237 (1963).
- [244] E. Newman and A. Janis, *J. Math. Phys. (N.Y.)* **6**, 915 (1965).
- [245] E. Newman, E. Couch, K. Chinnapared, A. Exton, A. Prakash, and R. Torrence, *J. Math. Phys. (N.Y.)* **6**, 918 (1965).
- [246] H. Reissner, *Ann. Phys. (Berlin)* **50**, 106 (1916).
- [247] G. Nordström, *Verhandel. Koninkl. Ned. Akad. Wetenschap., Afdel. Natuurk* **26**, 1201 (1918).
- [248] S. Carneiro, *Fund. Phys. Lett.* **11**, 95 (1998).
- [249] R. Rajaraman, *Phys. Rep.* **21**, 227 (1975).
- [250] V. G. Makhankov, *Phys. Rep.* **35**, 1 (1978).
- [251] R. Rajaraman, *Solitons and Instantons* (Elsevier, Amsterdam, North Holland, 1982).
- [252] T. D. Lee and Y. Pang, *Phys. Rep.* **221**, 251 (1992).
- [253] P. Jetzer, *Phys. Rep.* **220**, 163 (1992).
- [254] A. R. Liddle and M. S. Madsen, *Int. J. Mod. Phys. D* **01**, 101 (1992).
- [255] E. W. Mielke and F. E. Schunck, in *Proceedings of the 8th Marcel Grossmann Meeting*, edited by T. Piran (World Scientific, Singapore, 1998), arXiv:gr-qc/9801063.
- [256] F. E. Schunck and E. W. Mielke, *Gen. Relativ. Gravit.* **31**, 787 (1999).
- [257] E. W. Mielke and F. E. Schunck, *Nucl. Phys.* **B564**, 185 (2000).
- [258] F. E. Schunck and E. W. Mielke, *Classical Quantum Gravity* **20**, R301 (2003).
- [259] S. L. Liebling and C. Palenzuela, *Living Rev. Relativity* **20**, 5 (2017).
- [260] L. Visinelli, *Int. J. Mod. Phys. D* **30**, 2130006 (2021).
- [261] S. Krippendorf, F. Muia, and F. Quevedo, *J. High Energy Phys.* **08** (2018) 070.
- [262] E. Seidel and W. M. Suen, *Phys. Rev. Lett.* **72**, 2516 (1994).
- [263] D. Lynden-Bell, *Mon. Not. R. Astron. Soc.* **136**, 101 (1967).
- [264] P. H. Chavanis, *Eur. Phys. J. B* **95**, 48 (2022).
- [265] P. H. Chavanis, *Phys. Rev. D* **84**, 043531 (2011).
- [266] L. Hui, J. Ostriker, S. Tremaine, and E. Witten, *Phys. Rev. D* **95**, 043541 (2017).
- [267] P. H. Chavanis, *Phys. Rev. D* **103**, 123551 (2021).
- [268] H. Y. Schive, T. Chiueh, and T. Broadhurst, *Nat. Phys.* **10**, 496 (2014).
- [269] H. Y. Schive, M.-H. Liao, T.-P. Woo, S.-K. Wong, T. Chiueh, T. Broadhurst, and W.-Y. Pauchy Hwang, *Phys. Rev. Lett.* **113**, 261302 (2014).
- [270] B. Schwabe, J. Niemeyer, and J. Engels, *Phys. Rev. D* **94**, 043513 (2016).
- [271] P. Mocz, M. Vogelsberger, V. H. Robles, J. Zavala, M. Boylan-Kolchin, A. Fialkov, and L. Hernquist, *Mon. Not. R. Astron. Soc.* **471**, 4559 (2017).
- [272] P. Mocz, L. Lancaster, A. Fialkov, F. Becerra, and P. H. Chavanis, *Phys. Rev. D* **97**, 083519 (2018).
- [273] J. Veltmaat, J. C. Niemeyer, and B. Schwabe, *Phys. Rev. D* **98**, 043509 (2018).
- [274] P. Mocz *et al.*, *Phys. Rev. Lett.* **123**, 141301 (2019).
- [275] P. Mocz *et al.*, *Mon. Not. R. Astron. Soc.* **494**, 2027 (2020).
- [276] J. Veltmaat, B. Schwabe, and J. C. Niemeyer, *Phys. Rev. D* **101**, 083518 (2020).
- [277] P. H. Chavanis, J. Sommeria, and R. Robert, *Astrophys. J.* **471**, 385 (1996).
- [278] B. Moore, T. Quinn, F. Governato, J. Stadel, and G. Lake, *Mon. Not. R. Astron. Soc.* **310**, 1147 (1999).
- [279] A. Suárez, V. H. Robles, and T. Matos, *Astrophys. Space Sci. Proc.* **38**, 107 (2014).
- [280] T. Rindler-Daller and P. R. Shapiro, *Astrophys. Space Sci. Proc.* **38**, 163 (2014).
- [281] P. H. Chavanis, Self-gravitating Bose-Einstein condensates, in *Quantum Aspects of Black Holes*, edited by X. Calmet (Springer, New York, 2015).
- [282] D. Marsh, *Phys. Rep.* **643**, 1 (2016).
- [283] J. W. Lee, *EPJ Web Conf.* **168**, 06005 (2018).
- [284] J. C. Niemeyer, *Prog. Part. Nucl. Phys.* **113**, 103787 (2020).
- [285] E. Ferreira, *Astron. Astrophys. Rev.* **29**, 7 (2021).
- [286] L. Hui, *Annu. Rev. Astron. Astrophys.* **59**, 247 (2021).
- [287] A. Suárez and P. H. Chavanis, *Phys. Rev. D* **92**, 023510 (2015).
- [288] A. Suárez and P. H. Chavanis, *J. Phys. Conf. Ser.* **654**, 012008 (2015).
- [289] E. Madelung, *Z. Phys.* **40**, 322 (1927).
- [290] P. H. Chavanis and L. Delfini, *Phys. Rev. D* **84**, 043532 (2011).
- [291] M. Membrado, A. F. Pacheco, and J. Sañudo, *Phys. Rev. A* **39**, 4207 (1989).
- [292] S. Chandrasekhar, *An Introduction to the Study of Stellar Structure* (Dover, New York, 1958).
- [293] M. Membrado, J. Abad, A. F. Pacheco, and J. Sañudo, *Phys. Rev. D* **40**, 2736 (1989).
- [294] J. W. Lee and I. Koh, *Phys. Rev. D* **53**, 2236 (1996).
- [295] J. Goodman, *New Astron.* **5**, 103 (2000).
- [296] A. Arbey, J. Lesgourgues, and P. Salati, *Phys. Rev. D* **68**, 023511 (2003).
- [297] C. G. Böhrer and T. Harko, *J. Cosmol. Astropart. Phys.* **06** (2007) 025.
- [298] P. H. Chavanis, *Eur. Phys. J. Plus* **130**, 181 (2015).
- [299] J. M. Lattimer and M. Prakash, in *From Nuclei to Stars*, edited by S. Lee (World Scientific, Singapore, 2011), p. 275.
- [300] R. D. Peccei and H. R. Quinn, *Phys. Rev. Lett.* **38**, 1440 (1977).
- [301] J. E. Kim and G. Carosi, *Rev. Mod. Phys.* **82**, 557 (2010).
- [302] J. Preskill, M. Wise, and F. Wilczek, *Phys. Lett.* **120B**, 127 (1983).
- [303] L. Abbott and P. Sikivie, *Phys. Lett.* **120B**, 133 (1983).
- [304] M. Dine and W. Fischler, *Phys. Lett.* **120B**, 137 (1983).
- [305] R. L. Davis, *Phys. Lett. B* **180**, 225 (1986).
- [306] P. H. Chavanis, in *The Maximum Mass of Dilute Axion Stars Proceedings of the Sixteenth Marcel Grossman Meeting* (World Scientific, 2021).
- [307] P. H. Chavanis, *Phys. Rev. D* **94**, 083007 (2016).
- [308] D. G. Levkov, A. G. Panin, and I. I. Tkachev, *Phys. Rev. Lett.* **118**, 011301 (2017).
- [309] T. Helfer, D. J. E. Marsh, K. Clough, M. Fairbairn, E. A. Lim, and R. Becerril, *J. Cosmol. Astropart. Phys.* **03** (2017) 055.
- [310] F. Michel and I. G. Moss, *Phys. Lett. B* **785**, 9 (2018).
- [311] E. Braaten, A. Mohapatra, and H. Zhang, *Phys. Rev. Lett.* **117**, 121801 (2016).
- [312] J. Eby, M. Leembruggen, P. Suranyi, and L. C. R. Wijewardhana, *J. High Energy Phys.* **12** (2016) 066.
- [313] L. Visinelli, S. Baum, J. Redondo, K. Freese, and F. Wilczek, *Phys. Lett. B* **777**, 64 (2018).

- [314] J. Eby, M. Leembruggen, L. Street, P. Suranyi, and L. C. R. Wijewardhana, *Phys. Rev. D* **100**, 063002 (2019).
- [315] M. J. Ablowitz, D. J. Kaup, A. C. Newell, and H. Segur, *Phys. Rev. Lett.* **30**, 1262 (1973).
- [316] E. Braaten and H. Zhang, *Rev. Mod. Phys.* **91**, 041002 (2019).
- [317] D. Guerra, C. F. B. Macedo, and P. Pani, *J. Cosmol. Astropart. Phys.* **09** (2019) 061.
- [318] S. Davidson and T. Schwetz, *Phys. Rev. D* **93**, 123509 (2016).
- [319] E. Cotner, *Phys. Rev. D* **94**, 063503 (2016).
- [320] P. H. Chavanis, *Eur. Phys. J. Plus* **132**, 248 (2017).
- [321] P. H. Chavanis, *Phys. Rev. D* **100**, 083022 (2019).
- [322] P. H. Chavanis, *Phys. Rev. D* **100**, 123506 (2019).
- [323] P. H. Chavanis, *Phys. Rev. D* **101**, 063532 (2020).
- [324] L. E. Padilla, T. Rindler-Daller, P. Shapiro, T. Matos, and J. A. Vázquez, *Phys. Rev. D* **103**, 063012 (2021).
- [325] B. Eggemeier and J. C. Niemeyer, *Phys. Rev. D* **100**, 063528 (2019).
- [326] N. Bar, D. Blas, K. Blum, and S. Sibiryakov, *Phys. Rev. D* **98**, 083027 (2018).
- [327] N. Musoke, S. Hotchkiss, and R. Easther, *Phys. Rev. Lett.* **124**, 061301 (2020).
- [328] J. C. Niemeyer and R. Easther, *J. Cosmol. Astropart. Phys.* **07** (2020) 030.
- [329] B. Eggemeier, J. C. Niemeyer, and R. Easther, *Phys. Rev. D* **103**, 063525 (2021).
- [330] B. Eggemeier, B. Schwabe, J. C. Niemeyer, and R. Easther, *Phys. Rev. D* **105**, 023516 (2022).
- [331] L. E. Padilla, J. C. Hidalgo, and K. A. Malik, *Phys. Rev. D* **106**, 023519 (2022).
- [332] V. Desjacques, A. Kehagias, and A. Riotto, *Phys. Rev. D* **97**, 023529 (2018).
- [333] K. Fujikura, M. Hertzberg, E. Schiappacasse, and M. Yamaguchi, *Phys. Rev. D* **104**, 123012 (2021).
- [334] J. Chen, X. Du, E. Lentz, D. Marsh, and J. Niemeyer, *Phys. Rev. D* **104**, 083022 (2021).
- [335] N. Glennon and C. Prescod-Weinstein, *Phys. Rev. D* **104**, 083532 (2021).
- [336] J. Eby, S. Shirai, Y. V. Stadnik, and V. Takhistov, *Phys. Lett. B* **825**, 136858 (2022).
- [337] B. K. K. Lee, M. C. Chu, and L. M. Lin, *Astrophys. J.* **922**, 242 (2021).
- [338] M. Jain, *Phys. Rev. D* **106**, 085011 (2022).
- [339] M. Jain and M. A. Amin, [arXiv:2211.08433](https://arxiv.org/abs/2211.08433).
- [340] J. Binney and S. Tremaine, *Galactic Dynamics*, Princeton Series in Astrophysics (Princeton, NJ, 1987).
- [341] A. Ritter, *Wiedemann's Ann.* **11**, 332 (1880).
- [342] P. S. Laplace, *Traité de Mécanique Céleste, vol. V, livre XI* (Bachelier, Paris, 1825).
- [343] G. Choi, H. J. He, and E. D. Schiappacasse, *J. Cosmol. Astropart. Phys.* **10** (2019) 043.
- [344] P. Amaro-Seoane, J. Barranco, A. Bernal, and L. Rezzolla, *J. Cosmol. Astropart. Phys.* **11** (2010) 002.
- [345] D. Croon, J. Fan, and C. Sun, *J. Cosmol. Astropart. Phys.* **04** (2019) 008.
- [346] A. Suárez and P. H. Chavanis, *Phys. Rev. D* **95**, 063515 (2017).
- [347] B. Schwabe, M. Gosenca, C. Behrens, J. C. Niemeyer, and R. Easther, *Phys. Rev. D* **102**, 083518 (2020).
- [348] J. Kormendy and K. C. Freeman, in *Proceedings of IAU Symposium 220, Dark Matter in Galaxies*, edited by S. D. Ryder, D. J. Pisano, M. A. Walker, and K. C. Freeman (Astronomical Society of the Pacific, San Francisco, 2004), p. 377.
- [349] M. Spano, M. Marcelin, P. Amram, C. Carignan, B. Epinat, and O. Hernandez, *Mon. Not. R. Astron. Soc.* **383**, 297 (2008).
- [350] F. Donato, G. Gentile, P. Salucci, C. Frigerio Martins, M. I. Wilkinson, G. Gilmore, E. K. Grebel, A. Koch, and R. Wyse, *Mon. Not. R. Astron. Soc.* **397**, 1169 (2009).
- [351] R. Easther, R. Flauger, and J. B. Gilmore, *J. Cosmol. Astropart. Phys.* **04** (2011) 027.
- [352] S. Hawking, *Commun. Math. Phys.* **43**, 199 (1975).
- [353] P. H. Chavanis (to be published).
- [354] P. H. Chavanis, *Phys. Rev. D* **106**, 043538 (2022).
- [355] L. D. Landau and E. M. Lifshitz, *Fluid Mechanics* (Pergamon Press, London, 1959).
- [356] L. de Broglie, *J. Phys. Radium* **8**, 225 (1927).
- [357] L. de Broglie, *C. R. Acad. Sci. Paris* **185**, 380 (1927).
- [358] L. de Broglie, *C. R. Acad. Sci. Paris* **185**, 1118 (1927).
- [359] P. H. Chavanis, *Phys. Rev. D* **106**, 063525 (2022).
- [360] P. H. Chavanis, *Phys. Rev. D* **106**, 043502 (2022).
- [361] T. Matos, A. Avilez, T. Bernal, and P. H. Chavanis, *Gen. Relativ. Gravit.* **51**, 159 (2019).
- [362] J. C. Hwang and H. Noh, *J. Cosmol. Astropart. Phys.* **03** (2022) 001.
- [363] J. C. Hwang and H. Noh, [arXiv:2211.02197](https://arxiv.org/abs/2211.02197).
- [364] B. Li, T. Rindler-Daller, and P. R. Shapiro, *Phys. Rev. D* **89**, 083536 (2014).
- [365] D. R. Karkevandi, S. Shakeri, V. Sagun, and O. Ivanytskyi, *Phys. Rev. D* **105**, 023001 (2022).
- [366] S. Shakeri and D. R. Karkevandi, [arXiv:2210.17308](https://arxiv.org/abs/2210.17308).
- [367] E. Witten, *Ann. Phys. (N.Y.)* **128**, 363 (1980).
- [368] P. Di Vecchia and G. Veneziano, *Nucl. Phys.* **B171**, 253 (1980).
- [369] L. Diósi, *Phys. Lett.* **105A**, 199 (1984).
- [370] P. Jetzer and J. van der Bij, *Phys. Lett. B* **227**, 341 (1989).
- [371] P. Jetzer, *Phys. Lett. B* **231**, 433 (1989).
- [372] A. D. Vlasov, *Phys. Usp.* **36**, 94 (1993).
- [373] L. P. Pitaevskii, *Phys. Usp.* **36**, 760 (1993).
- [374] H. Poincaré, *Comptes Rendus* **140**, 1504 (1905).
- [375] P. Caldirola, *Nuovo Cimento* **45**, 549 (1978).
- [376] H. A. Lorentz, *Proc. R. Netherland Acad. Arts Sci.* **1**, 427 (1899).
- [377] H. A. Lorentz, *Proc. R. Netherlands Acad. Arts Sci.* **6**, 809 (1904).
- [378] M. Abraham, *Phys. Z.* **5**, 576 (1904).
- [379] A. Einstein, *Ann. Phys. (Berlin)* **322**, 891 (1905).
- [380] F. Rohrlich, *Am. J. Phys.* **28**, 639 (1960).
- [381] J. J. Thomson, *Philos. Mag.* **11**, 229 (1881).
- [382] G. G. Stokes, *Trans. Cambridge Philos. Soc.* **8**, 105 (1844).
- [383] O. Heaviside, *Philos. Mag.* **27**, 324 (1889).
- [384] J. J. Thomson, *Notes on Recent Researches in Electricity and Magnetism* (Clarendon Press, Oxford, 1893).
- [385] G. F. C. Searle, *Philos. Mag. Ser. 5* **44**, 329 (1897).
- [386] M. Abraham, *Ann. Phys. (Berlin)* **315**, 105 (1902).
- [387] H. A. Lorentz, *Arch. Néer. Sci. Exact. Nat.* **25**, 363 (1892).
- [388] W. Wien, *Ann. Phys. (Berlin)* **310**, 501 (1900).